

A COMPARISON STUDY OF GRACE-BASED GROUNDWATER MODELING FOR
DATA-RICH AND DATA-POOR REGIONS

A THESIS IN
Environmental and Urban Geosciences

Presented to the Faculty of the University of
Missouri-Kansas City in partial fulfillment of
the requirements for the degree

MASTER OF SCIENCE

By
ALLA SKASKEVYCH

B.S., Computer Environmental and Economic Monitoring
Sevastopol National University of Nuclear Energy and Industry, 2009

Kansas City, Missouri
2014

© 2014

ALLA SKASKEVYCH

ALL RIGHTS RESERVED

A COMPARISON STUDY OF GRACE-BASED GROUNDWATER MODELING FOR
DATA-RICH AND DATA-POOR REGIONS

Alla Skaskevych, Candidate for the Master of Science Degree

University of Missouri-Kansas City, 2014

ABSTRACT

Gravity Recovery and Climate Experiment (GRACE) modeling in water resources is an emerging field in hydrology. Investigation of groundwater change using remote sensing data helps overcome data limitation at a regional scale. We present a GRACE modeling approach to estimate the variations of groundwater for two case studies, the Upper Mississippi Basin in the US as a relatively data-rich region and the Ngadda catchment of the Lake Chad Basin in Africa as a data-poor region. It is critical to understand whether GRACE data is capable of analyzing groundwater change in data-poor regions as much as in data-rich regions.

The GRACE data is applied first to analyze groundwater changes at the Upper Mississippi Basin, and compare it with ground truth data. The modeling conditions that affect the model accuracy are soil moisture models, groundwater fluctuations in the monitoring well, and the matter of the aquifer. The most successful GRACE modeling approach determined the effect of soil moisture model and aquifer. The strong correlation of 86.1%

and 73.4%, respectively, verifies a good match between GRACE-based and ground truth time series.

After the successful modeling approach is verified for the data-rich region, the technique was employed for the Ngadda Catchment of the Lake Chad Basin, as a data-poor region, to analyze groundwater changes. We investigated the effect of soil moisture models, scales, groundwater fluctuations in the individual cell, and the coverage area parameters in the GRACE modeling for the data-poor region. The most successful GRACE modeling approach determined the effect of soil moisture model.

APPROVAL PAGE

The faculty listed below, appointed by the Dean of the College of Arts and Sciences have examined a thesis titled “A Comparison Study of Grace-Based Groundwater Modeling for Data-Rich and Data-Scarce Regions” presented by Alla Skaskevych, candidate for the Master of Science degree, and hereby certify that in their opinion it is worthy of acceptance.

Supervisory Committee

Jejung Lee, Ph.D., Committee Chair and Research Advisor
Department of Geosciences

James B. Murowchick, Ph.D.
Department of Geosciences

Wei Ji, Ph.D.
Department of Geosciences

CONTENTS

ABSTRACT	iii
ILLUSTRATIONS	viii
TABLES	xi
ACKNOWLEDGEMENTS	xii
Chapter	
1. INTRODUCTION	1
1.1 Statement of Problems	1
1.2 GRACE in General	4
1.3 Lake Chad Basin.....	6
1.4 Objectives.....	10
2. LITERATURE REVIEW	12
2.1 Groundwater and Remote Sensing Studies for the Lake Chad Basin.....	12
2.2 GRACE Modeling Studies for Groundwater	15
3. METHODOLOGY	18
3.1 Basic Theory of GRACE.....	18
3.2 GLDAS in General	21
3.3 Implementation	24
3.3.1 Implementation of GRACE	25
3.3.2 Implementation of GLDAS	28
3.3.3 Groundwater Anomalies from the Ground-Truth Data.....	29
3.4 Statistical Analysis	30
4. RESULTS AND DISCUSSION	33
4.1 Data-rich Region: Upper Mississippi Basin	33

4.1.1 Effect of Soil Moisture Models.....	37
4.1.2 Effect of Groundwater Fluctuations	46
4.1.3 Effect of Aquifer	54
4.2 Data-Poor Region: Lake Chad Ngadda Catchment	59
4.2.1 Ground Truth Data for the Lake Chad Region	59
4.2.2 Effect of Soil Moisture Models.....	62
4.2.3 Effect of Scales	63
4.2.4 Effect of Individual Cell	63
4.2.5 Effect of Coverage Area	64
5. CONCLUSION	70
APPENDIX.....	74
REFERENCES.....	89
VITA.....	94

ILLUSTRATIONS

Figure	Page
1.1. The Lake Chad Basin and approximate location of Lake Chad.	3
1.2. The twin GRACE satellites with ranging link between the two crafts.....	6
1.3. Hydrogeological cross section of Lake Chad.....	8
1.4. Sampling area and boundaries of the study area.	10
3.1. A flowchart to estimate the groundwater storage anomalies.	21
3.2. The example case of the Upper Mississippi Basin boundary.	27
3.3. Downscaling of ΔGW using 1° GRACE and 0.25° GLDAS data.....	29
4.1. The Upper Mississippi Basin boundaries.	35
4.2. The Upper Mississippi Basin inputs (Rodell et al., 2007).	36
4.3. The Upper Mississippi Basin inputs.....	36
4.4. The Upper Mississippi Basin outputs (Rodell et al., 2007).	37
4.5. Soil moisture anomalies.....	38
4.6a. Effect of three soil moisture models average on groundwater storage anomalies.	39
4.6b. Correlation between GW anomalies from GRACE with three soil moisture models average and from well observations.....	40
4.7a. Effect of CLM soil moisture model on GW storage anomalies.	41
4.7b. Correlation between GW anomalies from GRACE and CLM soil moisture model and from well observations.	42
4.8a. Effect of Noah soil moisture model on GW storage anomalies.	43
4.8b. Correlation between GW anomalies from GRACE and Noah soil moisture model and from well observations.	44

4.9a. Effect of Mosaic soil moisture model on GW storage anomalies.	45
4.9b. Correlation between GW anomalies from GRACE and Mosaic soil moisture model and from well observations.	46
4.10. Location of groundwater wells.	48
4.11. Effect of GW fluctuations.	49
4.12. Effect of groundwater fluctuations: Thiessen Polygon distribution.	50
4.13. Effect of GW fluctuations: GW storage estimates.	51
4.14. Correlation between GW anomalies from GRACE and fluctuations from well observations.	53
4.15. Effect of aquifer.	55
4.16. Effect of aquifer: GW storage anomalies from monitoring wells.	56
4.17. Correlation between GW Anomalies from GRACE with three soil moisture models average and well observations.	58
4.18. Site map with GRACE domain.	60
4.19. Groundwater table in 1960's and location of Bornu piezometric depression.	60
4.20. Kriging of groundwater depths and sampling data.	61
4.21. Effect of soil moisture models.	65
4.22. Effect of scales.	66
4.23. Division of 2x2 area into 1° individual cells.	66
4.24. Effect of individual cell of 2x2 area.	67
4.25. The coverage area of the Lake Chad Ngadda Catchment using a sub-basin area boundary and 2° by 2° area.	68
4.26. Effect of coverage area: sub-basin area boundary and 2x2 area.	69

5.1. Effect of CLM and 11 groundwater monitoring wells.	71
5.2. Correlation between groundwater anomalies from GRACE and CLM soil moisture model and from 11 well observations.	72

TABLES

Table	Page
3.1. Vertical layering structure of three LSM models.	24
3.2. TWS and SM data description.	25
4.1. Monitoring well observations.....	47

ACKNOWLEDGEMENTS

First and foremost, I am thankful to God for the wisdom and perseverance he has been giving me during this research journey. Indeed, I can do everything through him who gives me strength. In particular, God helps me through different people, and without their contribution this research would not be possible.

My deepest gratitude is to my advisor and mentor, Dr. Jejung Lee who continuously supports me in my study and research. His patience, motivation, enthusiasm, and immense knowledge helped me overcome many difficulties and finish this thesis. His time and effort have been crucial in the development of this thesis.

Besides my advisor, I am also indebted to Professors James Murowchick and Wei Ji for serving in my Supervisory Committee, spending time reading this thesis and encouraging me throughout my coursework.

I am also grateful to John Bolten and Ebo from the NASA's Goddard Space Flight Center in Maryland for giving me their valuable time, numerous advices and a research opportunity to learn about GRACE. During my one-week visit, I have been trained to analyze GRACE data for groundwater storage monitoring. This knowledge has become a basis for this research.

I am thankful to Ken Kieffer, an expert in Python programming language, for assisting me in my entry-level programming skills. I appreciate his willingness to find time for helping me with coding and be there when I needed.

I sincerely acknowledge my fellow labmate, Rakiya Baba-maaji for her assistance in our Hydro Lab and valuable discussions on the Lake Chad that helped me understand my

research area better. Also, I am grateful to my friend Jenya for her support and help throughout these years. Thank you, girls, for a true friendship.

Most importantly, I am heartily thankful to my two families. I would like to express endless gratitude to my American family, Bill and Mary Beard for their generosity and care. Finally, I am most grateful to my parents whom this thesis is dedicated to. Despite the geographical challenges, they have always financially and emotionally supported me and helped me achieve the high standards I set for myself in all aspects of life.

CHAPTER 1

INTRODUCTION

1.1 Statement of Problems

Freshwater is the most vital resource for the healthy life of all ecosystems today. While nearly 70% of the world is covered by water, only 2.5% of it is fresh. The rest is saline and unsuitable for human consumption. Less than 1% out of 2.5% the world's freshwater is accessible for direct human uses at the land surface as rivers, lakes, and reservoirs. The land surface water is regularly renewed by rain and snowfall, and is therefore available on a sustainable basis. Less than about two-thirds of all freshwater on earth is stored as ice caps and glaciers, and almost a third is stored in deep underground aquifers as groundwater. However, groundwater is a non-renewable resource and is distributed extremely unevenly both in space and time around the globe. For instance, in the mid-latitude and semi-arid regions, groundwater is the primary source of freshwater which people exploit for domestic, agricultural and industrial uses. By this fact, more and more regions around the world are facing water stress and scarcity by their population and overuse growth, and climate change.

Since groundwater reservoir are experiencing increasing demands, a better monitoring system is critical to understanding proper management of these resources. However, in many parts of the world, data is complicated by sparsely distributed and spatially inconsistent monitoring wells, by temporal data gaps, and limitation in access to data by political boundaries. Especially analysis of groundwater variability requires a continuous time series data. For instance, the Lake Chad used to be one of the largest freshwater lakes in Africa. The Lake has been dramatically shrinking to about 1/20 of its original size since the 1960's and its own ecosystem is at risk. The shrinkage of Lake Chad

has been caused by natural and anthropogenic impacts (Fortnam and Oguntola, 2004). Anthropogenic activities such as fisheries, agriculture, animal farming, fuel wood provision, and wetland economic services suffer from the lack of main water resources. As Lake Chad has been used mainly for irrigation purposes, groundwater became the predominant source of potable water supply for domestic livestock consumption. Therefore, the demand on freshwater sources has been increasing for decades, and so groundwater consumption and abstraction rates have been increasing as well.

Besides the political instability of the surrounding countries of Lake Chad (Figure 1.1), there are other challenges and limitations for its data-poor conditions. The majority of the wells in the region are hand-dug, unlined or concrete-lined open wells with a diameter of about 1 m. The wells are mostly located in local villages, therefore wells distribution is clustered and hard to approach and maintain in time. Consequently, there is no continuous monthly groundwater station data available in the region. To overcome such limitations, computational modeling is a necessary step. Specifically, remote sensing offers free access datasets that can help further investigations of groundwater change. Groundwater hydrology is one of the last areas in the study of remote sensing. The most recent approach of remote sensing is to estimate the variations of groundwater by using Gravity Recovery and Climate Experiment (GRACE) data. Due to the limited accessibility to the Basin and lack of ground-truth data, the use of a GRACE-derived model would help understand the change of groundwater over certain periods of time.



Figure 1.1. The Lake Chad Basin and approximate location of Lake Chad.

I present an estimation of groundwater changes using ground truth and remote sensing data techniques for data-rich and data-poor regions. This work presents two case studies of modeling groundwater changes, one in a relatively data-rich region such as the Upper Mississippi Basin in the US and the other in a data-poor region such as the Lake Chad Basin in Africa. Data-rich and data-poor definition separated by data limitation at a regional scale. Data-rich region is considered to have a dense monitoring network of groundwater with periodic monitoring data. For example, the United States Geological Survey (USGS) provides spatially distributed groundwater data that are approved for public release over the past 100 years. The data-poor region is where such monitoring systems are lacking.

In the present study, I compare ground truth and GRACE-based data on the Upper Mississippi Basin to verify the accuracy of GRACE modeling and understand how modeling conditions would affect the model accuracy. After finding the most accurate GRACE modeling setup, I apply the same setup by only using GRACE data to the Ngadda catchment, a sub-basin of the Lake Chad Basin. My goal is to understand the spatial and temporal variability of groundwater near the Lake Chad since there is no ground-based monitoring effort. Consequently, I would be able to answer how the GRACE modeling can help investigate groundwater at the data poor regions. In addition, I discuss the challenges of using ground truth and remote sensing data with their advantages and disadvantages.

1.2 GRACE in General.

GRACE is a twin-satellite mission launched by the National Aeronautics and Space Administration (NASA) and the German Aerospace Center (DLR) in March 17th 2002, to make detailed measurements of Earth's gravity field and investigate Earth's water reservoirs, over land, ice and oceans. In addition, the mission has several partners for design, construction and launch, such as Jet Propulsion Laboratory (JPL), the University of Texas Center for Space Research (CSR), the German Research Centre for Geosciences (GFZ), as well as Astrium GmbH, Space System Loral (SS/L), Onera and Eurocke GmbH.

The basic concept of GRACE is based on gravity and its proportional relationship with earth density. Gravity is a force that pulls two masses together, while density is defined as mass in a given volume. Isaac Newton first discovered the law of gravity, and correlated gravity and density. If the object is denser, its mass increases, then the exerted gravitational force increases as well. The Earth's surface is not uniform as it includes objects with different density, such as mountains, valleys, oceans, and ice caps. Therefore, the density

varies from place to place on the Earth's surface. Consequently, these variations in density make slight variations in the gravitational field. As a result, GRACE is the only mission to detect those changes from space.

In Figure 1.2, the two satellites stay apart at a distance of about 220 km (137 miles), and the orbit altitude is about 500 km (311 miles). These satellites spin around the Earth 16 times a day, and produces global coverage every 30 days (a month) from a single source or position in space. The satellites detect minute variations in the Earth's surface mass below as well as variations in the Earth's gravitational force. When the satellites travel 500 km above the earth in space, the front satellite captures the area with higher gravity; it is slightly pulled toward the area with higher density and speeds up. As soon as the front satellite passed over the area of higher gravity, it slows down, but the trailing satellite speeds up. The distance between two satellites changes again. As the trailing satellite passes the region of higher density it slows down as well which does not affect the front satellite in the same time. These minute expansions and contractions of the distance between satellites are measured using the microwave K-band ranging instrument, thus are able to map the gravitational field of the Earth surface. In any one place of the measurement, the data is exactly positioned from Global Positioning System (GPS) receivers. The main advantage of the GRACE mission is the high-precision of GPS receiver, which helps precisely map Earth's gravity field within 1 micron (or the width of a human hair). Consequently, high-resolution maps allow looking at the Earth's gravitational field from the large scale to finer-scale over both land and sea.

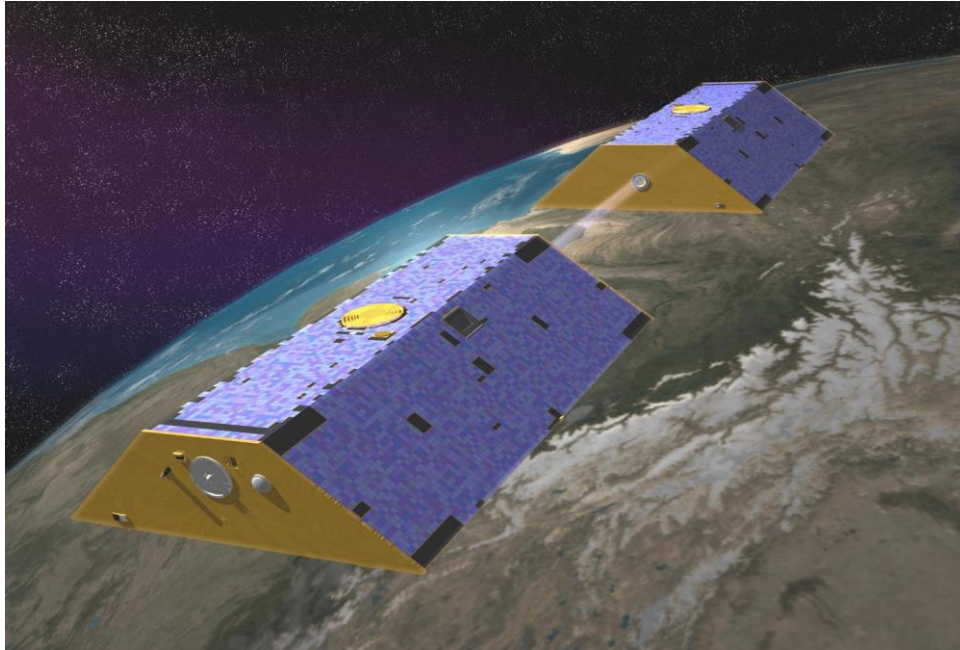


Figure 1.2. The twin GRACE satellites with ranging link between the two crafts (NASA/JPL, 2002).

The hydrologic product from the GRACE is expressed as Total Water Storage (TWS). TWS measures the distribution of mass above and below the Earth's surface. In other words, TWS represents a vertically integrated water storage system including groundwater, soil moisture, surface water, and snow. The GRACE data provides monthly anomalies in TWS on the basis of the Earth's global gravity field measurements (Wahr, et al., 2004).

1.3 Lake Chad Basin

In the last century, many closed lakes and seas all over the world have declined in size or completely dried out due to anthropogenic or natural causes (Thomas, Meybeck and Beim, 1992). The Lake Chad in Figure 1.1 is one of them; it used to be one of the largest endorheic lakes in the world with an area of $25,000 \text{ km}^2$ in 1963. The lake area has declined to less than 2000 km^2 in the 1990's (Grove, 1996). Many studies explain human and natural

impacts on the water resources of the Lake Chad, such as: two severe droughts that occurred in the periods 1972-1974 and 1983-1987 (Kimmage and Adams, 1992); desertification (Intergovernmental Panel on Climate Change (IPCC), 2001); overgrazing (Food and Agriculture Organization (FAO), 2009); irrigation activities (Isiorho and Njock-Libii, 1996); vegetation removal and modification (Keith & Plowers, 1997); deforestation (Neiland and Verinumbe, 1990); along with population increase (UN Population Division, 2002).

Although the Lake Chad shrinkage has been studied broadly, understanding of groundwater variations remains poor in the region due to lack of data and challenges to direct access in the region.

Since Lake Chad is a closed lake, its surface water completely depends on its inflow. The largest sub-system feeding the lake is the Chari-Logone River system (650,000 km^2 basin area) which supplies 95% of total inflow to the lake (FAO, 2009). The Chari River flows from the Central African Republic in the south-southeast from the lake, and reaches the southern pool of the Lake. The second important sub-system is Komadugu-Yobe River (148,000 km^2 basin area) which flows in from northern Nigeria and Niger. Although the river contributes only about 2.5% of the total inflow to the Lake, it is the only persistent river flowing into the northern pool of the Lake.

The Lake Chad Basin was formed during the Cretaceous Period and consists of three major aquifers: the upper, middle, and lower aquifers. Figure 1.3 shows hydrogeological cross section representing the Chad Formation consisting of three major aquifers to show the hydrodynamic linkages with the Lake Chad. The Chad Formation mostly consists of sand and clay. The upper aquifer is located at depths approximately 30 m thick and contained within the Quaternary fine-grained sediments (Edmunds, Fellman and Goni, 2002). The

aquifer is hydrologically connected to the Lake Chad. Groundwater at this aquifer is suitable mainly for domestic use through wells and boreholes (Odada, Oyebande and Oguntola, 2006). While the upper aquifer is unconfined, the middle aquifer is a confined aquifer consisting of fine sands and clays between 450 and 620 m depths from the surface (Kindler, et al. 1990). The water from middle aquifer is mainly used for domestic and livestock use. Finally, lower aquifer is also a confined aquifer consisting mostly of sand and clayey sand deposited in the Cretaceous period. The lower aquifer is hardly explored as the approximate depth to the aquifer is more than 700 meters from the ground surface. The city Maiduguri heavily drilled boreholes in and around the city for water and gas exploration, which provides most of the information about the lithology, geometry and hydrogeology of the aquifers (Bumba, Kida and Bunu, 1985).

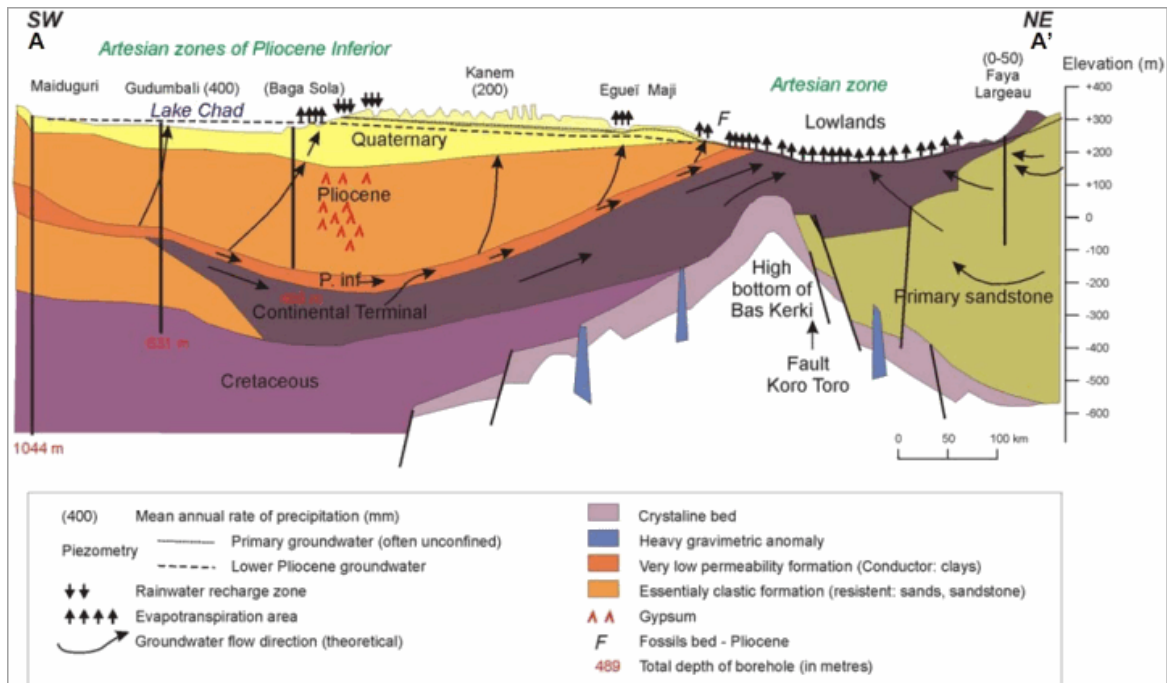


Figure 1.3. Hydrogeological cross section of Lake Chad (Source: Schneider, 1991).

As a case study, the present study focuses on the Ngadda River system (14,400 km^2 catchment area) as shown in Figure 1.4. The area of study is about 48,633 km^2 . The climate is semiarid with a long dry season and a short rainy season lasting generally between May and September. The main city in the area is Maiduguri with a population of 1,197,497 by 2009. The Ngadda River system originates in the Mandara Hills (Northern Cameroon) and passes through the city of Maiduguri before entering the lake. There is an 80 km^2 swamp further downstream of the Ngadda Catchment (Nigeria side) which is formed from where the river does not provide a consistent water supply to the Lake (FAO 1997). However, the Ngadda River makes a very negligible contribution to the Lake's inflow in the wet season since it loses most of its water in a 7 km wide flood plain and swamps in its northwestern flow. In addition, the system includes the Alau Dam (162 million m^3 reservoir), which is located in the southeast of Maiduguri. After its construction, the Alau reservoir had never filled to its expected level (Olofin, 1997).

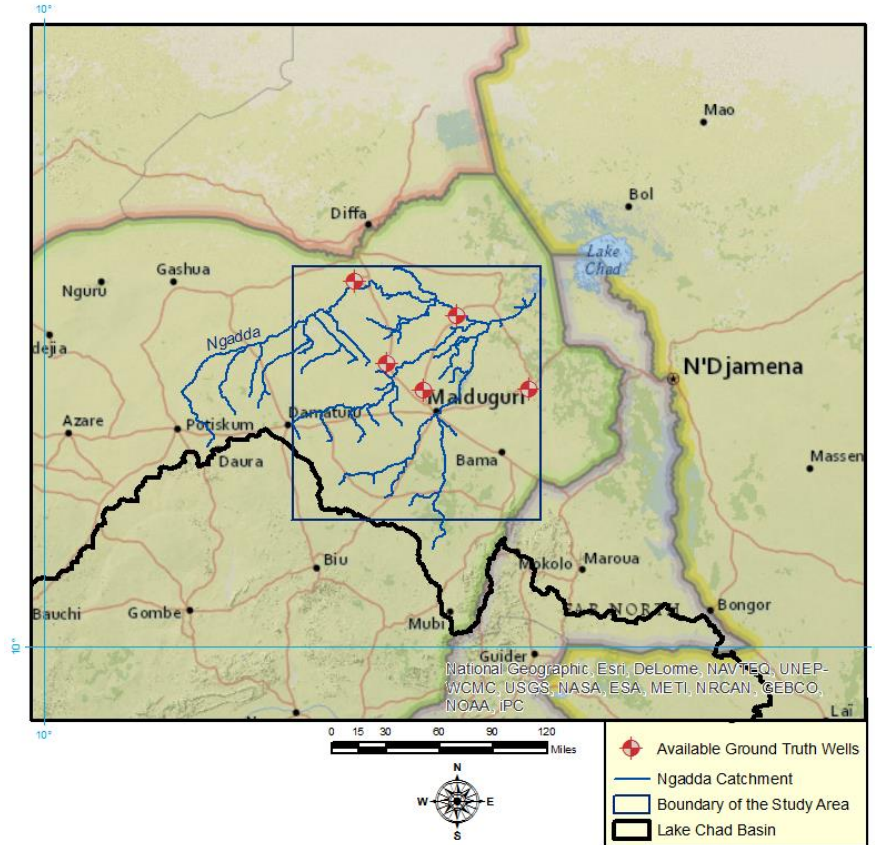


Figure 1.4. Sampling area and boundaries of the study area.

1.4 Objectives

The main purpose of the research is to investigate monthly groundwater variations near Lake Chad by using remotely sensed GRACE data and ground-truth groundwater data. The goal of this research is to determine whether GRACE data is capable of analyzing a groundwater change in data-poor regions as much as in data-rich regions, and to determine how results vary from the ground-truth measurements. This approach would help fill the data gap in Lake Chad area as a data-poor region.

The period of time was chosen from November 2005 to July 2009. In addition, multiple geostatistical methods were applied, including Kriging interpolation and Thiessen polygons, in order to analyze the spatiotemporal changes in groundwater over 2005-2009.

In order to assure that GRACE data is applicable to the analysis of groundwater changes and compare it with ground-truth data, the GRACE modelling was applied to the Upper Mississippi Basin as an example of a data rich region. After the verification of a successful modeling approach, the technique was employed to Lake Chad as a data poor region. The specific objectives of the research are as follows:

- To evaluate applicability and accuracy of GRACE satellite data for monitoring of groundwater in a data-poor region,
- To investigate the effects of physical parameters and model parameters in the GRACE modeling for data rich and data poor regions,
- To understand advantages and disadvantages of GRACE modeling for groundwater monitoring in the Lake Chad Basin as a data poor region.

CHAPTER 2

LITERATURE REVIEW

2.1 Groundwater and Remote Sensing Studies for the Lake Chad Basin

Groundwater in the Lake Chad Basin is the predominant source of potable water supply for domestic livestock consumption while surface water of the Lake Chad is used mainly for irrigation purposes. Overall, water balance assumes that decrease in rainfall amount causes decreasing in surface runoff and stream discharge equally well. As a consequence, groundwater levels have had moderate declines due to a decrease in aquifer recharge and the increased sinking of boreholes (Fortnam and Oguntola, 2004). Some specific groundwater reserves decreased due to overexploitation. For instance, Isiorho, Oguntola and Olojoba (2000) confirmed groundwater drawdowns of several tens of meters in the Maiduguri area of Nigeria due to groundwater overexploitation. Isiorho et al. (2000) stated that about 537 wash boreholes were drilled between 1985 and 1989 after droughts of the 1980s. The quality of the drilling work was unsatisfactory since the contractors did not use hydro-geological data when locating wells. Additionally, local people leave them uncapped for their own use. As a result, most of these boreholes are opened and free flowing. Consequently, this free flow is inefficient and results loss of a great amounts of water with high evaporation rates in the region (Isiohro, et al., 2000).

On the other hand, some catchment areas showed an increase in runoff and discharge, and following increase of groundwater. For example, Niger River and the Nakambe River in the West Africa had increasing discharge and runoff over a severe drought period between 1968 and 1995 (Descroix, et al., 2009). During the same drought period, there was an increase of groundwater at Niamey in Niger. Albergel (1987) called this phenomena as a

‘Sahelian Paradox’ which might happen as a result of deforestation by irrigation, biomass burning, and soil compaction. Favreau et al. (2002) discovered a rise of groundwater near the Niger River as a result of increased runoff and recharge through topographic depression zones. Luxereau, Genthon and Karimou (2012) found out that the discharge was almost constant in the last five decades at Diffa in the downstream of the Yobe River in spite of a rainfall decline. Therefore, another assumption is that when runoff increases, discharge into the River increases as well due to deforestation or cultivation since the 1950s (Mahe’ and Paturel, 2009; Luxereau, et al., 2012).

The Quaternary aquifer of the Lake Chad has large natural piezometric depressions, which are found in the southeast of Niger, central Chad, and northeastern Nigeria (Leblanc, et al., 2007). Schneider (1966) and Lake Chad Basin Commission (LCBC) (1969) first reported the piezometric depressions, but the origins of the depressions are not yet well understood. The piezometric depressions might occur due to recharge changes, aquifer characteristics, land cover and vegetation changes, interactions with surface water, and overexploitation. Arad and Kafri (1975) made a hypothesis of a perched “hollow” aquifer existence. They believed that a perched aquifer consists of discontinuous semi-pervious aquicludes, which provides a form of a hydrological sink with its separation. However, this theory has not been proved due to lack of subsurface information. The area of the present study includes one of those depressions named as Bornu piezometric depression. It is certainly important to understand the behavior of the piezometric depression and the sensitivity of the aquifer to related climate changes, but the investigation is challenged due to lack of data.

Remote sensing and satellite data have been widely applied to the Lake Chad region to find the causes of the lake shrinkage. Most of these hydrologic studies focus on the changes of the Lake (Leblanc, et al., 2003; Schuster, et al., 2005; Cretaux and Birkett, 2006; Leblanc, et al., 2007), and changes in stream flow pattern connected to the Lake (Coe and Foley, 2001; Li, et al., 2007, 2012; Le Coz, et al., 2009). Coe and Foley (2001) used an integrated biospheric model (IBIS) and a hydrological model (HYDRA) to simulate the changes in lake level, lake area and stream discharge along the Chari-Logone River. However, remote sensing applications for groundwater modeling has not been fully defined yet. Most studies were based on estimation of groundwater recharge by using geochemical isotope analysis (Goni, Fellman and Edmunds, 2001; Favreau, et al., 2002; Edmunds, et al., 2002) or a soil water balance model in the near surface (Rushton, Eilers and Carter, 2006; Eilers, Carter and Rushton, 2007). For instance, Edmunds, et al. (2002) estimated groundwater recharge using the chloride mass-balance method from collected moisture samples of unsaturated zone in the northern Nigeria of the Lake Chad.

Just few studies used remote sensing data for investigating groundwater recharge, but nobody has tried to define time series data of groundwater depending on the nature and fluctuations of groundwater in space and time.

Leblanc et al. (2003, 2007) used satellite images (Meteosat thermal data) combined with hydrogeological data to identify the thermal change of groundwater in the depression zones, and then estimate values of recharge and discharge of the area. Boronina and Ramillien (2008) calculated actual evapotranspiration and the maximum and the mean annual recharge over the Lake Chad basin using AVHRR (The Advanced Very High Resolution Radiometer) imagery and GRACE measurements. The calculated evapotranspiration was

compared to the evapotranspiration estimates derived from the GRACE solutions. LeCoz, et al. (2009) simulated the water balance of the Lake Chad basin using SRTM (the Shuttle Radar Topography Mission) with six algorithms (mean, median, mode, nearest neighbor, maximum and minimum).

2.2 GRACE Modeling Studies for Groundwater

GRACE modeling in water resources is an emerging field in hydrology. Since GRACE is able to produce a precise model of the geoid and gravitational field, its practical usage finds various applications in hydrology, oceanography, geology, understanding climate change and related disciplines, and is used for a variety of applications including:

- measuring water fluctuations on and beneath Earth's surface;
- measuring sea level changes;
- detecting ocean currents near the surface and far beneath the waves;
- understanding the structure changes of the solid Earth.

The application of GRACE modeling in hydrological mass redistribution over Earth's surface has been well performed by Schmidt, et al. (2006, 2008), Swenson, et al. (2006, 2008), Wang, et al., (2011), Scanlon, Lonquevergne and Long (2012). The monthly-derived GRACE data was applied globally in defining the dominating seasonal components of the continental water cycle. In other studies, GRACE data has been extended to the definition of individual hydrological components from the integral GRACE signals such as the estimates of groundwater variations, snow cover variations or the evapotranspiration. Strassberg, et al. (2009) proved that the GRACE-derived modeling is capable of addressing the observational gap in monitoring groundwater storage changes over the observed basin.

Zaitchik, Rodell and Reichle (2008) states that monthly water storage anomalies must be varied horizontally and vertically for a better understanding of the full potential application of GRACE for hydrology. Looking at GRACE TWS anomalies and its individual components would greatly improve their scientific value for hydrological research and applications. Currently, GRACE is the only remote sensing data capable of detecting changes in TWS at any depth, under any conditions.

One of the approaches that has been performed by the vertical disaggregation of GRACE data is to assimilate anomalies of TWS into the NASA Catchment land surface model (LSM), applied in western and central Europe, (Koster, et al., 2000). Originally, the LSM model was developed for global scale and coupled land and atmosphere modeling. There were some improvements in stream flow estimates, but groundwater was not validated directly due to the lack of in situ measurements. With the Catchment LSM, GRACE data assimilation had a large influence on the detection of groundwater change and its seasonality in several basins.

GRACE has no vertical resolution. In cases, where it is necessary to determine one individual component of water storage anomalies, TWS must be disaggregated horizontally, vertically, and temporally. Rodell, et al. (2007) computed and averaged groundwater storage variations over the Mississippi River basin and its four major sub-basins by using soil moisture and snow water equivalent components from the Global Land Data Assimilation System (GLDAS). It was used to estimate and remove groundwater storage components from GRACE TWS, assuming vegetation and surface water contributions to be negligible. This is a simple approach for estimating groundwater storage variability on medium scale regions and large aquifer systems, but it has not been applied to finer scale data-poor regions. The

GRACE modeling could be a feasible alternative to fill the data gap and analyze groundwater changes in a data-poor region such as the Lake Chad Basin.

CHAPTER 3

METHODOLOGY

3.1 Basic Theory of GRACE

Wolf (1969) presented the first realization of the satellite-to-satellite tracking concept in the low-low mode. The basics of this concept was to trace the spatio-temporal gravity field with an increased sensitivity by means of micrometer-precise inter-satellite observation of two co-planar orbiting satellites. Onboard GPS receivers determine the position of each spacecraft in a geocentric reference frame, while onboard accelerometers detect the non-gravitational acceleration. As soon as the residuals infer the gravitational acceleration, the gravity field is mapped. The desired inter-satellite distance should be smaller than the altitude; otherwise data will be lost or distorted. Also, since satellites are in such low orbit, the gravity field determines orders of magnitude more accurately. Relative motion between satellites is proportional to the integrated differences of the gravity accelerations at its individual position. The differences are correlated with conservative (gravitational force, elastic spring force, electric force) and non-conservative forces (tension, air resistance, normal force).

The dynamic approach for the recovery of global gravity models is based on Newtonian formulation of the satellites' equation of motion. Isaak Newton expressed the interaction force between two masses by the Universal Law of Gravitation:

$$F = G \frac{M \times m}{R^2} \quad (1)$$

where F [N] is the gravitational force,

M and m [kg] are two masses,

R [m] is the distance between two masses,

G is the Gravitational constant, $G = 6.673 \times 10^{-11} \text{ Nm}^2/\text{kg}^2$.

The second law of Newton's Law of Motion states that a force (F) is equal to the change in momentum per change in time:

$$F = m \times g \quad (2)$$

where m is the mass of the object,

g is the gravity acceleration.

By combining both equations (1) and (2):

$$g = \frac{G \times M}{R^2} \quad (3)$$

The Earth's gravity varies with space and time. Spatial gravity variations might be caused by latitude, altitude, and the geological settings. Temporal gravity signal is a combination of different gravity variation sources, such as tide effects, effects from polar motion, atmospheric effects, the effect of water mass variations, and other factors (Schrama, Wouters and Lavallee, 2007).

Before this idea with low-altitude satellites, there were only high-altitude satellites, which provided useful information only at relatively long wavelengths (Tapley, et al., 2004). The advantage of the low-altitude satellites is the degradation of the gravity inversions at all wavelengths due to considerably larger non-gravitational forces, primarily from the atmosphere.

GRACE is a twin-satellite mission, launched by National Aeronautics and Space Administration (NASA) and German Center for Air and Space Flight (Deutsches Zentrum für Luft und Raumfahrt, or DLR) on March 16, 2002. GRACE is able to track how water is transported and stored within the Earth's environment by its variation in gravity field. The mission measures the changes in the speed and distance between two identical spacecraft

named GRACE-A and GRACE-B in a polar orbit about 220 kilometers apart and altitude of 500 kilometers.

There are three levels GRACE data produce:

1. Level 1 (Level-1A): the raw data to be calibrated and time-tagged in a non-destructive sense. Level-1A data products are not distributed to public.
2. Level 2 (Level-1B): the processed products to generate the monthly gravity field estimates in form of spherical harmonic coefficients.
3. Level 3: the processed data for users who are not familiar with the concept of spherical harmonics and prefer to access GRACE data products as mass anomalies (Sources: GRACE Tellus and ICEGM).

The present study adopted the Level 3 data for monthly changes in terrestrial water storage (TWS) on the basis of the Earth's global gravity field measurements (Wahr, et al., 2004). TWS represents a vertically integrated water storage including groundwater, soil moisture, surface water, snow, and biomass (Strassberg, et al., 2009). To estimate the monthly groundwater storage variations using GRACE, we adopted a water storage anomalies equation (Scanlon, et al., 2012):

$$\Delta TWS = \Delta GW + \Delta SM + \Delta SW + \Delta SWE, \quad (4)$$

where ΔTWS is the terrestrial water storage anomalies, ΔGW is the groundwater (GW) storage anomalies, ΔSM is the soil moisture (SM) anomalies, ΔSW is the surface water (SW) anomalies, and ΔSWE is the snow water equivalent (SWE) anomalies. If we assume ΔSW is negligible for the area where no surface water body exists, the ΔGW is defined as:

$$\Delta GW = \Delta TWS - (\Delta SM + \Delta SWE), \quad (5)$$

ΔTWS calculates as a difference between the TWS and its mean:

$$\Delta TWS_{i,j,k} = TWS_{i,j,k} - \sum_{k=1}^n TWS_{i,j,k}/n \quad (6)$$

Similarly, ΔSM calculates as a difference between the SM and its mean:

$$\Delta SM_{i,j,k} = SM_{i,j,k} - \sum_{k=1}^n SM_{i,j,k}/n \quad (7)$$

Figure 3.1 is a flowchart to estimate the groundwater storage anomalies. TWS data comes from GRACE Level 3, while SM data is obtained from GLDAS. Initially, we have TWS from GRACE and SM from GLDAS as an input files. After applying equations (6) and (7), we define ΔTWS and ΔSM storage anomalies which then applied in equation (5) to find out ΔGW storage anomalies. Ground truth data from well observations is processed using a Thiessen Polygon technique to define ΔGW . Then, remote sensed ΔGW and the field surveyed ΔGW are compared to verify the accuracy of the GRACE modeling.

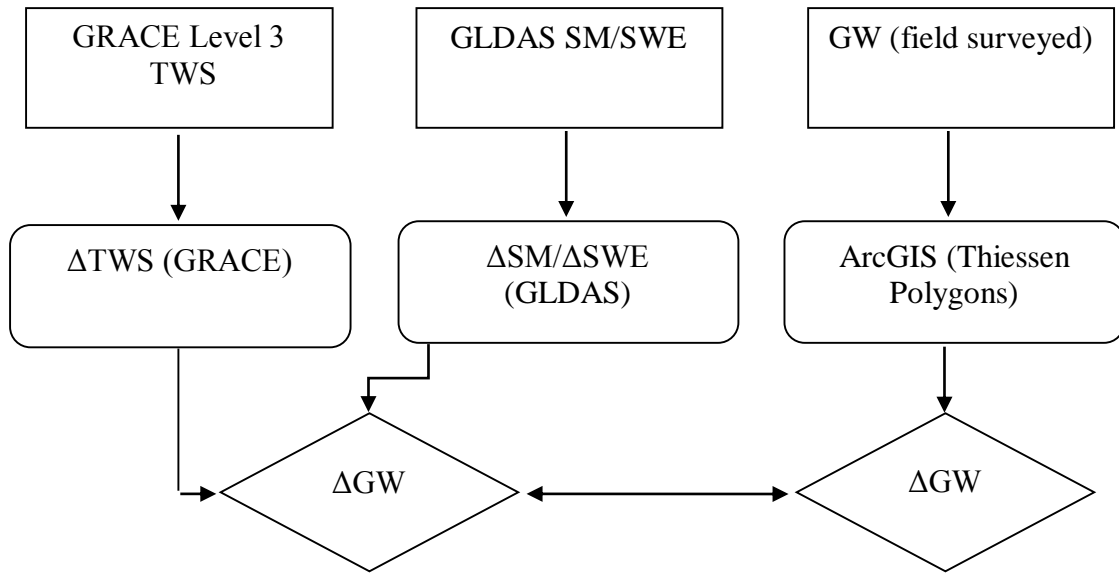


Figure 3.1. A flowchart to estimate the groundwater storage anomalies.

3.2 GLDAS in General

Global Land Data Assimilation System (GLDAS) provides optimal estimates of land surface fluxes and storages of water and energy using satellite and ground-based data.

GLDAS derives land surface state (soil moisture, surface temperature), and flux (evaporation, sensible heat flux) parameters. As a land surface component of the hydrological cycle, soil moisture is the most critical to link the atmospheric and climate processes to the terrestrial water processes.

GLDAS consists of two versions, GLDAS Version 1 (GLDAS-1) and GLDAS Version 2 (GLDAS-2). GLDAS-1 includes high quality observational precipitation and solar radiation input datasets for the period 1979 to present. Specifically, GLDAS-1 is a combination of NOAA/GDAS fields, NOAA Climate Prediction Center Merged Analysis of Precipitation (CMAP) (Xie and Arkin, 1997), and the Air Force Weather Agency (AFWA). In comparison, GLDAS-2 uses reanalyzed meteorological input datasets that have been corrected using ground-based products for the period 1948-2010. Consequently, GLDAS-2 is more applicable for a long-term analysis that requires consistency over a long period of time. In the present study we used GLDAS-1 since we were interested in the recent period, roughly 2002 to present, and the data is updated to within 1-2 months of time.

Currently, GLDAS runs four land surface models (LSMs):

1. The Common Land Model (CLM) is the land model for the Community Earth System Model (CESM) and Community Atmosphere Model (CAM). It is a collaborative project between scientists in the Terrestrial Science Section (TSS) and the Climate and Global Dynamics Division (CGD) at the National Center for Atmospheric Research (NCAR) and the CESM Land Surface Model (LSM) Working Group. CLM can be run as a stand-alone one-dimensional model in a coupled and uncoupled to the atmosphere (offline) mode. The soil model is divided into 10 horizontal layers (Table 1). Thus, CLM model has more dynamic

soil moisture with a smaller depth range, which tends to produce higher runoff and lower evapotranspiration under wet conditions (Zaitchik, Rodell and Olivera, 2010).

2. The National Centers for Environmental Prediction (NCEP)/Oregon State University/Air Force/Hydrologic Research Lab Model (Noah) was developed by a collaboration of public and private institutions with the leadership of the NCEP. Like CLM, Noah is a stand-alone, uncoupled and coupled one-dimensional model. Noah simulates soil temperature and moisture (both liquid and frozen) for all soil layers (four in this model), snowpack depth, snowpack water equivalent (one layer model), canopy water content, and the energy flux and water flux of the surface energy and water balance.

3. The Mosaic model originally was developed for the NASA global climate change. Like CLM and Noah, Mosaic is a stand-alone, one-dimensional model that can be run both uncoupled and coupled to the atmospheric models. The model is based on one of the simple biosphere model with its physics and surface flux calculations. The Mosaic model consists of three soil layers and a simple one layer snow model.

4. The Variable Infiltration Capacity (VIC) Model was developed, maintained and upgraded by the University of Washington. Unlike the other three models, VIC is an uncoupled, calibrated hydrology model, but can be adjusted as a coupled with climate models. Currently, VIC is running only in a water balance mode, and applied at the continental and global scales. Therefore, this model is not considered in this study.

The present study considers only two water balance parameters of GLDAS-1 version: average layer soil moisture and snow water equivalent from CLM, Noah, and Mosaic LSMs respectively. The average layer soil moisture is the depth-averaged amount of water in a specific soil layer beneath the surface. The soil moisture content can be measured by

Gravimetric Soil Moisture (GSM) or by Volumetric Soil Moisture (VSM). By GSM, soil moisture content is the mass of water compared to the mass of solid materials per unit volume of soil. By VSM, it is the volume of water per unit volume of soil where the mass of water determined per unit volume of soil (kg/m^2). Table 3.1 describes the specific number of vertical layers for soil moisture in different LSMs.

Table 3.1. Vertical layering structure of three LSM models.

GLDAS LSMs (no scale; vertical layers in m)		
CLM (10 layers)	Noah (4 layers)	Mosaic (3 layers)
0-0.018	0-0.1	0-0.02
0.045		
0.091		
0.166	0.4	1.50
0.289		
0.493		
0.829	1.0	3.50
1.383		
2.296	2.0	
3.433		

3.3 Implementation

As shown in Table 3.2, TWS and SM have different spatial resolution and data format. TWS is available only as a 1° monthly data, but SM has 1° and 0.25° monthly data. The units of the original files for TWS and SM are different as well. SM is measured in mm,

which should be converted to cm to make it consistent with the unit of TWS. Therefore, the GRACE modeling outputs are presented in cm as well.

Table 3.2. TWS and SM data description.

Component	Source	Data description	Units	File Format
TWS	GRACE Tellus	1° monthly data	cm	ASCII
SM	GLDAS	1° and 0.25° monthly data	kg/m ² or mm	NetCDF

3.3.1 Implementation of GRACE

GRACE level 3 product is based on the RL05 spherical harmonics version from JPL, which can be downloaded from the GRACE Tellus website gracetellus.jpl.nasa.gov. As mentioned before this Level 3 product is spatially smoothed during the data processing for Level 3. The sampling of all cells is 1° in both latitude and longitude which is approximately 111 km near the Equator. The downloadable GRACE Level 3 product is formatted for 360 longitudes (0.5,1.5,2.5,...,359.5), and 180 latitudes (-89.5,-88.5,...,-0.5,+0.5,...,+89.5). The time period for the present study is from January 2003 to July 2005 for the Upper Mississippi Basin and from January 2005 to November 2009 for the Ngadda catchment in the Lake Chad Basin.

In applying GRACE data to the GW estimation, small scale surface tends to be attenuated due to the sampling and post-processing of GRACE observations (Landerer and Swenson, 2012). To overcome the attenuation problem, the user should multiply the GRACE Level 3 data by a set of scaling coefficients provided in the scaling grid file from the GRACE Tellus website. The time series at one grid (1° bin) location must be multiplied by the scaling factor at the same 1° bin position. The ascii file with gain factors is

CLM4.SCALE_FACTOR.DS.G300KM.asc stored in the ascii directory of GRACE Tellus website.

After scaling GRACE input data, we created a Python program to estimate the GW anomalies. The program is coded in Python 2.7 version. The full program code is available in Appendix A.

Below is a procedure for the GW calculations:

Step 1. Create a separate folder for monthly GRACE data files in a Python directory.

Step 2. Set the boundaries of the study area in GRACE files. One month GRACE file consists of 1 degree grid resolution file (360 x 180 degrees) for the entire globe. To specify exact boundaries of the interested area, we need to open GRACE ascii file in ArcGIS and overlap it with a map of the basin boundaries. Using the 'Identify' tool in ArcGIS, we define the GRACE values over the basin. Then, we open the GRACE file in Microsoft Excel and define the boundaries of the area by known values. Then, in the program code, we isolate the rows and columns of the data of interest.

Step 3. Create a basin area mask. If the area of interest is a rectangular shape, completing Step 2 would be enough. For example, the Ngadda catchment in the present study is 2°x2° rectangular area. Therefore, using Step 2 we identify the boundaries of the study area, and isolate it in the Python program. However, the boundary of the entire Upper Mississippi Basin is located in the 11°x11° area with irregular shape of the basin. In Figure 3.2, the red cells are the Upper Mississippi Basin cells. In this case, we have to eliminate the cells that do not fall into the basin by using a mask file. In the program, we set the cells we need as 'True', and the cells we do not need as 'False' as a logical variable.

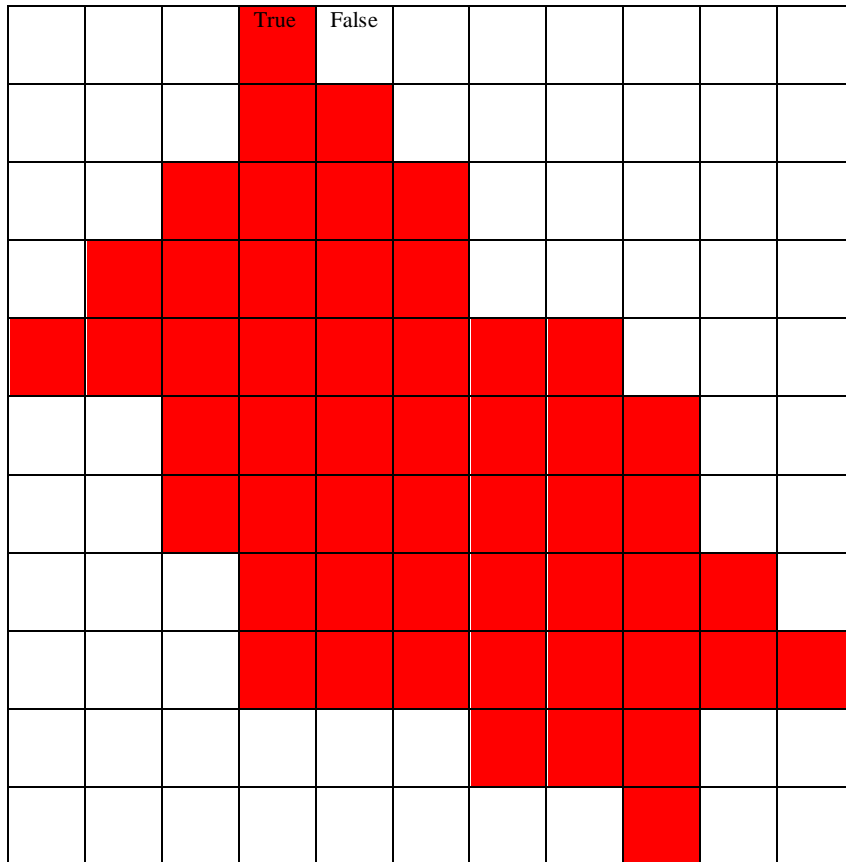


Figure 3.2. The example case of the Upper Mississippi Basin boundary.

Step 4. Remove the time average from the monthly anomalies. Each monthly GRACE Level 3 grid value represents the surface mass deviation for that month relative to the baseline average over January 2004 to December 2009. The period of time we use is different. In that case, it is critical to have anomalies relative to the same time-average. For instance, the period of time considered for the Upper Mississippi Basin is from January 2003 to July 2005. We average the GRACE Level 3 grid values over 01/2003 to 07/2005, and subtract this time average from all other monthly grid values. Basically, we apply equation (6) into the program. To calculate the total mean in Python we use the numpy module at the beginning of the program (Appendix A). To find the total average of all monthly GRACE grids, we used the average function from the numpy module.

3.3.2 Implementation of GLDAS

GLDAS can be downloaded from the GES GISC website

<http://disc.sci.gsfc.nasa.gov/hydrology/data-holdings>. The data was downloaded using search for data with Mirador database. Mirador is an earth science data search tool developed at the GES DIS. This database allows selection of the area by latitude and longitude, so we do not have to download an entire world map as we do in the acquisition of the GRACE data. All three LSMs with 1° and 0.25° resolution are available on the website. The period of time is the same as in the GRACE.

The implementation of the GLDAS data into the GW calculations is:

Step 1. Create a separate folder for monthly GLDAS data files in a Python directory.

Step 2. GLDAS data has NetCDF format. NetCDF is a file format for storing multidimensional scientific data (variables) such as temperature, pressure, wind speed, etc. In our case, we downloaded NetCDF files with two parameters: soil moisture and snow water equivalent (for the Upper Mississippi Basin). The NetCDF file can be opened in ArcGIS and verified the values using the ‘Identify’ tool in ArcGIS. GLDAS data does not require setting up basin boundaries since this procedure was performed during downloading.

Step 3. Average the GLDAS values over the target period of time, and subtract this average value from all other monthly grid values. Basically, we apply equation (7) into the program. If we use all three LSMs, we need to find an average of each model value.

Step 4. Convert GLDAS data from mm to cm by dividing by 10.

Step 5. Downscaling the GW. When we consider the Ngadda catchment, we apply a downscaling method to the rectangular area of interest. First, we estimate GW using 1° GRACE and 1° GLDAS data. Secondly, we estimate GW using 1° GRACE and 0.25°

GLDAS data. Figure 3.3 shows the illustration of the downscaling method. The smaller scale of the region, the more precise results are desired.

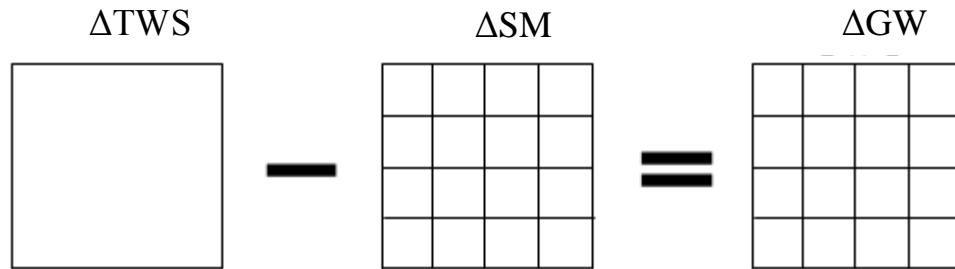


Figure 3.3. Downscaling of ΔGW using 1° GRACE and 0.25° GLDAS data.

3.3.3 Groundwater Anomalies from the Ground-Truth Data

Thiessen polygons method was adopted to estimate ΔGW anomalies from ground truth data. Thiessen polygons are Voronoi cells constructed from a set of points with known values. Set of points is a set of observed monitoring wells over the area. Each monitoring well has a groundwater level value. The goal of applying Thiessen polygons is to find the average groundwater level for each study area. The groundwater anomaly calculation for the ground-truth data using Thiessen polygons is performed in ArcGIS 10.1 with the following steps:

Step 1. Construct Thiessen polygons from each well using Analysis tools > Proximity > Create Thiessen Polygons. Once created, each value of monitoring well is now distributed throughout the N-polygon.

Step 2. Using Analysis tools > Overlay > Intersect, intersect Basin and Thiessen polygons to create new polygons within Basin boundary.

Step 3. Calculate the area of each polygon by creating a new field in the attribute table of groundwater file. Right click on groundwater shapefile > Open Attribute Table. In

the Table Options select Add Field. In the Add Field window Name the field; Type select Double > OK. When the new field is added to the attribute table, right click the new field > Calculate Geometry. Before calculating geometry, verify that the right coordinate system and display units are chosen.

Step 4. Calculate a percent area for each polygon that represents a portion of the entire basin. We need to create a new field to calculate this proportion > Field Calculator from the right click on the new field. The percent area can be defined as:

Percent Area = Intersecting Thiessen Polygon Area / Total Area of a basin.

Step 5. Create a new field and multiply the percent for each Thiessen polygon by groundwater level value for the polygon it spatially corresponds with. This gives the weighted groundwater level for each polygon.

Step 6. Sum all the values generated in the previous step to find the weighted average groundwater level over the basin using Thiessen polygons.

3.4 Statistical Analysis

In this work, trend and linear regression analysis performed to discuss the results. Trend analysis method of time series data involves comparison of monthly groundwater storage anomalies from satellite and field measurements over the long period of time to detect general pattern of a relationship between groundwater storage variables. Linear regression calculates an equation that minimizes the distance between the fitted line and all of data points. In general, a model fits the data well if the difference between the observed values and the model's predicted values are small and unbiased. Linear regression analysis consists of linear correlation coefficient and coefficient of determination.

The linear correlation coefficient (r) is a measure of the degree of linear relationship between two variables. The value of r varies $-1 \leq r \leq +1$. The r value of exactly $+1$ indicates a perfect positive fit. Positive correlation means that as the value of one variable increases, the value of the other variable increases, as one decreases the other decreases. The r value of exactly -1 indicates a perfect negative fit. Negative correlation means that as one variable increases, the other decreases, and vice versa. The value of r close to zero means that there is a random, nonlinear relationship between two variables. A correlation greater than 0.8 is generally describes as strong, whereas a correlation less than 0.5 is generally described as weak.

The coefficient of determination or R-squared value (r^2) is a statistical measure of how close the data are to the fitted regression line. If the regression line passes through every point on the scatter plot, it would be able to explain all of the variation. The farther the line is away from the points, the less it is able to explain. R-squared value varies $0 \leq r^2 \leq 1$ or between 0 and 100% , and represents the percent of the data that is the closest to the line of best fit. 0% indicates that the model explains none of the variability of the response data around its mean. 100% indicates that the model explains all the variability of the response data around its mean. However, in some applications low R-squared value indicates a good model, or a high R-squared value indicates a model that does not fit the data well. Therefore, R-squared values should be always evaluated in conjunction with residual plots and correlation coefficient where r is the square root of r^2 .

The Root Mean Square (RMS) deviation is a measure of the difference between values predicted by a model and the values actually observed from the environment that is being

modelled. The difference between values occur due to randomness or inaccurate estimation.

The RMS of a model prediction is defined as the square root of the mean squared error:

$$RMS = \sqrt{\frac{\sum_{i=1}^n (X_{obs,i} - X_{model,i})^2}{n}} \quad (8)$$

where X_{obs} is observed values

X_{model} is modelled values at time/place i .

Standard Deviation (STD) provides an understanding of how much variation there is from mean. In other words, the standard deviation measures how concentrated the data are around the mean; the more concentrated, the smaller the standard deviation. A large standard deviation indicated that data values are far from the mean.

CHAPTER 4

RESULTS AND DISCUSSION

4.1 Data-rich Region: Upper Mississippi Basin

The data-rich region is represented by the Upper Mississippi Basin, one of the four major sub-basins of the Mississippi River Basin, which stretches from northwest to southeast of the Upper Midwest of the United States (Figure 4.1). The Upper Mississippi Basin drains approximately 491,756km², including a large area of the states of Illinois, Iowa, Minnesota, Missouri, and Wisconsin. Small portions of Indiana, Michigan, and South Dakota are also within the basin.

Natural and human factors affect surface and groundwater hydrology over the Mississippi River Basin as well as its quality, aquatic life in rivers and streams (Stark, et al., 1999). Besides GRACE satellite-based data, investigation of groundwater changes over the Upper Mississippi Basin is possible using ground truth data from the USGS Groundwater Watch Data. The USGS maintains the network of groundwater wells with daily, monthly, or seasonal observations to monitor the effects of droughts and other climate variability on groundwater levels. Monitoring groundwater level changes over the Upper Mississippi Basin is a good case study to find capability of GRACE modeling since there is enough time-series data. However, many of the groundwater well records have missing daily or monthly values. To overcome such a limitation, continuous time series for each monitoring station was first generated using linear interpolation.

Therefore, the methodology of GRACE modeling was applied to the Upper Mississippi Basin for verification of GRACE efficiency. In the present study, I used a case study of Rodell, et al. (2007). They estimated groundwater storage anomalies from GRACE water storage data

and average GLDAS soil moisture and snow data for the entire Mississippi River Basin ($3,247,804 \text{ km}^2$), and its separate four sub-basins: the Missouri ($1,323,998 \text{ km}^2$), Arkansas-Red-White-Lower Mississippi ($903,918 \text{ km}^2$), Ohio-Tennessee ($528,132 \text{ km}^2$), and Upper Mississippi ($491,756 \text{ km}^2$) using equation (5). Figures 4.2 and 4.3 show the inputs to equation (5) for the Upper Mississippi Basin from Rodell et al. (2007) and this thesis work. TWS from GRACE and the average SM and SWE from the three GLDAS land surface models are anomalies or deviations from the time series mean. The effect of SWE to terrestrial water storage is almost negligible compared to that of soil moisture.

Then, they evaluated results using groundwater level of 58 well observations in the unconfined or semi-confined aquifer evenly distributed over the Upper Mississippi basin. Groundwater levels were converted to regional average groundwater storage variations. Specific yield estimates were determined over the basin from USGS available metadata and reports. The Rodell's work considers specific yield value depending on the sub-basin to be in the range from 0.02 to 0.32, and its mean of 0.14. I considered specific yield depending only on the Upper Mississippi Basin as its mean value 0.14. Thiessen polygons were then created from a set of groundwater levels over the basin to find average groundwater anomalies for each basin. Figure 4.4 represents the groundwater storage estimated from GRACE-GLDAS, and monitoring well observations. Rodell, et al. (2007) found out that groundwater anomalies estimates for smaller sub-basins have larger seasonal amplitudes which makes results poorer in comparison with larger sub-basins since there is little similarity with monitoring well observation based results. Rodell and Famiglietti (1999) confirmed that the minimum region area in which GRACE can resolve water mass changes should be no less than $500,000 \text{ km}^2$. Based on the results for the Mississippi River basin and its four sub-basins, they confirmed

that the approach is appropriate for larger regions with about $900,000 \text{ km}^2$. However, in this case it should be considered that GRACE and GLDAS data are updated versions with better usage of data filtering and smoothing techniques since 2007. Also, investigation shows more limitations such as that mostly groundwater storage outcomes affected by soil moisture models, individual fluctuation in the monitoring well, and matter of the aquifer. In the present study, these three cases were investigated for the Upper Mississippi Basin.



Figure 4.1. The Upper Mississippi Basin boundaries.

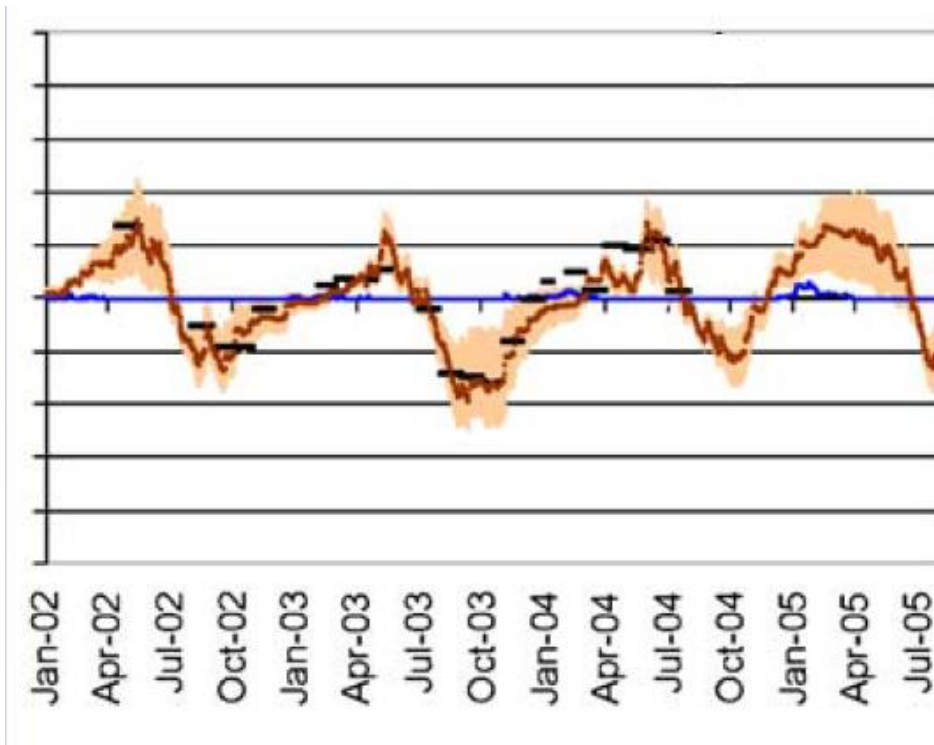


Figure 4.2. The Upper Mississippi Basin inputs: GRACE derived TWS (black bars), and the averaged three land surface models of SM (brown dots) and SWE (blue line). The tan shaded area is the range of the modeled soil moisture values (Rodell, et al., 2007).

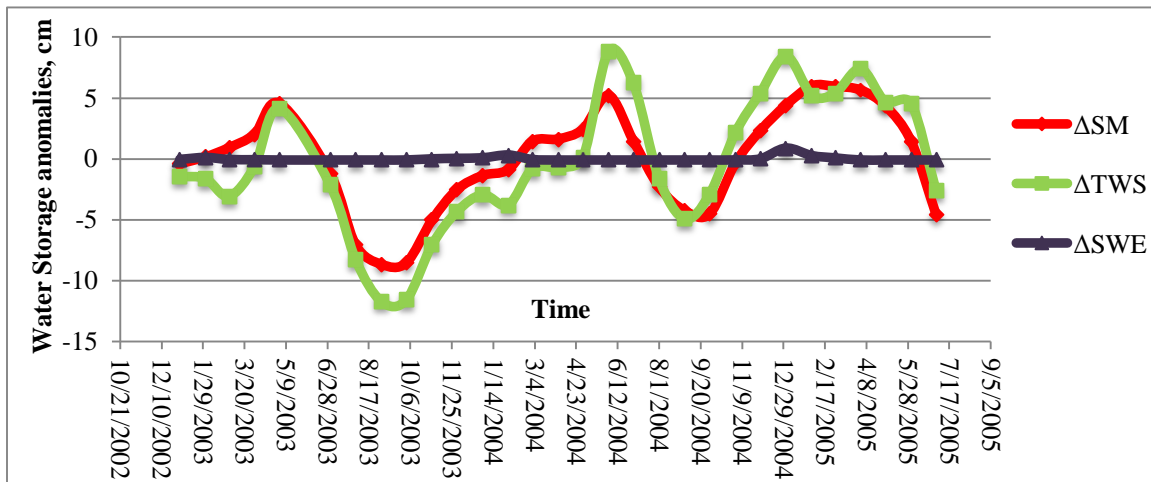


Figure 4.3. The Upper Mississippi Basin inputs.

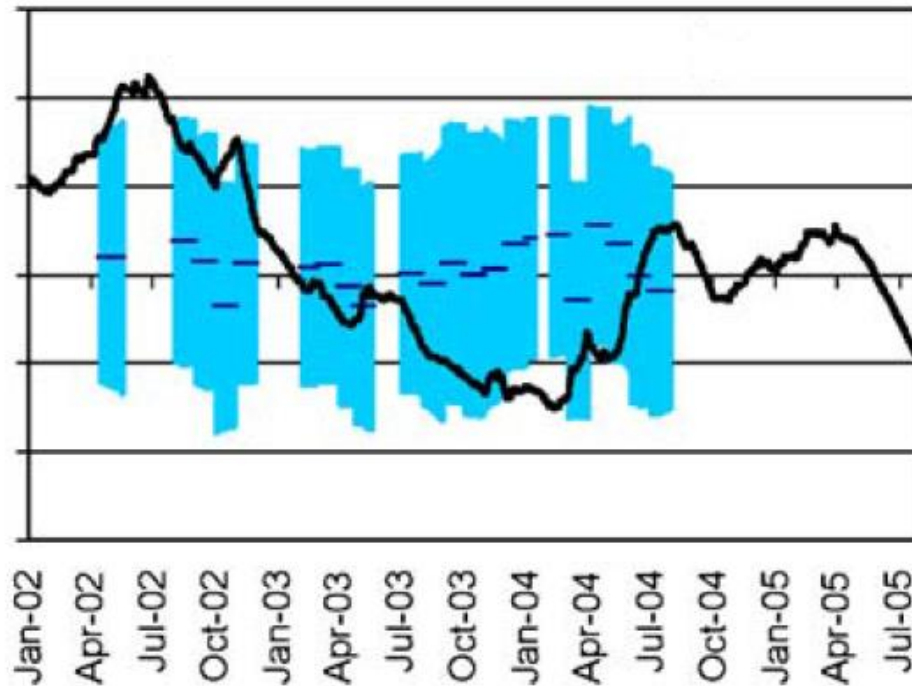


Figure 4.4. The Upper Mississippi Basin outputs: GW storage estimated from GRACE and GLDAS (dark blue bars), and based on well observations (black line). The light blue shaded area is the uncertainty in the GRACE –GLDAS estimates (Rodell, et al., 2007).

4.1.1 Effect of Soil Moisture Models

All the graphs in this section depict the effect of Soil Moisture land surface models on groundwater variations. In time and space, X-axis represents the period of time data collection over Upper Mississippi Basin area which is from January 2003 to July 2005. Y-axis represents the water storage anomalies in cm. It compares outputs of groundwater changes derived from GRACE and GLDAS models with ground truth data.

Figure 4.5 shows the differences in soil moisture anomalies fluctuations as an input data. ΔSM is an average of three soil moisture models CLM, Noah, and Mosaic. ΔSM (CLM), ΔSM (Noah), and ΔSM (Mosaic) represent individual models' anomalous

fluctuations. Among three soil moisture models, CLM model shows less anomalous fluctuations, while the Mosaic model – the greatest respectively. In the following figures, we can see how difference in soil moisture models affects derived groundwater storage anomalies estimated from GRACE.

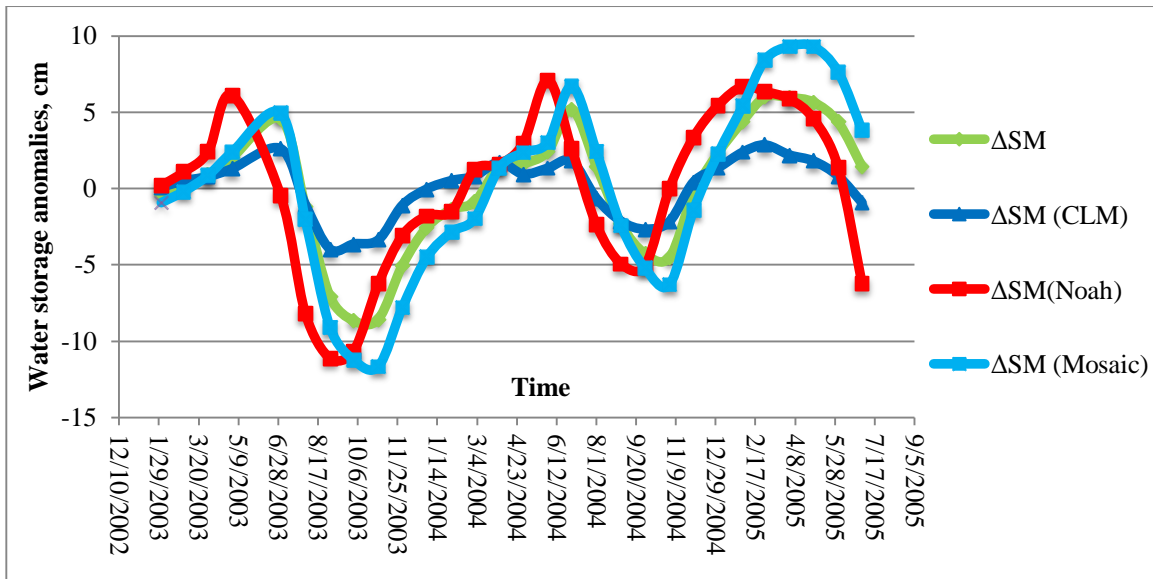


Figure 4.5. Soil moisture anomalies.

Figure 4.6a compares the groundwater storage anomalies estimated from GRACE and average soil moisture models, ΔGW (GRACE), and the groundwater storage anomalies based on 18 available monitoring well observations, ΔGW (GT). The maximum seasonal amplitude occurs in May-June and minimum in October-November. The curves line up over the period of time, but there are a few periods with significant gaps. One of them is from August 2003 to March 2003. The difference in ΔGW anomalies reaches up to 7 cm. Another gap is from September 2004 to July 2005 where ΔGW anomalies' difference is up to 4 cm. Overall, both groundwater storage anomalies (ΔGW) from satellite and ground truth data (18 wells) have

increasing trend from January 2003 to July 2005. ΔGW (GRACE) has a positive slope of 0.0056, while ΔGW (GT) regression line has a positive slope of 0.0107.

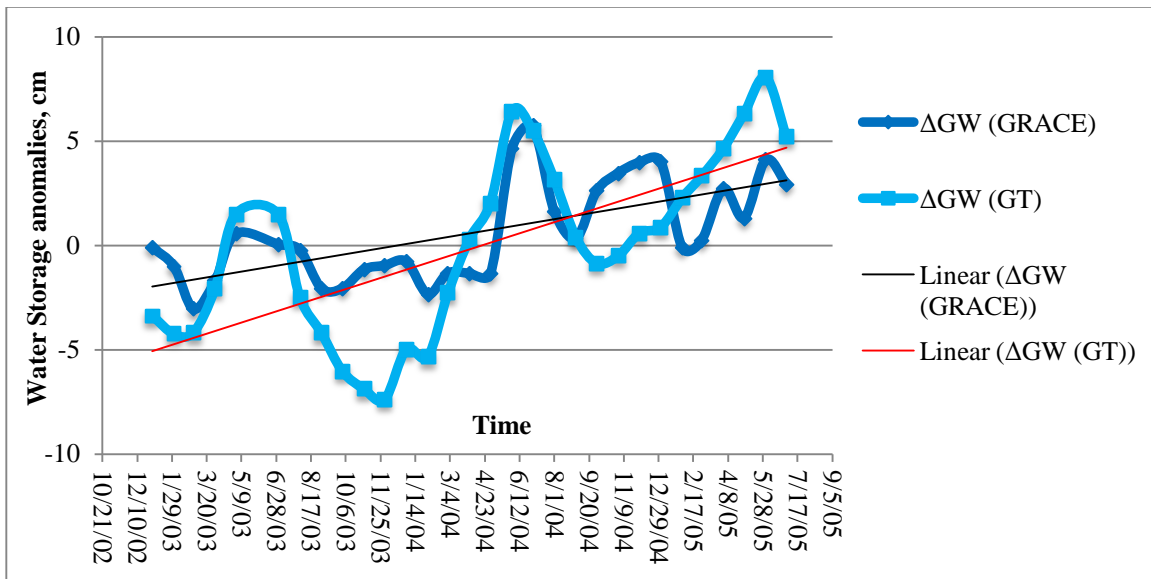


Figure 4.6a. Effect of three soil moisture models average on groundwater storage anomalies.

The two ΔGW time series appear to be well correlated and the calculated correlation coefficient confirms it. The value of r is 0.719, which means that these two time series are well correlated. Figure 4.6b shows a correlation scatterplot between ΔGW (GRACE) and ΔGW (GT) in cm. The scatterplot shows that the observed values fit the GRACE outputs well with an offset on both tails of the regression line. The coefficient of determination, whose value is 0.517, implies that 51.7% of the variations in ΔGW from GRACE can be explained by the variations in ΔGW from well observations. In this context, R-squared value is high enough, due to the present linear relationship between variables with strong correlation of 71.9%.

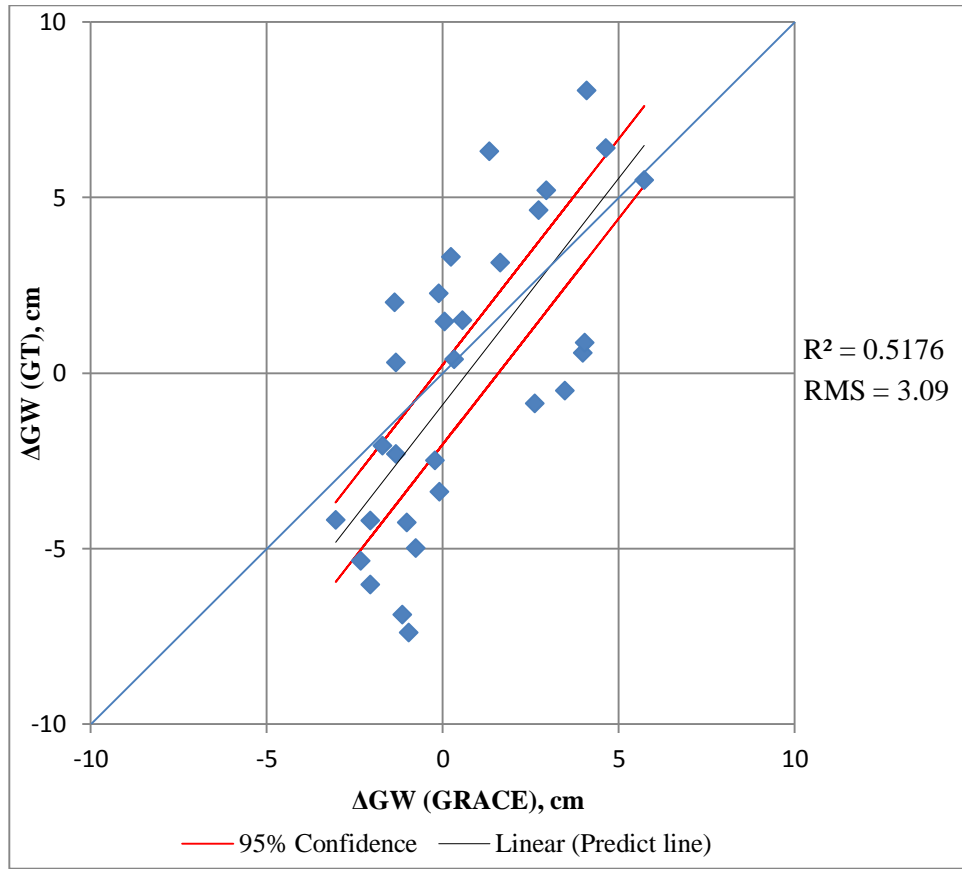


Figure 4.6b. Correlation between GW anomalies from GRACE with three soil moisture models average and from well observations.

Figure 4.7a shows outputs of ΔGW (CLM) soil moisture models alongside 18 well observations ΔGW (GT). In general, CLM soil moisture model improves the pattern of ΔGW between GRACE-GLDAS and well observations reducing the gaps between the curves.

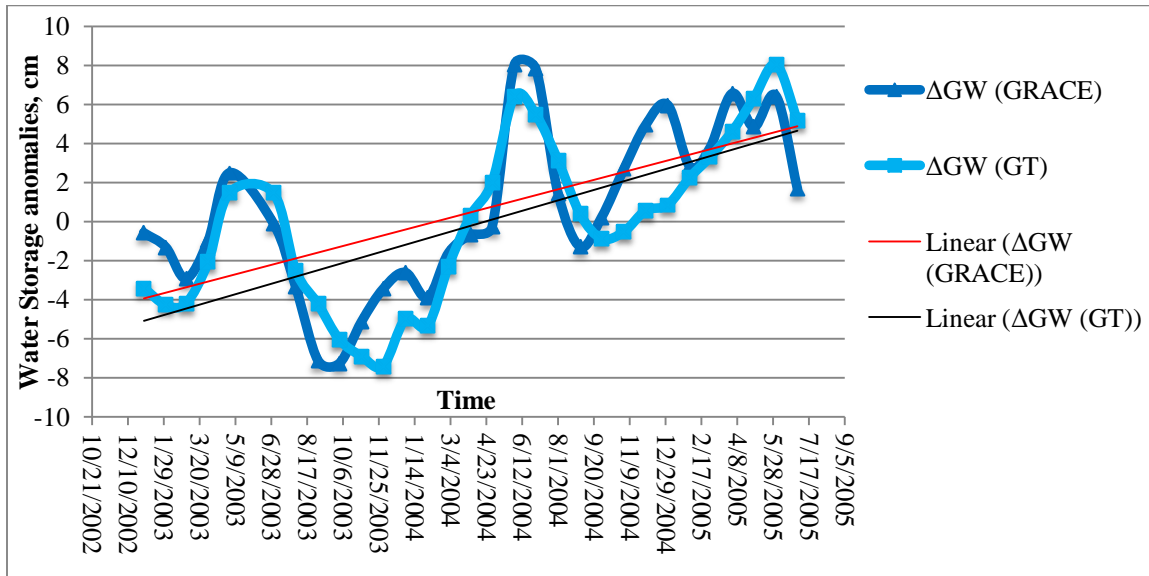


Figure 4.7a. Effect of CLM soil moisture model on GW storage anomalies.

The ΔGW curve from CLM soil moisture model matches ΔGW from well observations better over the period of time than ΔGW curves from the three soil moisture models' average. Overall, both groundwater storage anomalies (ΔGW) from satellite and ground truth data have a rising up trend from January 2003 to July 2005. ΔGW regression line from GRACE and CLM has a positive slope of 0.0097, while ΔGW regression line from well observations data remains slope value of 0.0107.

The two time series appear to be highly correlated and the calculated correlation coefficient confirms it. The value of r is 0.861, which signifies high correlation between these two time series. Figure 4.7b shows a correlation between ΔGW (CLM) and ΔGW (GT). The scatterplot shows that the observed values are uniformly distributed along its profit match line with slight offset on one of the tails. The coefficient of determination, whose value is 0.743, implies that 74.3% of the variations in ΔGW from GRACE can be explained

by the variations in ΔGW from well observations. In this context, R-squared value is high due to the present linear relationship between variables with strong correlation of 86.1%.

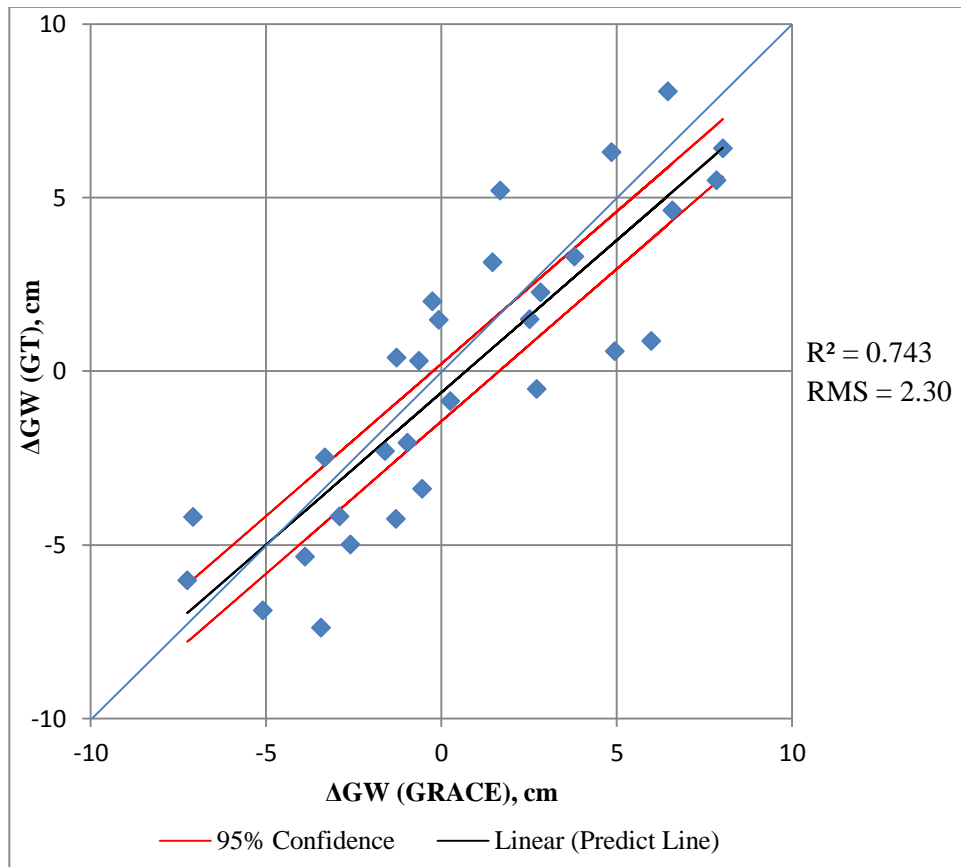


Figure 4.7b. Correlation between GW anomalies from GRACE and CLM soil moisture model and from well observations.

Figure 4.8a shows outputs of ΔGW from GRACE and Noah soil moisture models alongside 18 well observations, ΔGW (GT). Noah soil moisture model impairs the pattern of ΔGW between GRACE-GLDAS and well observations.

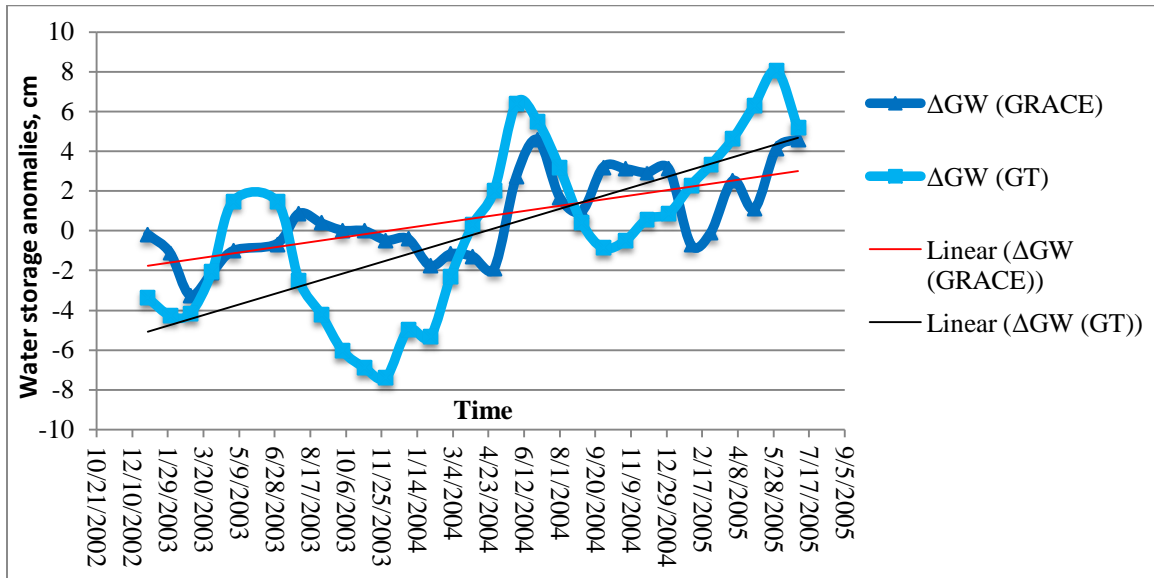


Figure 4.8a. Effect of Noah soil moisture model on GW storage anomalies.

The ΔGW curve from Noah soil moisture model and ΔGW from well observations does not line up well over the period of time. Overall, both groundwater storage anomalies (ΔGW) from satellite and ground truth data still have a rising up trend from January 2003 to July 2005. ΔGW regression line from GRACE and CLM has a positive slope of 0.0052, while ΔGW regression line from well observations data remains slope value of 0.0107.

The two time series appear to be moderately correlated and the calculated correlation coefficient r is 0.581 which is not a good correlation between these two time series. Figure 4.8b shows a correlation between ΔGW from GRACE and Noah and ΔGW from well observations. The scatterplot shows that the observed values scatter widely along its fitted regression line with offset from its mean. The coefficient of determination, whose value is 0.338, implies that 33.8% of the variations in ΔGW from GRACE can be explained by the variations in ΔGW from well observations. In this context, R-squared value is moderate due to the scattered pattern between variables with correlation of 58.1%.

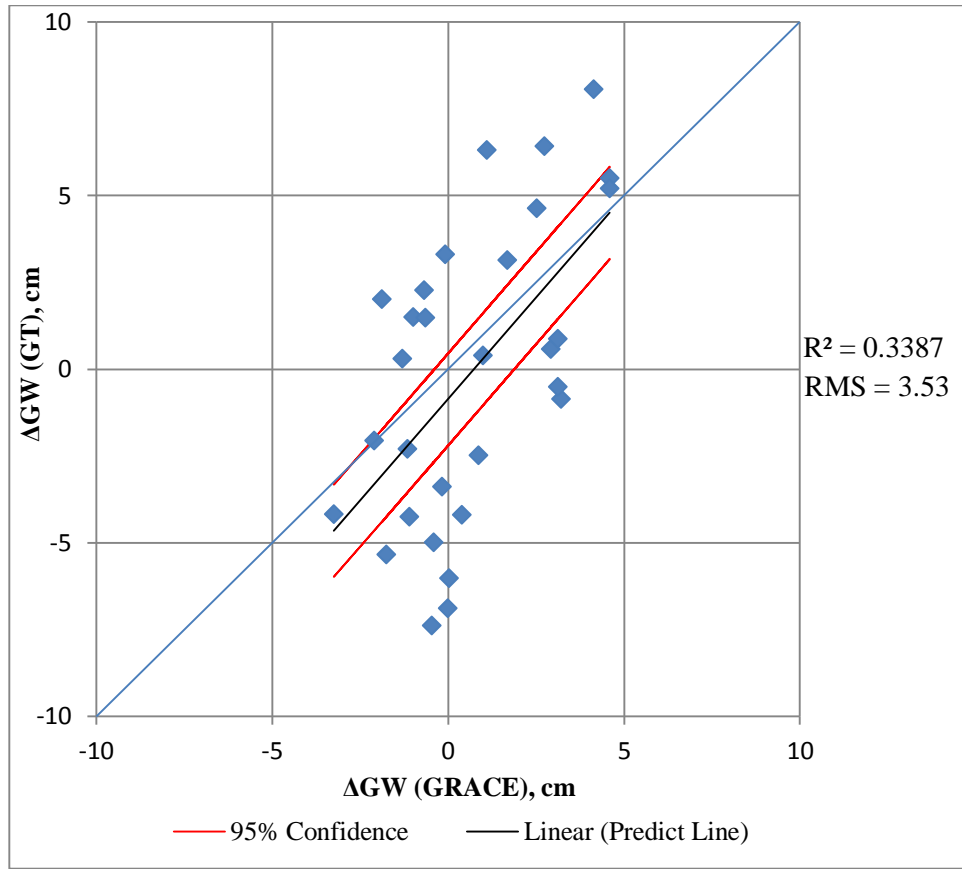


Figure 4.8b. Correlation between GW anomalies from GRACE and Noah soil moisture model and from well observations.

Figure 4.9a shows outputs of ΔGW from GRACE and Mosaic soil moisture models alongside with 18 well observations. Mosaic soil moisture model impairs the pattern of ΔGW between GRACE-GLDAS and well observations even more than Noah soil moisture model.

$RMS = 3.53$

The ΔGW curve from Mosaic soil moisture model and ΔGW from well observations has significant gaps over the period of time. Overall, both groundwater storage anomalies (ΔGW) from satellite and ground truth data still have a rising up trend from January 2003 to July 2005. ΔGW regression line from GRACE and Mosaic has a positive slope of 0.0018,

while ΔGW regression line from well observations data remains with a slope value of 0.0107.

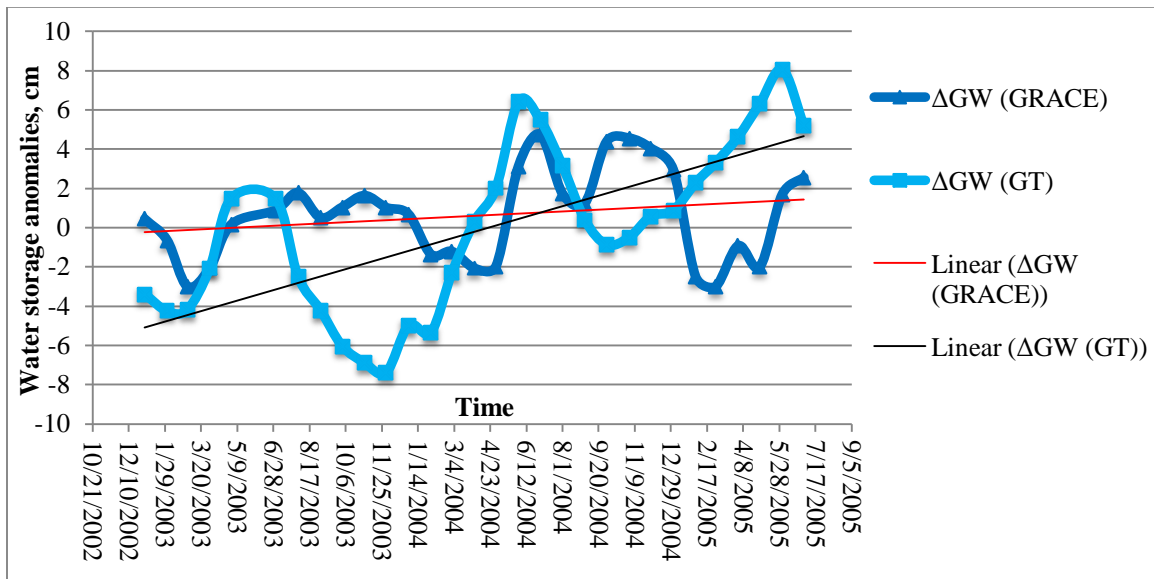


Figure 4.9a. Effect of Mosaic soil moisture model on GW storage anomalies.

The two time series appear to be weakly correlated. The calculated correlation coefficient r is 0.129, which is weak correlation between these two series. Figure 4.9b shows a correlation between ΔGW from GRACE and Mosaic and ΔGW from well observations. The scatterplot shows that the observed values scatter widely along its perfect match line with significant offset. The coefficient of determination, whose value is 0.017, implies that only 1.7% of the variations in ΔGW from GRACE can be explained by the variations in ΔGW from well observations. In this context, R-squared value is very low due to the widely scattered pattern between variables with correlation of 12.9%.

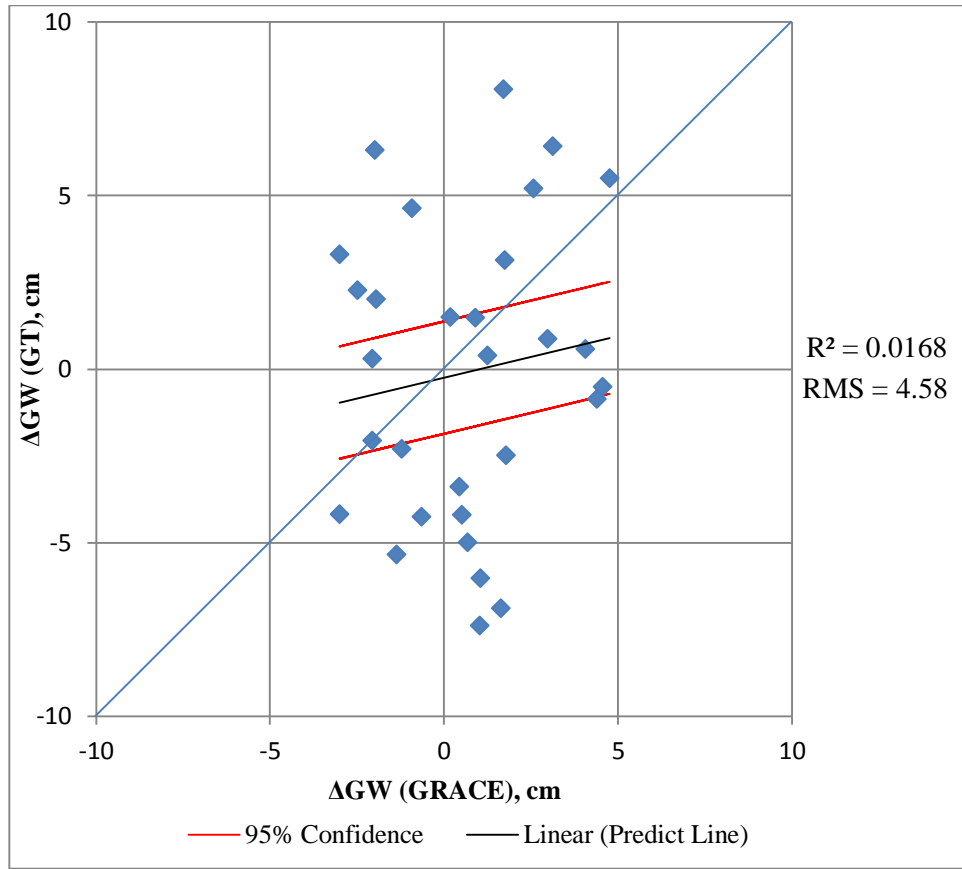


Figure 4.9b. Correlation between GW anomalies from GRACE and Mosaic soil moisture model and from well observations.

4.1.2 Effect of Groundwater Fluctuations

There are 18 monitoring wells provided from the USGS website (Table 4.1). The location of the monitoring wells is presented in Figure 4.10. Analysis of each well determined that some wells have significant fluctuation in groundwater changes, while some wells are more constant. Figure 4.11a represents groundwater level changes over the period of time at each monitoring well with its site number and location state. Monitoring wells were separated into the wells of greater and smaller fluctuations. Figures 4.11b and 4.11c show 10 wells with greater fluctuations and 8 wells with smaller fluctuation of groundwater

levels and its standard deviation (STD). Greater fluctuations mean greater STD. However, in this case STD of smaller fluctuations is greater because its depth varies in a big range from 5 to 19 meters. Whereas greater fluctuations depth varies in a small range.

Table 4.1. Monitoring well observations.

Well Name	Site Number	Latitude	Longitude	Aquifer	Depth, m
#12_WI	453013092314601	45.52875	-92.504611	"Sand and Gravel Aquifer"	15.85
#13_WI	453720089215401	45.62746	-89.366667	"Sand and Gravel Aquifer"	10.06
#8_WI	440713089320801	44.120251	-89.535677	"Sand and Gravel Aquifer"	5.48
#4_WI	431312089475301	43.22	-89.798056	"Sand and Gravel Aquifer"	44.5
#3_WI	425607088173001	42.93529	-88.29176	"Sand and Gravel Aquifer"	72.24
#30_MO	382100090592801	38.35025	-90.990389	"Ozark Plateaus aquifer system"	77.72
#36_MO	390207092570801	39.035278	-92.952222	"Ozark Plateaus aquifer system"	70.1
#39_MO	403452092292901	40.580917	-92.49175	"Sand and Gravel Aquifer"	8.23
#2_IL	374453088261701	37.748194	-88.438056	"Sand and Gravel Aquifer"	3.35
#1_KY	365210088391301	36.869444	-88.653611	"Mississippi embayment aquifer system"	32.31
#9_IL	402558087351501	40.433194	-87.590694	"Sand and Gravel Aquifer"	44.5
#6_IN	400541085213701	40.094722	-85.358333	"Sand and Gravel Aquifer"	27.74
#3_SD	434330096434801	43.725	-96.73	"Sand and Gravel Aquifer"	8.84
#1_ND	460120097591803	46.022222	-97.988333	"Alluvial aquifers"	17.37
#5_ND	462425096441202	46.406944	-96.736667	"Sand and Gravel Aquifer"	41.15
#3_IA	410057095075101	41.015833	-95.130556	"Sand and Gravel Aquifer"	12.19
#4_IA	414315091252002	41.721128	-91.422389	"Silurian-Devonian aquifers"	25.15
#2_MN	473416095052801	47.57093	-95.0914	"Sand and Gravel Aquifer"	6.94

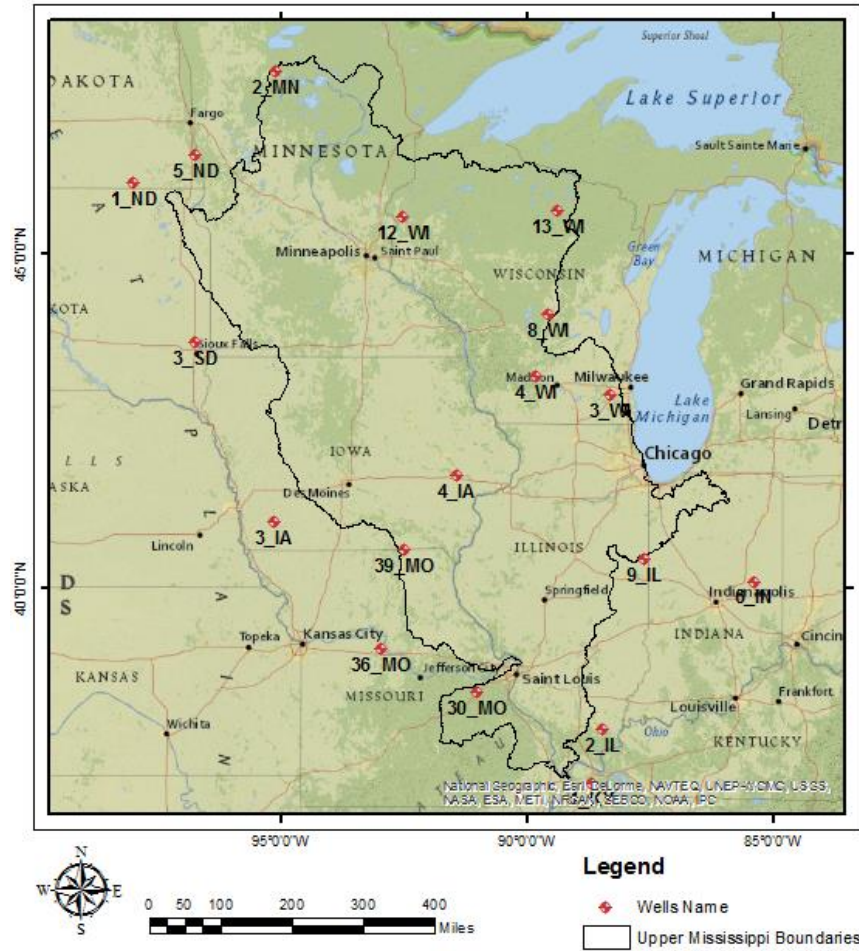
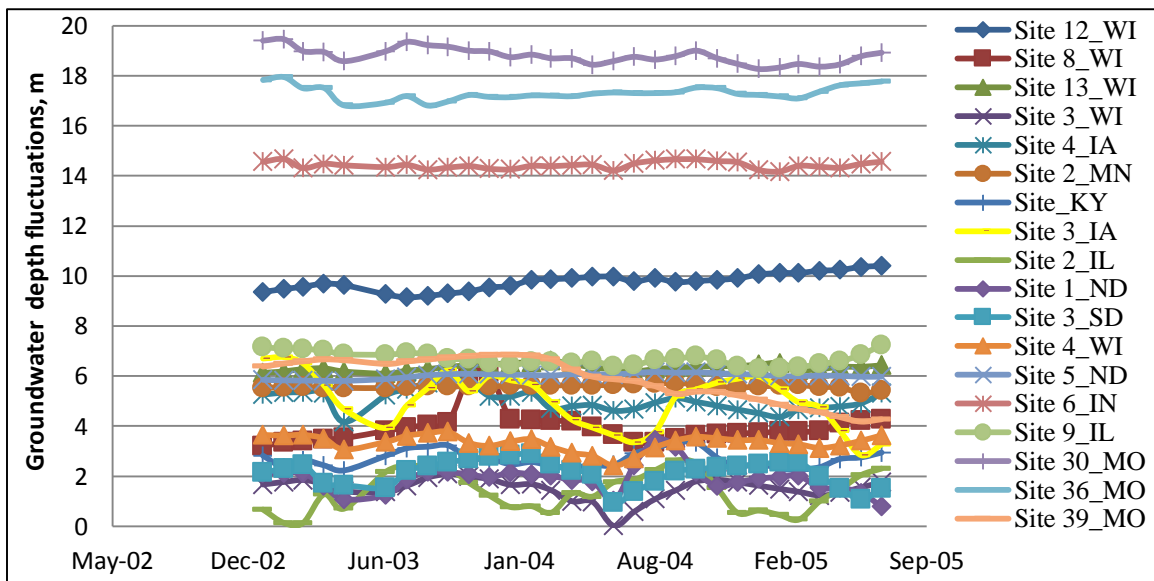
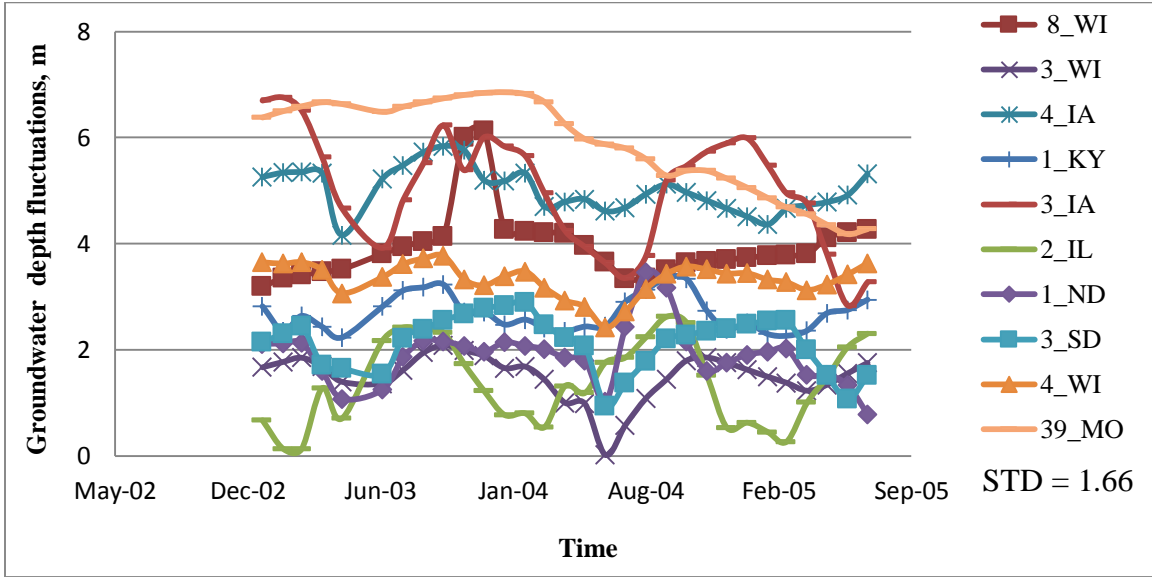


Figure 4.10. Location of groundwater wells.

a)



b)



c)

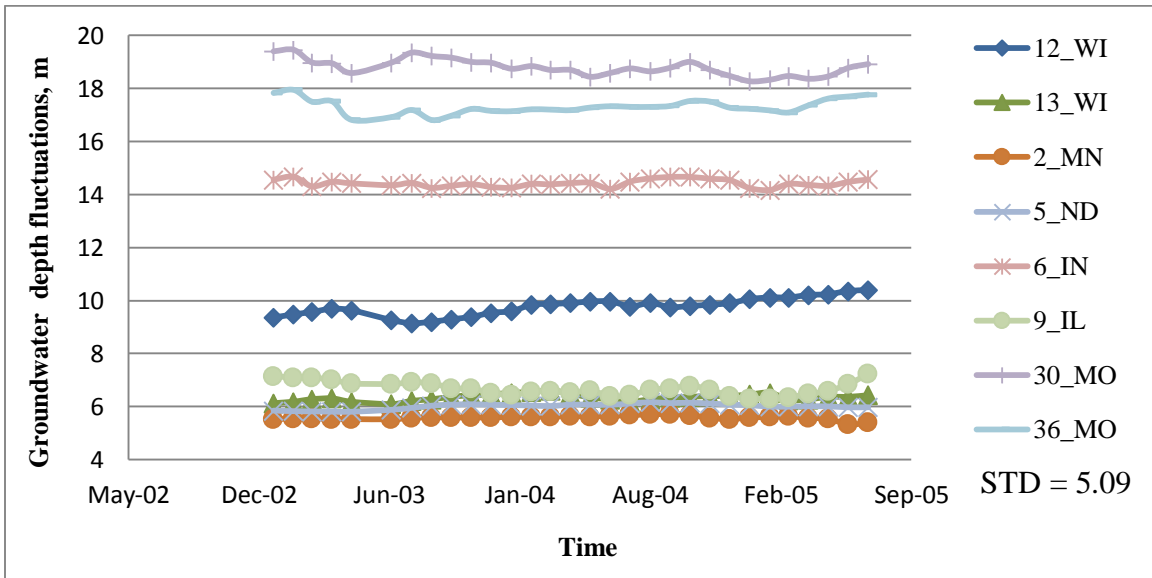


Figure 4.11. Effect of GW fluctuations: (a) Fluctuation of GW levels from the total 18 wells, (b) greater fluctuations of GW levels, (c) smaller fluctuations of GW wells.

Considering the distribution of well observations, the special selection of monitoring wells influences the distribution of Thiessen polygons over the basin. Figures 4.12a and 4.12b show different Thiessen Polygons distributions for greater and smaller fluctuations

respectively. Figures 4.13a and 4.13b compare the groundwater storage anomalies estimated from GRACE and average soil moisture models and the groundwater storage anomalies based on 10 wells with greater fluctuations and 8 wells with smaller fluctuations.

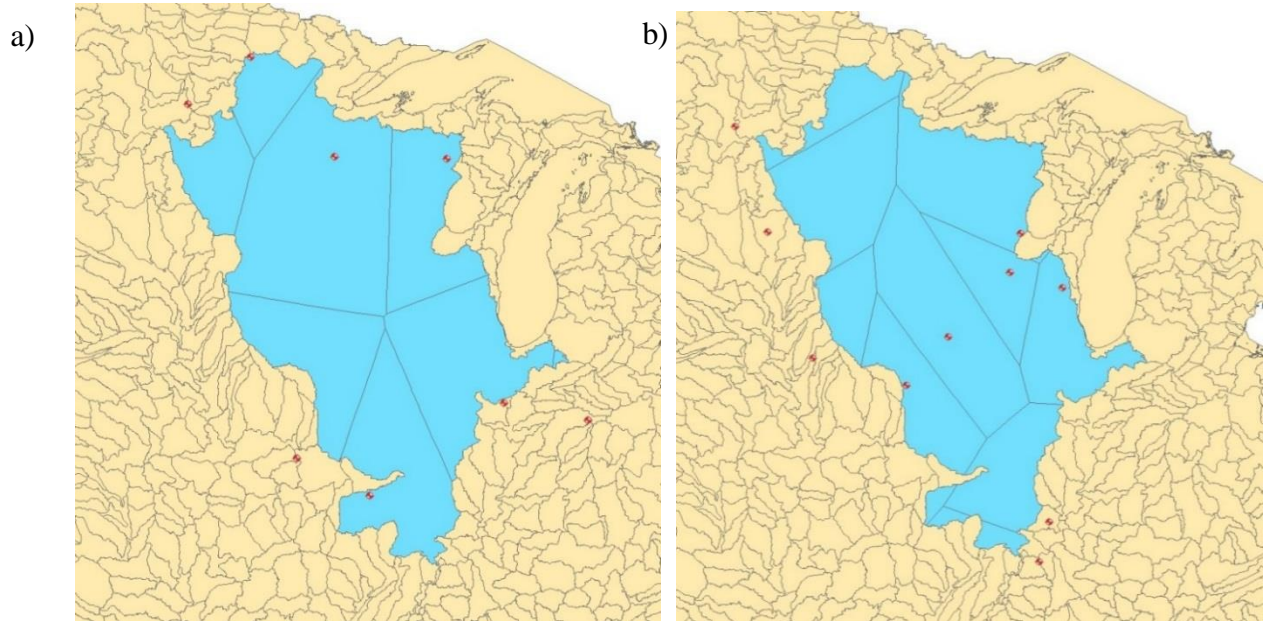
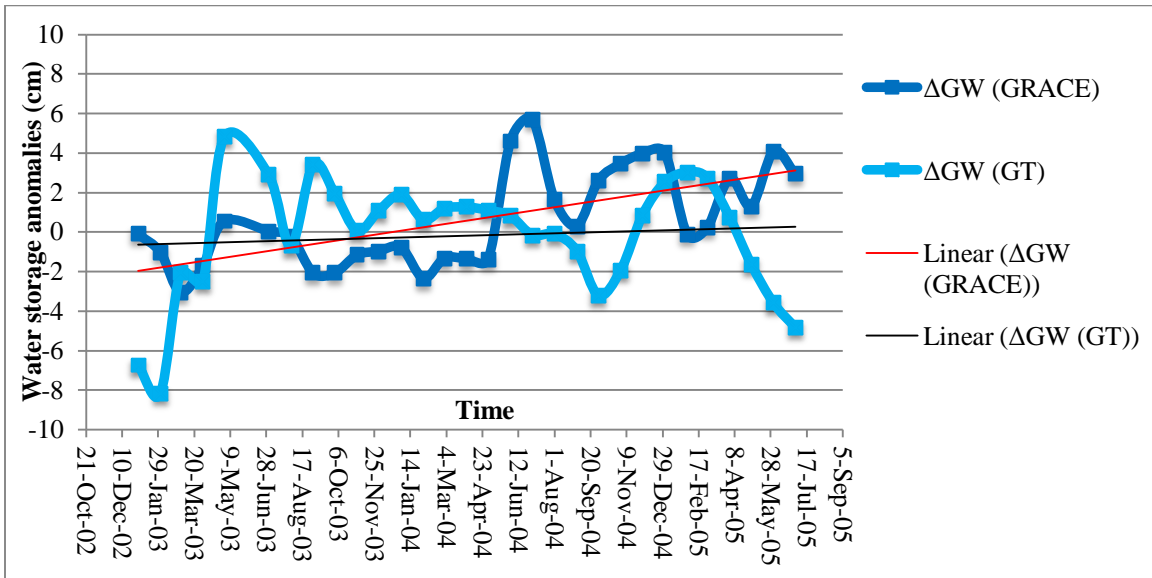


Figure 4.12. Effect of groundwater fluctuations: Thiessen Polygon distribution for (a) greater and (b) smaller groundwater fluctuations.

a)



b)

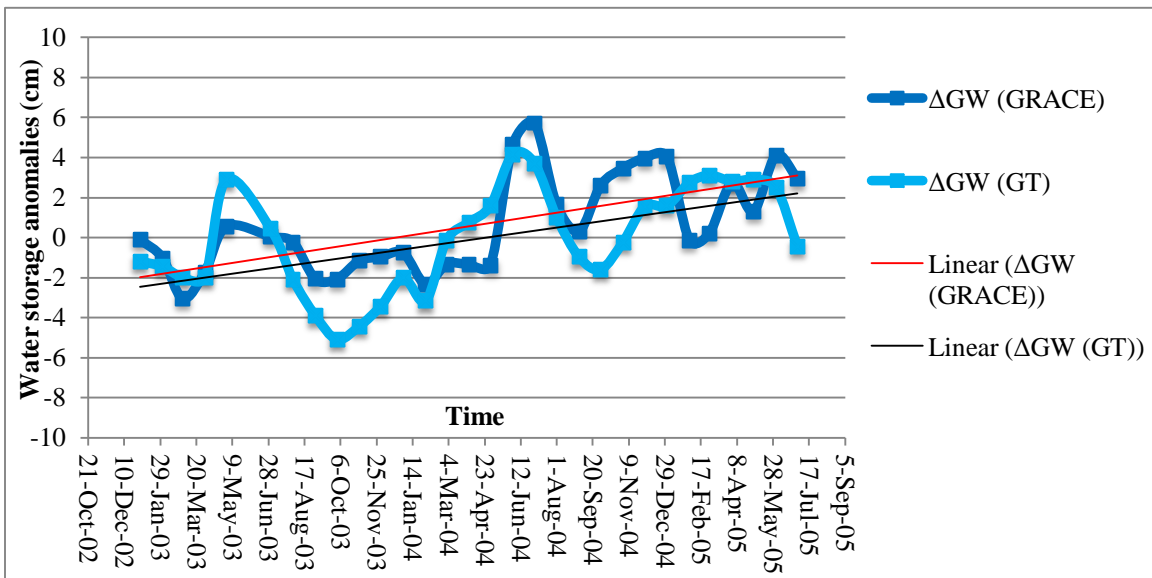


Figure 4.13. Effect of GW fluctuations: GW storage estimates from (a) greater and (b) smaller fluctuations.

Overall, both groundwater storage anomalies (ΔGW) from GRACE and ground truth data have an increasing trend from January 2003 to July 2005. ΔGW regression line from GRACE has a positive slope of 0.0056, while ΔGW regression line from well observations

data with greater fluctuations has a positive slope of 0.0010 and with smaller fluctuations has a positive slope of 0.0051.

The ΔGW time series for greater fluctuations appear to be poorly correlated and the calculated correlation coefficient explains it. The value of r is -0.105 or -10.5% which shows negative and low correlation. The ΔGW time series for smaller fluctuations appear to be well correlated with its value of 0.655 or 65.5% which shows positive and moderate correlation. Figure 4.14 shows a correlation between ΔGW (GRACE) and ΔGW (GT) of (a) greater and (b) smaller fluctuations from well observations. In figure 4.14a, the scatterplot shows that the observed values and its perfect match fit the data poorly. The majority of the observed points scatter widely about the plot, and falling roughly in the shape of a circle. In figure 4.14b, the scatterplot shows that the observed values and its perfect match fit the data well. As the linear relationship increases, the circle becomes more and more elliptical in shape and all points fall better on a straight line. The coefficient of determination for greater fluctuations, whose value is 0.011, implies that only 1.1% of the variations in ΔGW from GRACE can be explained by the variations in ΔGW from well observations. In this context, R-squared value is poor due to the weak linear relationship between variables. The coefficient of determination for smaller fluctuations, whose value is 0.428, implies that 42.8% of the variations in ΔGW from GRACE can be explained by the variations in ΔGW from well observations. In this context, R-squared value is good due to the stronger linear relationship between variables.

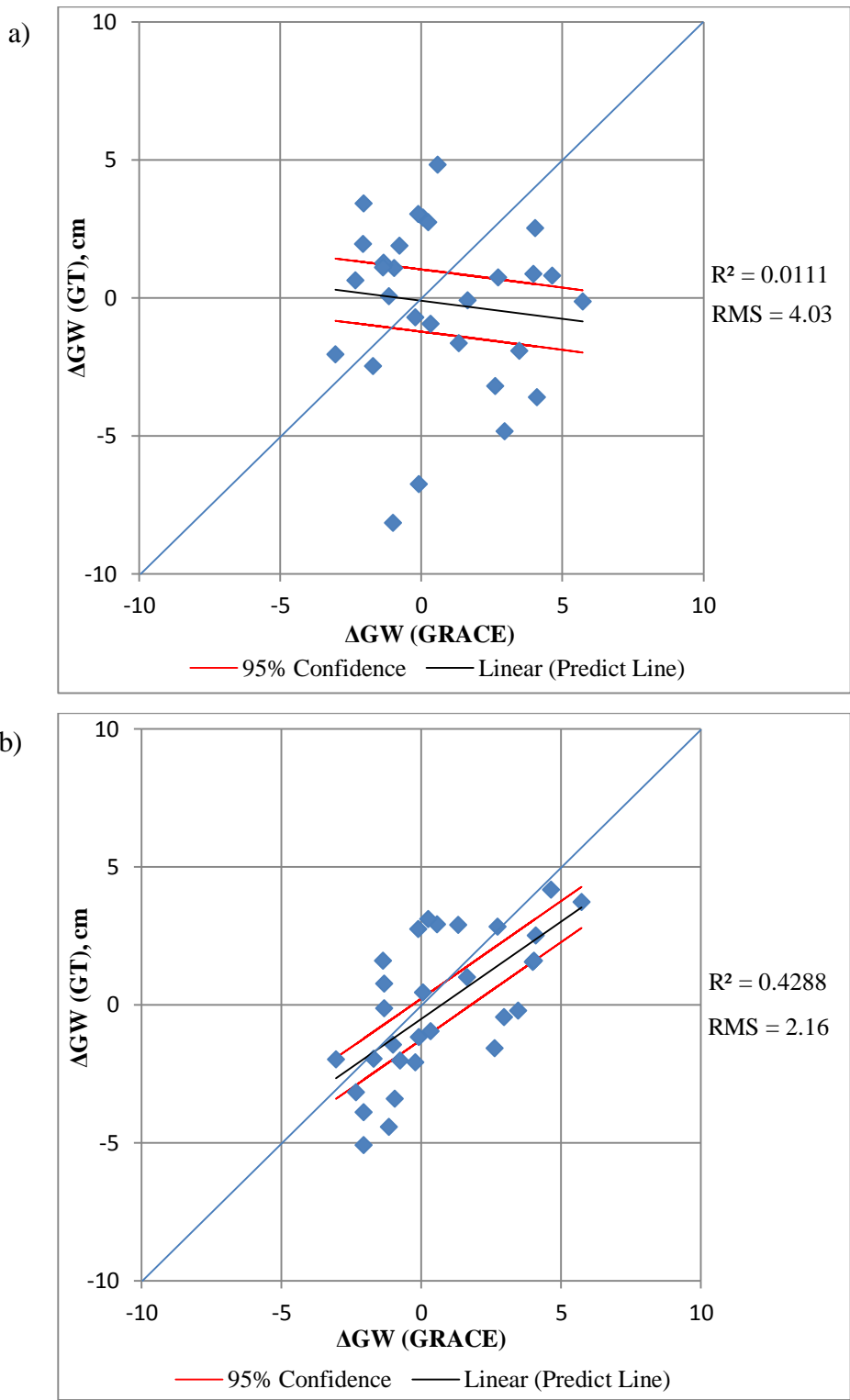
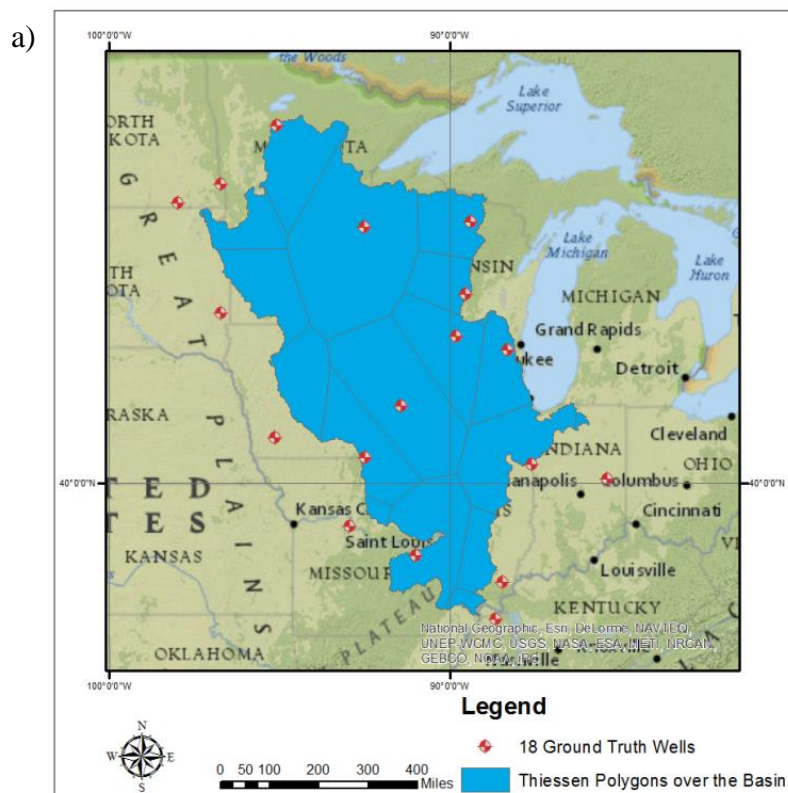


Figure 4.14. Correlation between GW anomalies from GRACE and (a) greater and (b) smaller fluctuations from well observations.

4.1.3 Effect of Aquifer

The Upper Mississippi Basin consists of different aquifer systems over the total 18 wells. Among them, Ozark Plateaus aquifer, Mississippi embayment aquifer, alluvial aquifer, Silurian-Devonian aquifer. However, the majority of the wells exists with Sand and Gravel aquifers. The effect of aquifers might be significant. Therefore, 11 observation wells with the same aquifer were selected out of 18 wells to determine the effect of an aquifer on groundwater storage anomalies.

Figures 4.15a and b show 18 and 11 observation wells and its Thiessen distribution over the basin. Groundwater observation wells distribute less uniformly for 11 wells rather than for 18 having a few sparseness areas which might affect the area of Thiessen polygons.



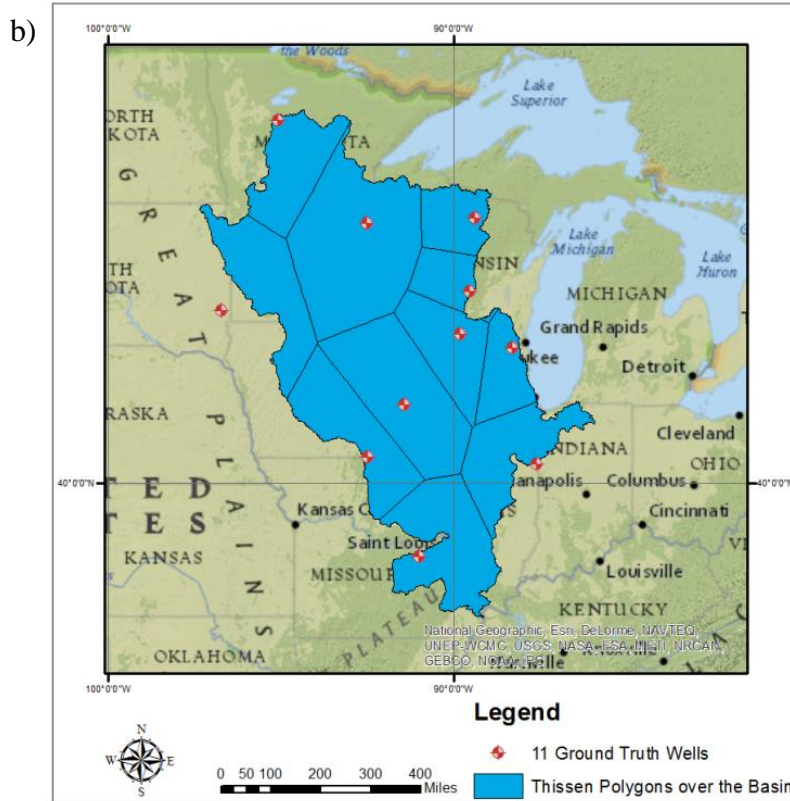


Figure 4.15. Effect of aquifer: Thiessen Polygon area distribution for (a) 18 and (b) 11 wells.

Figures 4.16a and b compare the groundwater storage anomalies estimated from GRACE and average soil moisture models, ΔGW (GRACE), and the groundwater storage anomalies, ΔGW (GT) based on 18 available and 11 selected monitoring well observations. Overall, both groundwater storage anomalies (ΔGW) from satellite and ground truth data (18 and 11 wells) have increasing trend from January 2003 to July 2005. ΔGW regression line from GRACE has a positive slope of 0.0056 in both figures 4.16a and b. ΔGW regression line from 18 well observations data has a positive slope of 0.0107, but ΔGW regression line from 11 well observations data has a positive slope of 0.0056 which matches ΔGW regression line from GRACE.

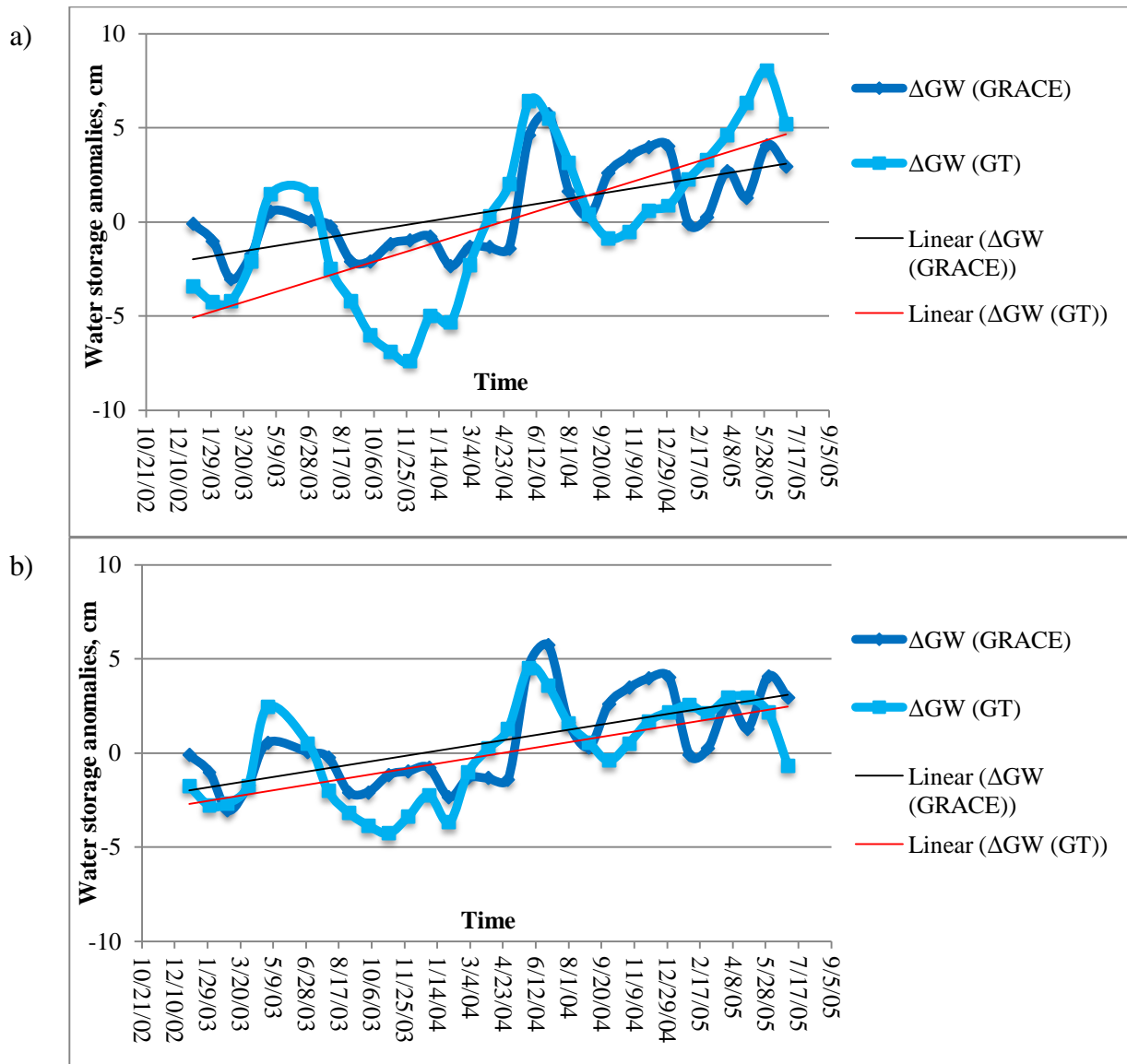
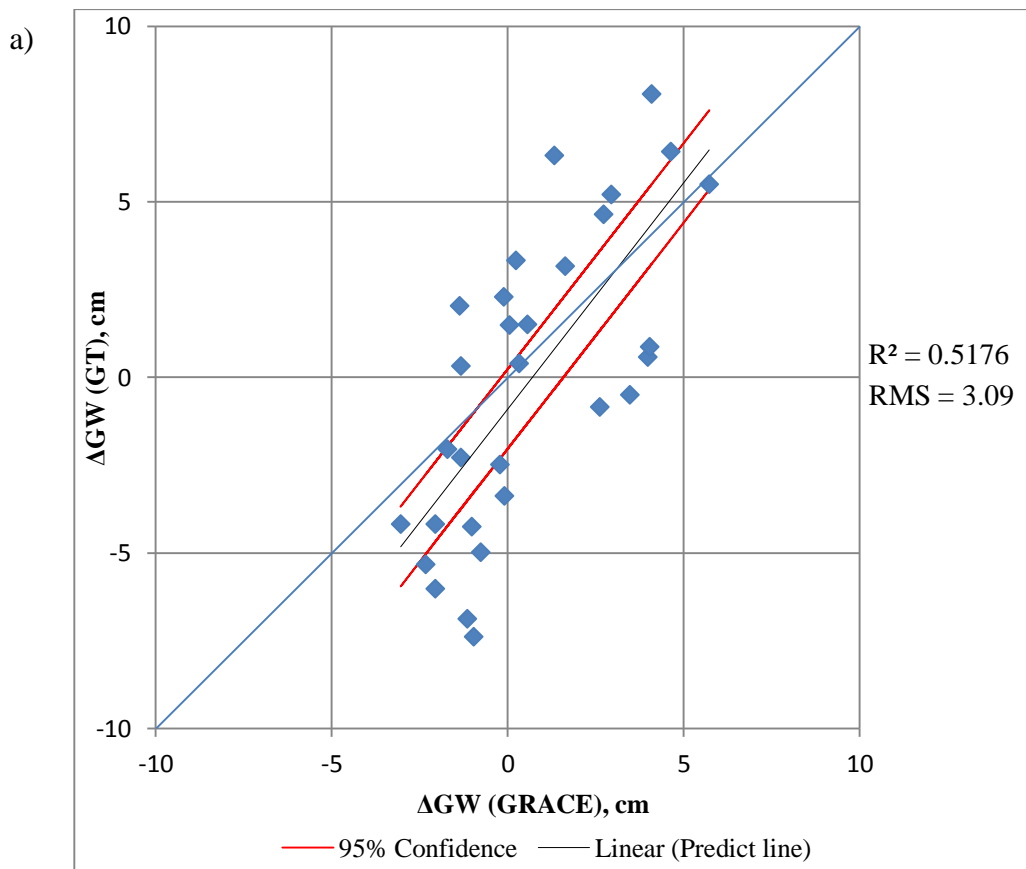


Figure 4.16. Effect of aquifer: GW storage anomalies from (a) 18 and (b) 11 monitoring wells.

Δ GW time series appear to be well correlated with calculated a correlation coefficient value of 0.719 or 71.9%, which means that these two series are good correlated. In figure 4.17b, Δ GW time series shows good correlation with calculated correlation coefficient value of 0.734 or 73.4%. The correlation relationships enhance only by 1.5%. Figures 4.17a and b

show a correlation between ΔGW from GRACE and ΔGW (GT) from 18 and 11 well observations. The scatterplot shows that the observed values and its perfect match fit the data well with an offset on both tails of the regression line. The coefficient of determination for 18 observation wells, whose value is 0.517, implies that 51.7% of the variations in ΔGW from GRACE can be explained by the variations in ΔGW from well observations. The coefficient of determination for 11 observation wells increases to 0.538, which describes 53.8% of the variation in ΔGW from GRACE can be explained by the variations in ΔGW from well observations. Although the difference in R-squared value is slight, the scatter plot for 11 wells show observed points closer to its fitted regression line. R-squared value is high enough due to the present linear relationship between variables with strong correlation of 71.9% and 73.4% respectively.



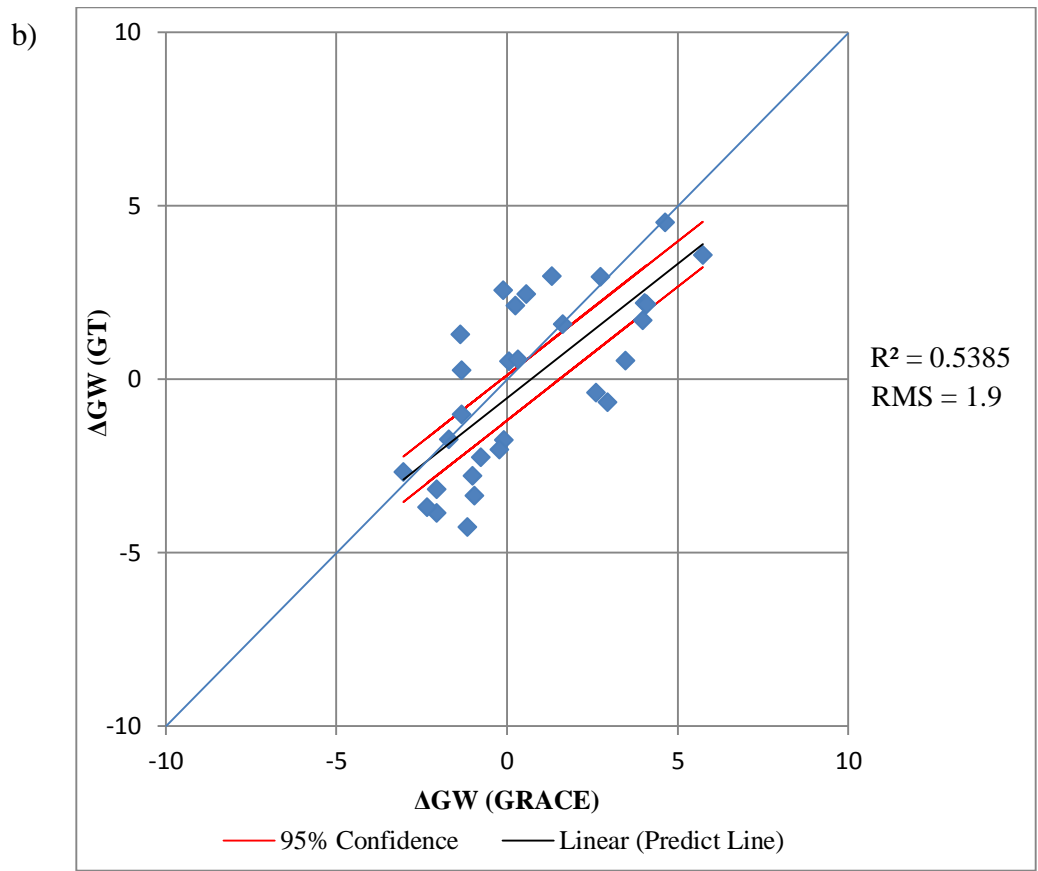


Figure 4.17. Correlation between GW Anomalies from GRACE with three soil moisture models average and from (a) 18 and (b) 11 well observations.

4.2 Data-Poor Region: Lake Chad Ngadda Catchment

4.2.1 Ground Truth Data for the Lake Chad Region

The data-poor region is presented by the Ngadda Catchment. For the Lake Chad Ngadda Catchment, the IRD (Institute of Research Development, France) collected groundwater depths in the southwest region (the Nigerian side) of the Lake in 2005, while the Hydrolab at the University of Missouri – Kansas City collected the groundwater depths in the same area in 2009. Thus the baseline maps of groundwater are constructed for November 2005 and July 2009. The site map with GRACE model domain is shown in Figure 4.18. There are five monitoring wells selected out of all available wells for the 2005 and 2009 years that have been selected with the same or close criteria by location. The area of study includes one of the largest natural piezometric depressions of the Quaternary aquifer which is named as the Bornu piezometric depression. Figure 4.19 shows the location of Bornu piezometric depression and groundwater table contour lines in the 1960s.

Due to the Lake Chad shrinkage over decades, and the Quaternary aquifer interconnection with the Lake, groundwater levels are supposed to decline in the vicinity of Lake Chad. Nevertheless, groundwater levels at the Bornu depression show an increase while the lake has shrunk from 1960s to 2009. The elevation and the direction of Ngadda Catchment have a direction from northwest to southeast. Groundwater-surface direction did not change since the 1960s. Figures 4.20a and 4.20b shows an increase in groundwater levels from 2005 to 2009, and the difference between groundwater depths and the location of monitoring wells using Kriging for 2005 and 2009. However, it is inappropriate to make a conclusion for the groundwater change from ground truth well observations since it is not continuous data, but two separate series of data.

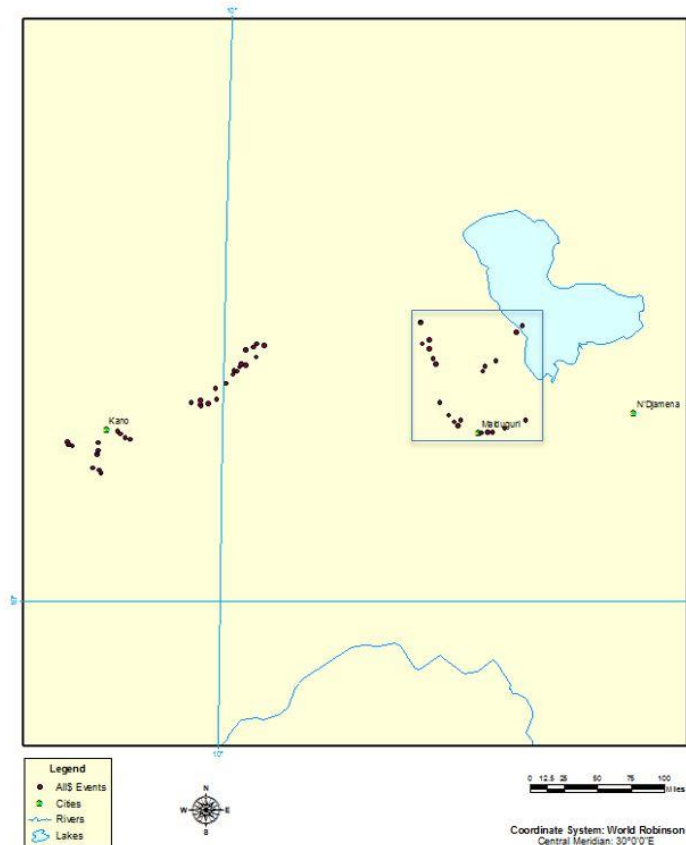


Figure 4.18. Site map with GRACE domain.

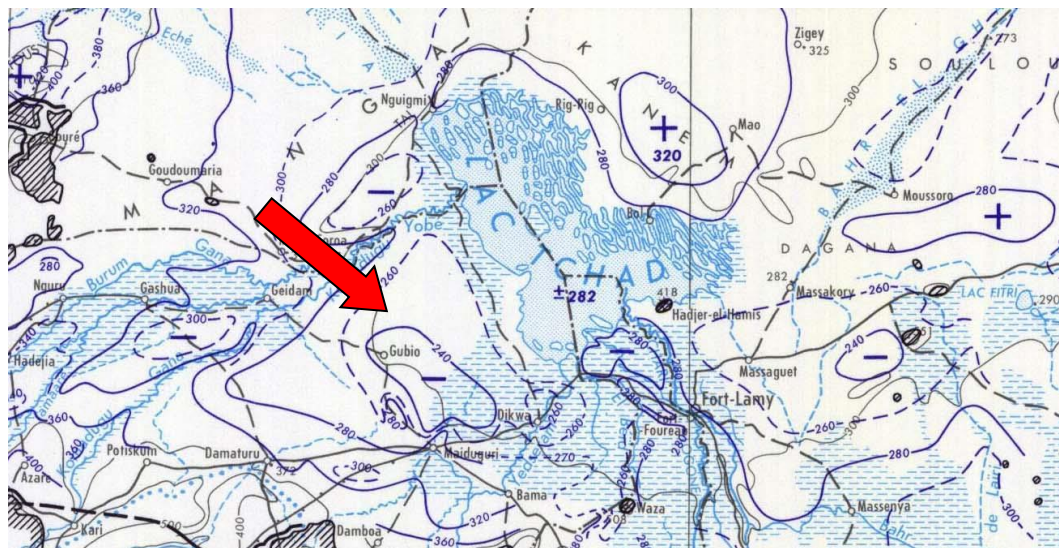


Figure 4.19. Groundwater table in 1960's and location of Bornu piezometric depression.

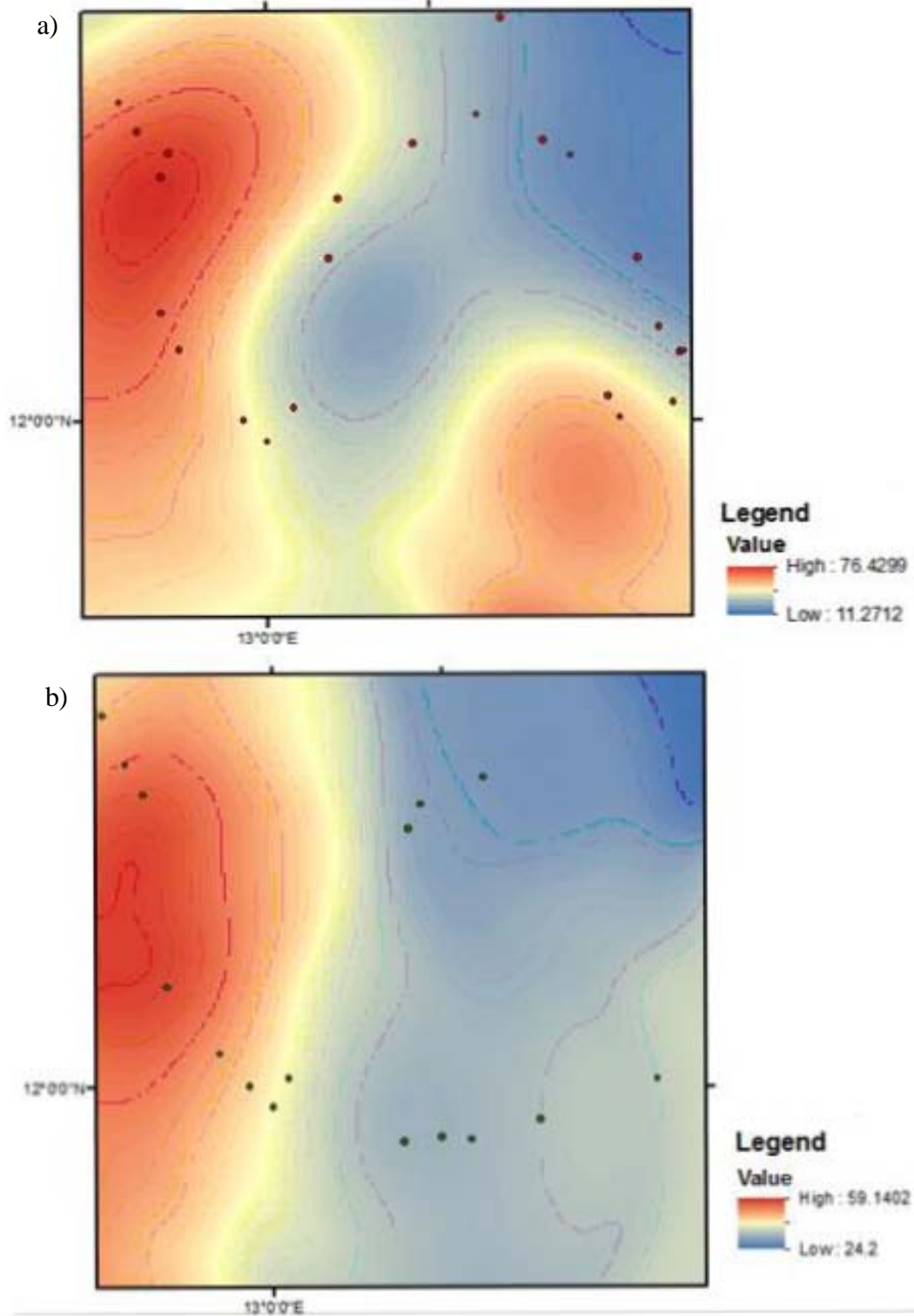


Figure 4.20. Kriging of groundwater depths and sampling data for (a) 2005 and (b) 2009.

4.2.2 Effect of Soil Moisture Models

Figure 4.21 depicts the effect of Soil Moisture land surface models on groundwater variations. In time and space, the period of time is from November 2005 to July 2009 and over the Lake Chad Ngadda Catchment area. It compares outputs of groundwater changes derived from GRACE and GLDAS models. Figure 4.21a shows inputs of ΔTWS and ΔSM and the groundwater storage anomalies ΔGW estimated from GRACE and GLDAS average soil moisture models. The high picks of seasonal amplitudes occur around September through November which is a wet season in the region, while low picks represents dry season from March to May. The seasonal variations of ΔTWS and ΔSM are up to 10 cm. The seasonal amplitudes reach up to 6 cm for ΔGW estimates. Figures 4.21b, 4.21c, and 4.21d show inputs of ΔTWS and ΔSM , and ΔGW from GRACE and individual soil moisture models (CLM, Noah, and Mosaic). CLM soil moisture model shows greater and more stable fluctuations of groundwater storage anomalies' ΔGW . High picks fluctuates up to 10 cm. Mosaic and Noah soil moisture models show similar pattern of groundwater storage changes. High picks of Mosaic and Noah models almost do not exceed 5 cm. Seasonal amplitudes fluctuate more often in compare with constant seasonal change of CLM model.

Out of three land surface models, the one with the greatest effect and reasonable result is the CLM model. The results from CLM model provide the most realistic simulations of mean annual runoff since the model has a small dynamic range of soil moisture in it. Mosaic and Noah models show greater soil moisture changes; consequently, groundwater storage fluctuation would be smaller.

4.2.3 Effect of Scales

TWS data derived from GRACE is available only as 1° resolution. However, GLDAS provides 1° and 0.25° resolution for LSMs. Figure 4.22a shows the groundwater storage changes computed from 1° TWS and 1° SM, while figure 4.22b shows groundwater storage changes computed from 1° TWS and 0.25° SM. The pattern of both GRACE-GLDAS groundwater storage estimates is almost identical with its seasonal amplitudes in wet and dry seasons. However, groundwater storage anomalies from 0.25° SM gives more detailed variations.

4.2.4 Effect of Individual Cell

The Lake Chad Ngadda Catchment covers 2° by 2° area of GRACE and GLDAS spatial resolution. The GRACE approach appears to be appropriate for regions equal or larger than 5° by 5° area. However, the area cannot be expanded due to the lack of well monitoring observations. Also, the Lake Chad Ngadda Catchment region covers Bornu piezometric depression. Therefore, it would be appropriate to look at each individual cell effect. In figure 4.23, a 2° by 2° area is divided into four separate 1° cells for better understanding of each cell impact. Southeastern and southwestern cells approximately cover the Bornu piezometric depression. Figures 4.24c and 4.24d show the inputs of GRACE and GLDAS estimates and output groundwater storage anomalies for southeastern and southwestern cells. The fluctuations are significantly great in those two cells. Seasonal amplitudes in the wet season can reach up to 10 cm of groundwater storage anomalies. Figure 4.24a and 4.24b show the inputs of GRACE and GLDAS estimates and output groundwater storage anomalies for northeastern and northwestern cells. The fluctuations of groundwater storage changes are half the size of those in figures 4.24c and 4.24d. Seasonal amplitudes in the wet season reach no

more than 5 cm of groundwater storage anomalies. The results proves the presence of the Bornu piezometric depression which takes place in southeastern and southwestern cells.

4.2.5 Effect of Coverage Area

Figure 4.25 shows the coverage area of the Lake Chad Ngadda Catchment using a sub-basin area boundary and 2° by 2° area. Groundwater observation wells show a few sparseness areas when the coverage area expands. Figures 4.26a and 4.26b represent groundwater storage anomalies from GRACE-GLDAS estimates over sub-basin and 2° by 2° area. GRACE-GLDAS estimates from sub-basin coverage area are greater than the estimates from 2° by 2° coverage area. Consequently, different fluctuations in GRACE-GLDAS estimates affect variations of groundwater storage anomalies. The seasonal fluctuations of groundwater storage anomalies for the sub-basin area reach up to 7 cm for high picks, while for 2° by 2° area the seasonal fluctuations do not exceed 5 cm.

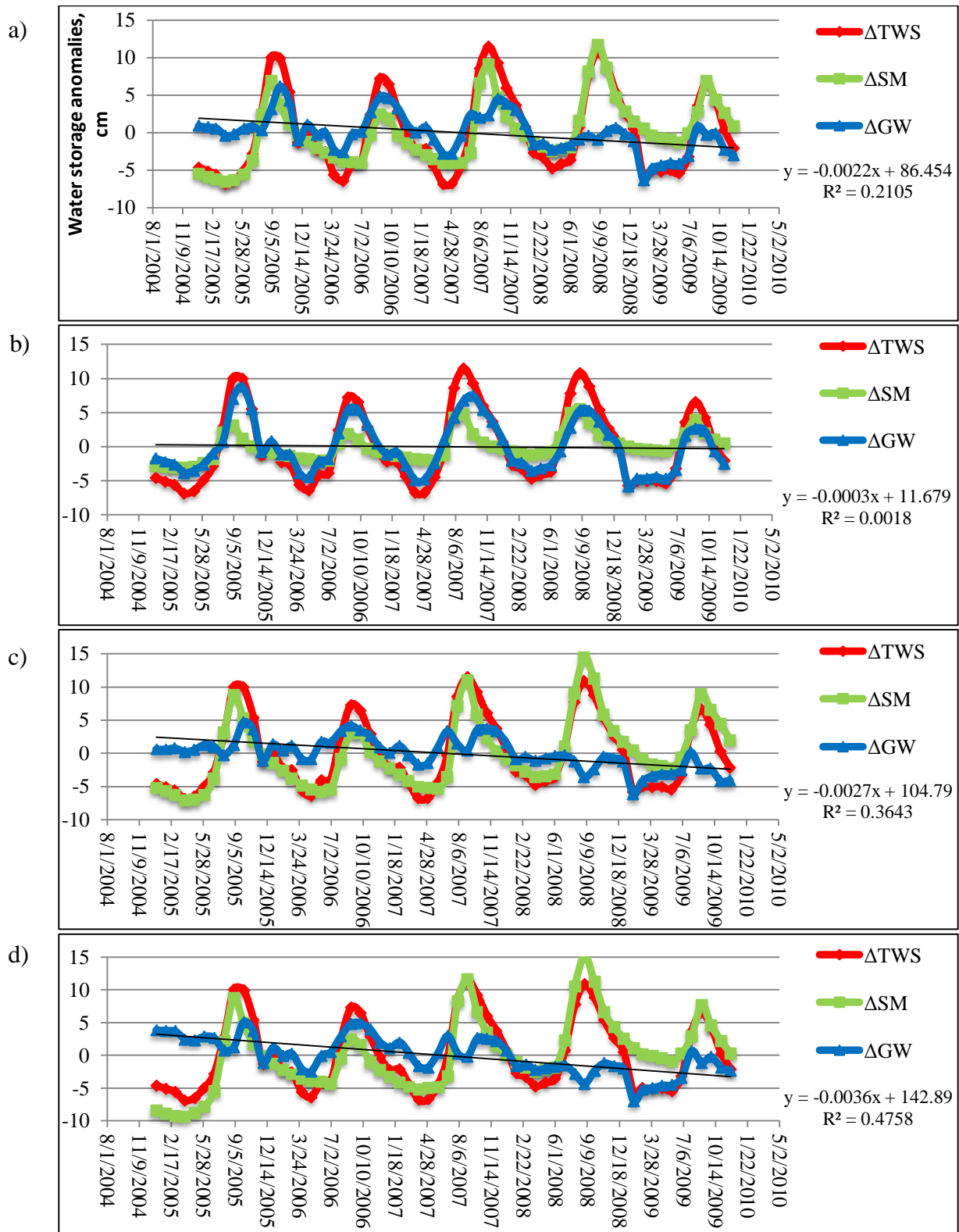


Figure 4.21. Effect of soil moisture models: (a) Average of three soil moisture models, (b)

CLM model, (c) Mosaic model, (d) Noah model.

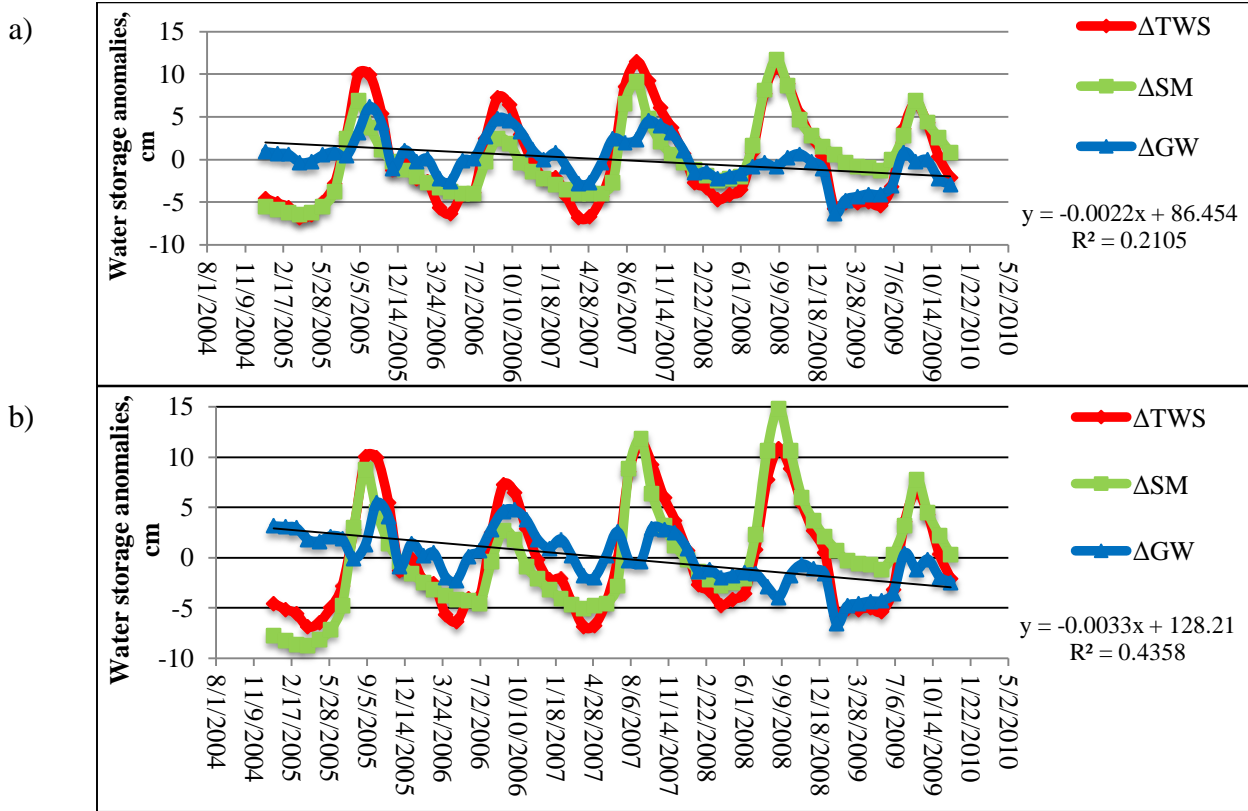


Figure 4.22. Effect of scales: The results of applying 1° TWS with (a) 1° SM, (b) 0.25° SM data.

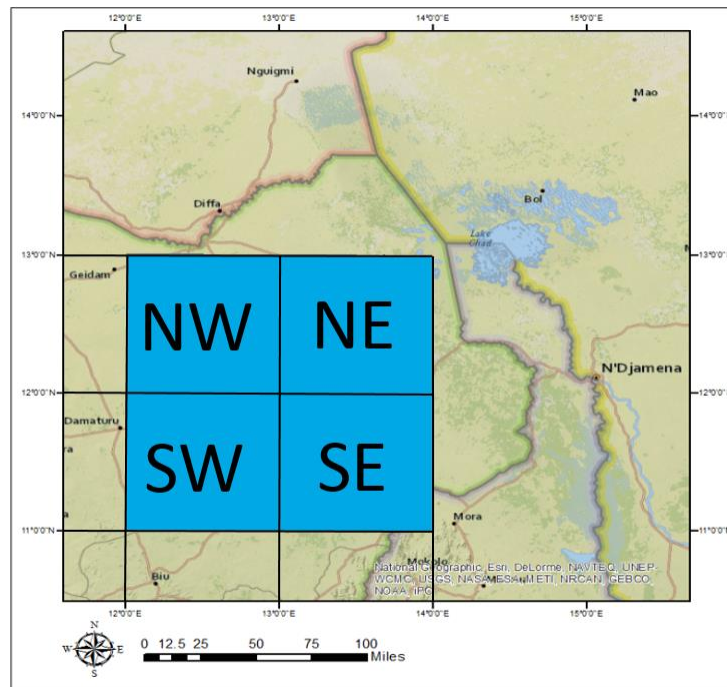


Figure 4.23. Division of 2x2 area into 1° individual cells.

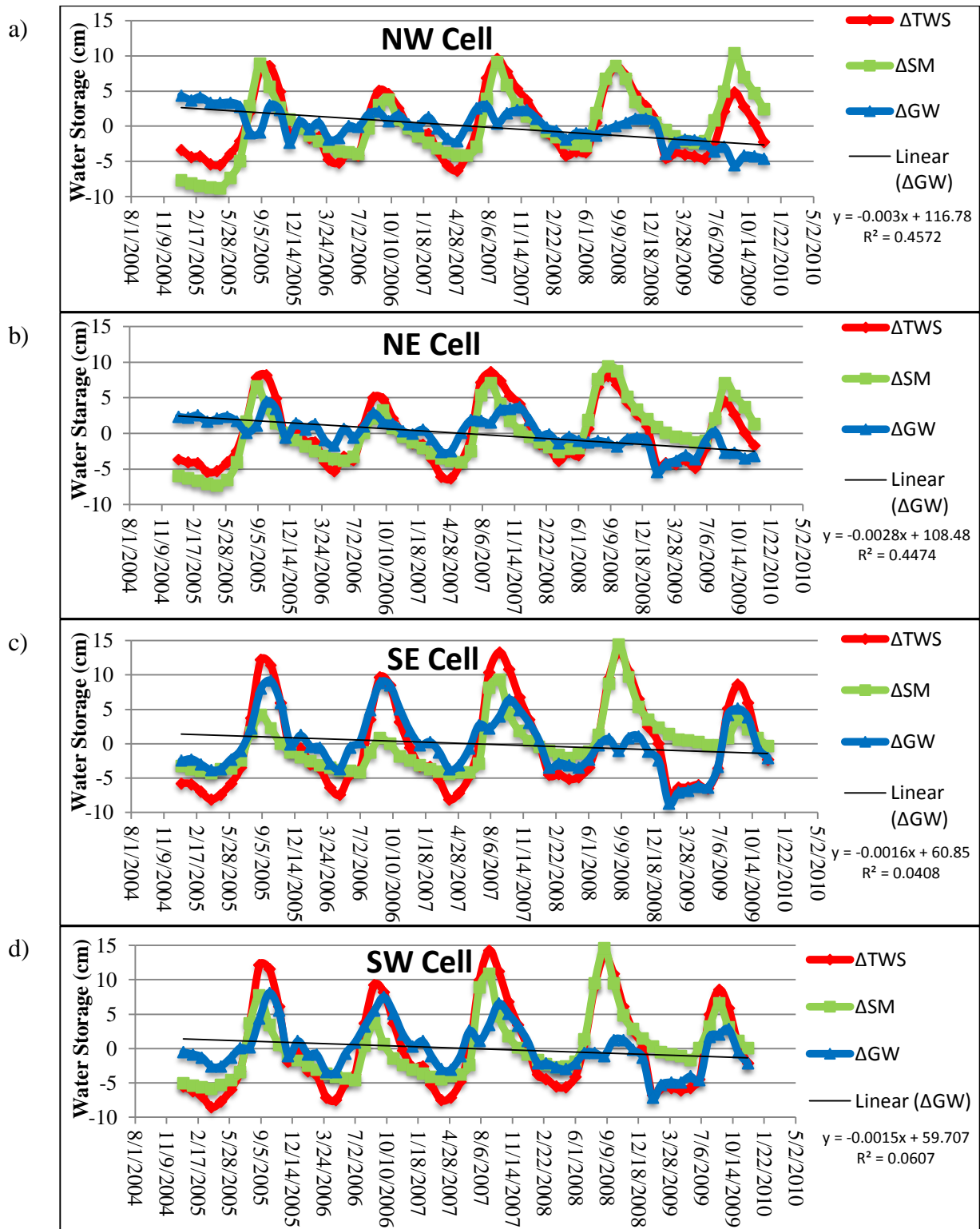


Figure 4.24. Effect of individual cell of 2x2 area: (a) northwestern, (b) northeastern, (c) southeastern, (d) southwestern cell.

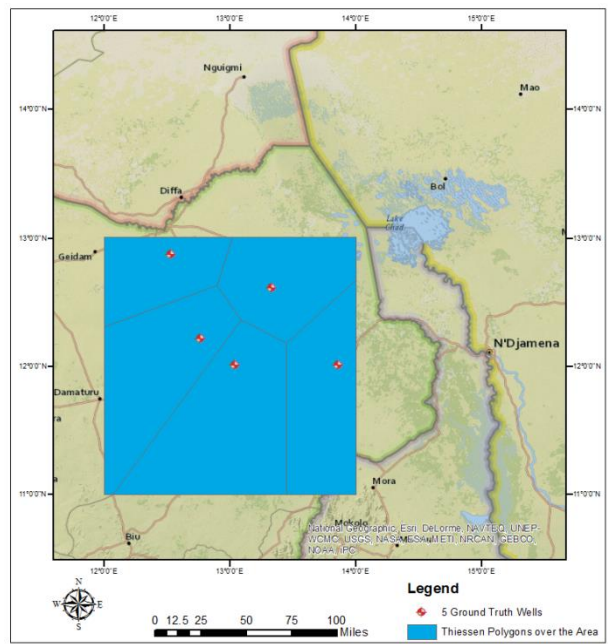
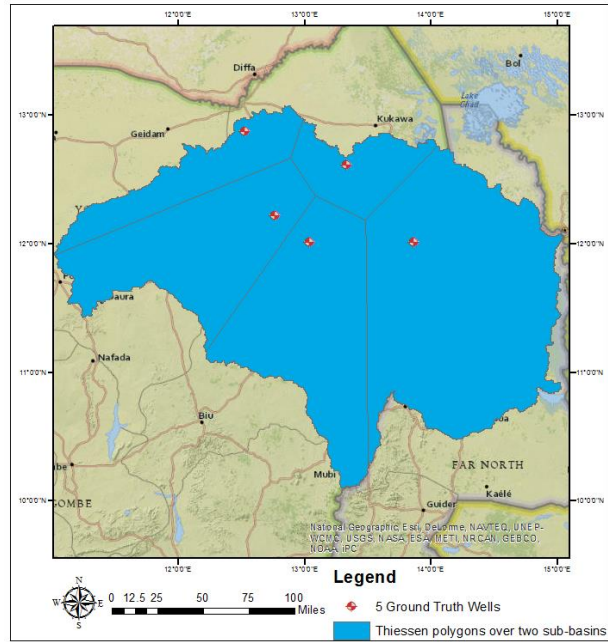


Figure 4.25. The coverage area of the Lake Chad Ngadda Catchment using a sub-basin area boundary and 2° by 2° area.

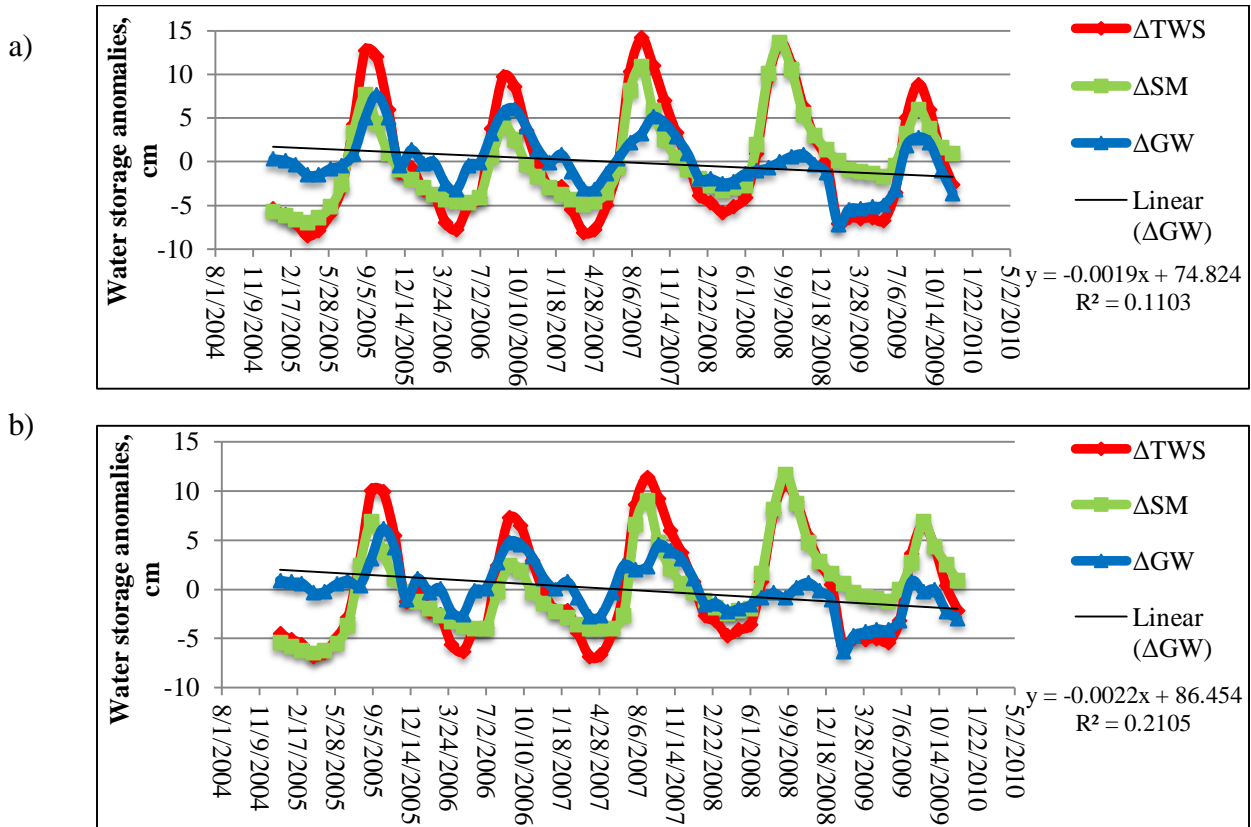


Figure 4.26. Effect of coverage area: The results of applying (a) sub-basin area boundary and (b) 2x2 area.

CHAPTER 5

CONCLUSION

We conducted a study to estimate the variations of groundwater using remotely sensed Gravity Recovery and Climate Experiment and ground truth data. We presented two case studies of modeling groundwater variations, one in a data-rich region and the other in a data-poor region. The advantage of using GRACE modeling is that it allows us to determine groundwater change over a continuous period of time in the region with limited accessibility to the Basin and a lack of ground truth data.

The Upper Mississippi Basin, as a data-rich region, verified the GRACE efficiency and accuracy in groundwater change estimations. The simulated results considered the effect of soil moisture models, groundwater fluctuations in the monitoring well, and the matter of the aquifer. The most accurate GRACE modeling setup determined the effect of soil moisture model and aquifer. The results showed that the best fit soil moisture model is CLM. The calculated correlation coefficient is 86.1%, which signifies strong correlation between remote sensed and ground truth time series. Also, the results showed that the best selection of well observations is from a homogeneous aquifer. The results showed that the best fit model is 11 well observations from the same sand and gravel aquifer with strong correlation of 73.4%. I would like to combine these two well correlated conditions in one case to find the best match of the data. Figure 5.1 performs the analysis using CLM soil moisture model and selecting 11 well observations from the same aquifer.

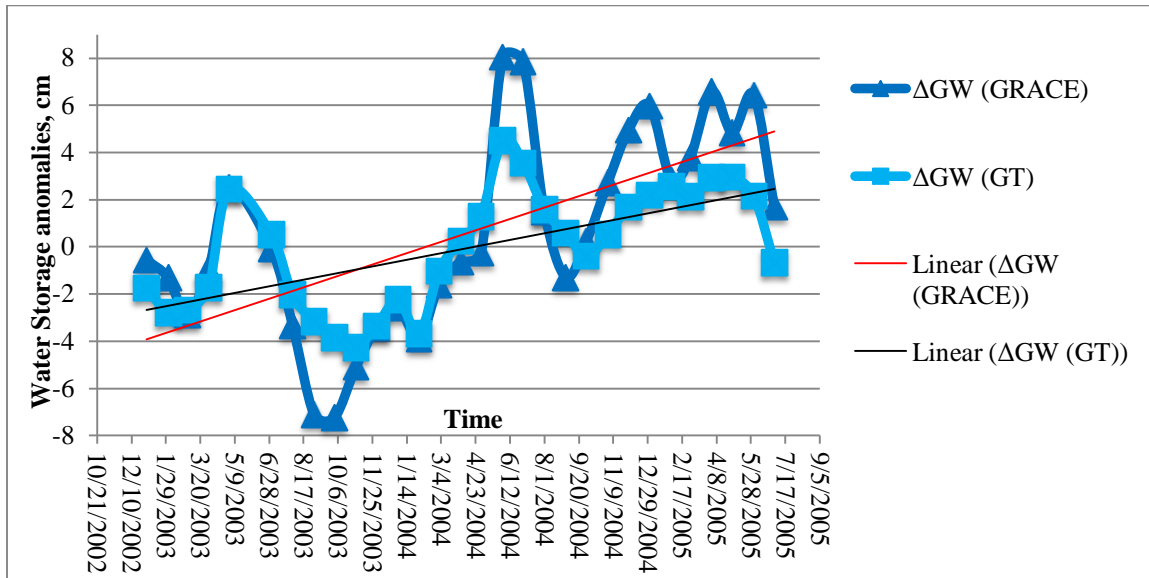


Figure 5.1. Effect of CLM and 11 groundwater monitoring wells.

The calculated correlation coefficient value is 0.918 or 91.8%, which means that these two series are highly correlated. This is the strongest relationship between groundwater estimates from GRACE and ground truth data. Figure 5.2 shows the closest fit of the observed points to its fitted regression line. The coefficient of determination is 0.844, which means that 84.4% of the variation in ΔGW from GRACE directly accounted for the variations in ΔGW from well observations.

The Ngadda catchment of the Lake Chad Basin as a data-poor region showed the ability of GRACE to analyze groundwater changes using the same modeling approach. The simulated results considered the effect of soil moisture models, scales, groundwater fluctuations in the individual cell, and the coverage area. Overall, the groundwater anomalies' in each parameter effect showed seasonal amplitudes pattern. The high picks occurred in a wet season, while low picks occurred during a dry season in the region. In addition, the results showed the negative regression line, which means that the groundwater

change has been decreasing since 2005. The results showed that CLM soil moisture model had the greatest effect and more stable fluctuations of groundwater storage anomalies. We assume that the result from CLM soil moisture provides the best fit match.

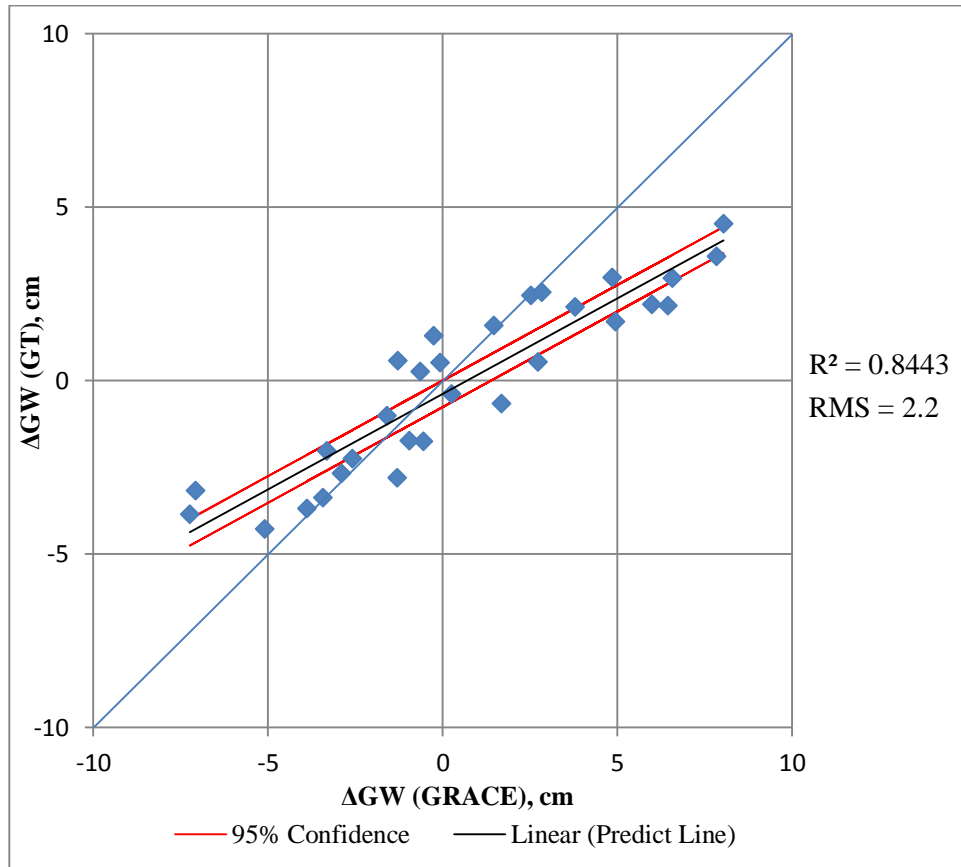


Figure 5.2. Correlation between groundwater anomalies from GRACE and CLM soil moisture model and from 11 well observations.

The present study shows that GRACE modeling approach is capable of investigating the groundwater changes in data-poor regions. We were able to fill the data gap from November 2005 to July 2009. The effect of soil moisture model is the most valuable condition for the study area. The disadvantage of GRACE is that data is available only in 1° degree resolution, which is coarse for the regional scale application. However, the solution in

this case would be to use 0.25° degree soil moisture data and downscale it as in the Ngadda catchment example.

APPENDIX

Python Program for the Upper Mississippi Basin

```
###imports
import os
import math
import numpy
from numpy.ma.core import is_masked
from netCDF4 import Dataset

###Constants
NODATA = '32767.000'

###Functions
def buildGraceData(graceFileName):
    f = open(graceFileName, 'rU')
    l = f.read()

    d = l.split('\n')
    #remove headers
    d = d[6:]

    #isolate the rows in the data we want
    d = d[42:53]
    grace_data = list()

    #isolate the columnar data we want
    for item in d:
        i = item.split(' ')
        j = i[263:274]
        grace_data.append(j)

    #reverse the data so that it will be in the same order as
    # Soil Moisture data
    grace_data.reverse()

    #close the file
    f.close()

    return grace_data

def buildSMDData(smFileName, num):
    ###For nc (soil moisture)
    rootgrp = Dataset(smFileName, 'r', format='NETCDF4')
    sm_data = list()
    swe_data = list()
    sizeY = len(rootgrp.variables['g0_lat_0'])
    tempSM = list()
    tempSW = list()

    for y in range(0, sizeY):

        for z in range(len(rootgrp.variables['SoilMoist1_GDS0_DBLV'][:,0][y])):
            totalSM = []
```

```

    for x in range(num):
        item = rootgrp.variables['SoilMoist1_GDS0_DBLV'][:,x][y][z]
        totalSM.append(item)
        if y == 0 and z == 0:
            pass
        sumSM = sum(totalSM)
        if numpy.isnan(sumSM):
            tempSM.append(rootgrp.variables['SoilMoist1_GDS0_DBLV'][:,x][y][z])
        else:
            tempSM.append(sumSM)
    for item in rootgrp.variables['SWE_GDS0_SFC'][:,y]:
        tempSW.append(item)

    sm_data.append(tempSM[2:])
    swe_data.append(tempSW[2:])
    #reset SM and SW temp lists
    tempSM = list()
    tempSW = list()
    sm_data = sm_data[1:12]
    swe_data = swe_data[1:12]
    return sm_data, swe_data

def basinAreaMask():
    mask = []
    mask.append([False, False, False, False, False, False, False, True, False, False, False])
    mask.append([False, False, False, False, False, False, True, True, False, False, False])
    mask.append([False, False, False, False, False, True, True, True, True, False, False])
    mask.append([False, False, False, False, False, True, True, True, True, True, False])
    mask.append([False, False, True, True, True, True, True, True, True, True, True])
    mask.append([False, False, True, True, True, True, True, True, True, False, False])
    mask.append([False, True, True, True, True, True, True, True, False, False, False])
    mask.append([True, True, True, True, True, True, True, True, False, False, False])
    mask.append([False, False, True, True, True, False, False, False, False, False, False])
    mask.append([False, False, True, False, False, False, False, False, False, False, False])

    return mask

def createFile(newFile, data):
    #Build "NODATA" line
    fullLineNoDataGrace = (NODATA + ' ') * 360
    fullLineNoDataGrace = fullLineNoDataGrace.strip().split(' ')

    #Write the data to a file
    #create a new list to hold the data we will write to a file
    newNCASCIIFile = list()

    #create first six lines
    newNCASCIIFile.append('ncols      11')
    newNCASCIIFile.append('nrows      11')
    newNCASCIIFile.append('xllcorner  -97.356126378418')
    newNCASCIIFile.append('yllcorner  36.961829841827')
    newNCASCIIFile.append('cellsize   1')
    newNCASCIIFile.append('NODATA_value -9999')

    #write actual SM data
    for val in data:

```

```

    newLine = list()
    for x in val:
        newLine.append(x)
    newNCASCIIFile.append(newLine)

#now that the data is compiled, write it to a file
#open a new file
g = open("UMB_results/" + newFile, 'w')

#Because the first 6 items of newNCASCIIFile are strings, and all
# the rest are lists, need to deal with them separately.
for n in range(0,6):
    g.write(newNCASCIIFile[n])
    g.write('\n')

for line in newNCASCIIFile[6:]:
    for x in line:
        g.write(str(x) + ' '),
    g.write('\n')

#close the file
g.close()

def findAvgDev(data, avg):
    summation = 0
    for item in data:
        summation += abs(item - avg)
    return summation / len(data)

###Start main
##def main():
#Build the list of nc files that we will be working with
smFiles = []
smCLMFiles = []
smMosaicFiles = []

#build file list for NOAH SM Files
for root, dirs, files in os.walk('SMandSWE'):
    for name in files:
        fname = os.path.join(root, name)
        #only add .nc files to the smFiles list
        if fname[-3:] == '.nc':
            smFiles.append(fname)

#build file list for CLM SM Files
for root, dirs, files in os.walk('CLM_SMandSWE'):
    for name in files:
        fname = os.path.join(root, name)
        #only add .nc files to the smFiles list
        if fname[-3:] == '.nc':
            smCLMFiles.append(fname)

#build file list for NOAH Mosaic Files
for root, dirs, files in os.walk('Mosaic_SMandSWE'):
    for name in files:
        fname = os.path.join(root, name)

```

```

    #only add .nc files to the smFiles list
    if fname[-3:] == '.nc':
        smMosaicFiles.append(fname)

#Build the list of GRACE data files that we will be working with
graceFiles = []

for root, dirs, files in os.walk('GRACE_data'):
    for name in files:
        fname = os.path.join(root, name)
        if 'CSR' in fname:
            graceFiles.append(fname)

#determine boundaries of data
rootgrp = Dataset(smFiles[0], 'r', format='NETCDF4')
sizeX = 11
sizeY = 11

#Build "NODATA" line
fullLineNoDataGrace = (NODATA + ' ') * 1440
fullLineNoDataGrace = fullLineNoDataGrace.strip().split(' ')

#Create the ground water "sum" data list
groundWaterData = list()
z = 0
for y in range(0, sizeY):
    lineList = []
    for x in range(0, sizeX):
        lineList.append(z)
    groundWaterData.append(lineList)

#create structures to hold the mean and the average deviation
smAvgDict = {}
swAvgDict = {}
grAvgDict = {}
gwAvgDict = {}
smSTDDict = {}
swSTDDict = {}
grSTDDict = {}
gwSTDDict = {}

smNOAASumDict = {}
smCLMSumDict = {}
smMOSAICSumDict = {}
#create mask file
mask = basinAreaMask()
#process each set of grace and sm files
for smF in smFiles:
    smAvg = []
    swAvg = []
    grAvg = []
    gwAvg = []

    #determine the year/month of the file from the filename
    x = smF.find('_M.A')
    tmpDate = smF[x+4:x+10]

```

```

#find the corresponding grace file, if it exists
for graceF in graceFiles:
    if tmpDate in graceF:
        #if found, remove it from the graceFiles list so we don't
        # have to look at it on the next search
        graceFiles.remove(graceF)
        #once found, stop looking through the graceFiles list
        break
for CLMF in smCLMFiles:
    if tmpDate in CLMF:
        #if found, remove it from the smCLMFiles list so we don't
        # have to look at it on the next search
        smCLMFiles.remove(CLMF)
        #once found, stop looking through the smCLMFiles list
        break

for mosaicF in smMosaicFiles:
    if tmpDate in mosaicF:
        #if found, remove it from the smMosaicFiles list so we don't
        # have to look at it on the next search
        #once found, stop looking through the smMosaicFiles list
        break

#extract the sm, sw and grace data from the files (the integer is the number of sublayers)

sm, sw = buildSMDData(smF, 4)
sm2, sw2 = buildSMDData(CLMF, 10)
sm3, sw3 = buildSMDData(mosaicF, 3)
##sum up all valid values
smTotal = 0
for line in sm:
    lineTotal = 0
    for item in line:
        if not is_masked(item):
            lineTotal += item
    smTotal += lineTotal
smNOAASumDict[tmpDate] = smTotal
smTotal = 0
for line in sm2:
    lineTotal = 0
    for item in line:
        if not is_masked(item):
            lineTotal += item
    smTotal += lineTotal
smCLMSumDict[tmpDate] = smTotal
smTotal = 0
for line in sm3:
    lineTotal = 0
    for item in line:
        if not is_masked(item):
            lineTotal += item
    smTotal += lineTotal
smMOSAICSumDict[tmpDate] = smTotal

grace = buildGraceData(graceF)
yVals = list()

```

```

for y in range(0, sizeY):
    xVals = list()
    for x in range(0, sizeX):
        if mask[y][x]:
            #calculate
            grAvg.append(float(grade[y][x]))

            if is_masked(sm[y][x]):
                xVals.append(NODATA)
                groundwaterData[y][x] = NODATA
            else:

                smAvg.append((sm[y][x] + sm2[y][x] + sm3[y][x]) /3 / 10)

                calc = float(grade[y][x]) - (((sm[y][x] + sm2[y][x] + sm3[y][x]) /3
                    + (sw[y][x] + sw2[y][x] + sw3[y][x])/3) /10.0)

                gwAvg.append(calc)
                xVals.append(calc)
                groundwaterData[y][x]+= calc

            if not is_masked(sw[y][x]):
                swAvg.append((sw[y][x] + sw2[y][x] + sw3[y][x]) /3 /10)
            else:
                xVals.append(-9999)

        yVals.append(xVals)
#calculate and store the average
smAvgDict[tmpDate] = numpy.average(smAvg)
swAvgDict[tmpDate] = numpy.average(swAvg)
grAvgDict[tmpDate] = numpy.average(grAvg)
if tmpDate == '200301':
    print grAvg
gwAvgDict[tmpDate] = numpy.average(gwAvg)
#calculate and store the average deviation
smSTDDict[tmpDate] = numpy.std(smAvg)
swSTDDict[tmpDate] = numpy.std(swAvg)
grSTDDict[tmpDate] = numpy.std(grAvg)
gwSTDDict[tmpDate] = numpy.std(gwAvg)

#reverse the data so that it will be written to the file in
# the correct order
yVals.reverse()

#write data to a file
createFile(tmpDate + '.asc', yVals)
#convert from double-value in groundwaterData to single-value

groundWaterData.reverse()
createFile("ground_water_sum_data.asc", groundWaterData)

#calculate the total average based on all monthly averages for sm and sw
totalMeansm = numpy.average(smAvgDict.values())
totalMeansw = numpy.average(swAvgDict.values())
totalMeangw = numpy.average(gwAvgDict.values())

```

```

keys = smAvgDict.keys()
smDeviation = {}
smDeviation1 = {}
for k in keys:
    D = totalMeansm - smAvgDict[k]
    D1 = smAvgDict[k] - totalMeansm
    smDeviation[k] = D
    smDeviation1[k] = D1

keys = swAvgDict.keys()
swDeviation = {}
swDeviation1 = {}
for k in keys:
    D = totalMeansw - swAvgDict[k]
    D1 = swAvgDict[k] - totalMeansw
    swDeviation[k] = D
    swDeviation1[k] = D1

keys = gwAvgDict.keys()
gwDeviation = {}
gwDeviation1 = {}
for k in keys:
    D = totalMeangw - gwAvgDict[k]
    D1 = gwAvgDict[k] - totalMeangw
    gwDeviation[k] = D
    gwDeviation1[k] = D1

#create a file with the averages of all types
f = open('UMB_results/avg.csv', 'w')
k = smAvgDict.keys()
k.sort()

#write header row
f.write('Date' + ',' + 'Soil Moisture Avg' + ',' + 'Snow Water Avg' + ',' + 'Grace Avg' +
',' + 'Ground Water Avg' + ',' + 'SM STD' + ',' + 'SW STD' + ',' +
'Grace STD' + ',' + 'GW STD' + ',' + 'SM Total M-Month M' + ',' +
'SW Total m-Month M' + ',' + 'GW Total M-Month M' + ',' +
'SM Month M-Total M' + ',' + 'SW Month M-Total M' + ',' + 'GW Month M-Total M' +
',' + 'NOAA SM Sum' + ',' + 'CLM SM Sum' + ',' + 'MOSAIC SM Sum\n')

#write the average (mean) and the average deviation
for key in k:
    f.write(key[0:4] + '-' + key[4:] + '-' + '01' + ',' + str(smAvgDict[key]) +
',' + str(swAvgDict[key]) + ',' + str(grAvgDict[key]) + ',' + str(gwAvgDict[key]) +
',' + str(smSTDDict[key]) + ',' + str(swSTDDict[key]) + ',' + str(grSTDDict[key]) +
',' + str(gwSTDDict[key]) + ',' + str(smDeviation[key]) +
',' + str(swDeviation[key]) + ',' + str(gwDeviation[key]) +
',' + str(smDeviation1[key]) + ',' + str(swDeviation1[key]) +
',' + str(gwDeviation1[key]) + ',' + str(smNOAASumDict[key]) + ',' +
str(smCLMSumDict[key]) + ',' + str(smMOSAICSumDict[key]) + '\n')

f.close()

### this is the boilerplate portion
##if __name__ == '__main__':
##    main()

```

Python Program for the Ngadda Catchment of the Lake Chad Basin

```
###imports
import os
import math
import numpy
from numpy.ma.core import is_masked
from netCDF4 import Dataset

###Constants
NODATA = '32767.000'

###Functions
def buildGraceData(graceFileName):
    f = open(graceFileName, 'rU')
    l = f.read()

    d = l.split('\n')
    #remove headers
    d = d[6:]

    #isolate the rows in the data we want
    d = d[76:79]

    grace_data = list()

    #isolate the columnar data we want
    for item in d:
        i = item.split(' ')
        j = i[12:14]
        grace_data.append(j)

    #reverse the data so that it will be in the same order as
    # Soil Moisture data
    grace_data.reverse()

    #close the file
    f.close()

    return grace_data

def buildSMDData(smFileName, num):
    ###For nc (soil moisture)
    rootgrp = Dataset(smFileName, 'r', format='NETCDF4')
    sm_data = list()
    swe_data = list()
    sizeY = len(rootgrp.variables['g0_lat_0'])
    tempSM = list()
    tempSW = list()
    for y in range(1, sizeY-1):

        for z in range(1, len(rootgrp.variables['SoilMoist1_GDS0_DBL Y'][:,0][y])-1):
            totalSM = []
            for x in range(num):
                item = rootgrp.variables['SoilMoist1_GDS0_DBL Y'][:,x][y][z]
```

```

        totalSM.append(item)
        if y == 0 and z == 0:
            pass
            #print item, totalSM
        sumSM = sum(totalSM)
        if numpy.isnan(sumSM):
            tempSM.append(rootgrp.variables['SoilMoist1_GDS0_DBLV'][:,x][y][z])
        else:
            tempSM.append(sumSM)
    for item in rootgrp.variables['SWE_GDS0_SFC'][:,y]:
        tempSW.append(item)
        if item > 0:
            print "Snow Water > 0 Detected!"

    sm_data.append(tempSM)
    swe_data.append(tempSW)
    #reset SM and SW temp lists
    tempSM = list()
    tempSW = list()

return sm_data, swe_data

def basinAreaMask():
    mask = []
    mask.append([True, True])
    mask.append([True, True])
    mask.append([False, False])

return mask

def createFile(newFile, data):
    #Build "NODATA" line
    fullLineNoDataGrace = (NODATA + ' ') * 360
    fullLineNoDataGrace = fullLineNoDataGrace.strip().split(' ')

    #Write the data to a file
    #create a new list to hold the data we will write to a file
    newNCASCIIFile = list()

    #create first six lines
    newNCASCIIFile.append('ncols      8')
    newNCASCIIFile.append('nrows      8')
    newNCASCIIFile.append('xllcorner  12')
    newNCASCIIFile.append('yllcorner  11')
    newNCASCIIFile.append('cellsize  0.25')
    newNCASCIIFile.append('NODATA_value -9999')

    ## #create next 41 lines of NODATA
    ## for n in range(41):
    ##     newNCASCIIFile.append(fullLineNoDataGrace)

    #write actual SM data
    for val in data:
        newLine = list()
        for x in val:
            newLine.append(x)

```

```

    newNCASCIIFile.append(newLine)

#now that the data is compiled, write it to a file
#open a new file
g = open("LCB_results_025//" + newFile, 'w')

#Because the first 6 items of newNCASCIIFile are strings, and all
# the rest are lists, need to deal with them separately.
for n in range(0,6):
    g.write(newNCASCIIFile[n])
    g.write('\n')

for line in newNCASCIIFile[6:]:
    for x in line:
        g.write(str(x) + ' '),
    g.write('\n')

#close the file
g.close()

def findAvgDev(data, avg):
    summation = 0
    for item in data:
        summation += abs(item - avg)
    return summation / len(data)

def createGraceCellAvg(fileList):
    grace = buildGraceData(fileList[0])
    y = len(grace)
    x = len(grace[0])
    avgList = list()
    for z in range(y):
        tmpList = list()
        for w in range(x):
            tmpList.append(0)
        avgList.append(tmpList)

    for f in fileList:
        grace = buildGraceData(f)
        for z in range(y):
            for w in range(x):
                avgList[z][w] += float(grace[z][w])

    numFiles = len(fileList)
    for z in range(y):
        for w in range(x):
            avg = avgList[z][w] / numFiles
            avgList[z][w] = avg
    print 'grace avg = ', avgList

    return avgList

def createSMCellAvg(fileList, numLayers):
    sm, sw = buildSMData(fileList[0], numLayers)

    y = len(sm)

```

```

x = len(sm[0])

avgList = list()
for z in range(y):
    tmpList = list()
    for w in range(x):
        tmpList.append(0)
    avgList.append(tmpList)

for f in fileList:
    sm, sw = buildSMData(f, numLayers)

    for z in range(y):
        for w in range(x):

            avgList[z][w] += sm[z][w]

numFiles = len(fileList)
for z in range(y):
    for w in range(x):
        avg = avgList[z][w] / numFiles
        avgList[z][w] = avg
print 'avg = ', avgList
print numFiles

return avgList

###Start main
##def main():
#Build the list of nc files that we will be working with
smFiles = []
smCLMFiles = []
smMosaicFiles = []

#build file list for NOAH 0.25 degree SM Files
for root, dirs, files in os.walk('LCB_NOAH_025deg'):
    for name in files:
        fname = os.path.join(root, name)
        #only add .nc files to the smFiles list
        if fname[-3:] == '.nc':
            smFiles.append(fname)

#Build the list of GRACE data files that we will be working with
graceFiles = []

for root, dirs, files in os.walk('GRACE_data_LCB'):
    for name in files:
        fname = os.path.join(root, name)
        if 'CSR' in fname:
            graceFiles.append(fname)

graceAvgCellList = createGraceCellAvg(graceFiles)
smAvgCellList = createSMCellAvg(smFiles, 4)

#determine boundaries of data

```

```

rootgrp = Dataset(smFiles[0], 'r', format='NETCDF4')
sizeX = 8
sizeY = 8

#Create the ground water "sum" data list
groundWaterData = list()
z = 0
for y in range(0, sizeY):
    lineList = []
    for x in range(0, sizeX):
        lineList.append(z)
    groundWaterData.append(lineList)

#create structures to hold the mean and the average deviation
smAvgDict = {}
swAvgDict = {}
grAvgDict = {}
gwAvgDict = {}
smSTDDict = {}
swSTDDict = {}
grSTDDict = {}
gwSTDDict = {}

smNOAASumDict = {}

#create mask file
mask = basinAreaMask()
#process each set of grace and sm files
for smF in smFiles:

    smAvg = []

    swAvg = []
    grAvg = []
    gwAvg = []

    #determine the year/month of the file from the filename
    x = smF.find('_M.A')
    tmpDate = smF[x+4:x+10]
    #find the corresponding grace file, if it exists
    for graceF in graceFiles:
        if tmpDate in graceF:
            #if found, remove it from the graceFiles list so we don't
            # have to look at it on the next search
            graceFiles.remove(graceF)
            #once found, stop looking through the graceFiles list
            break

    #extract the sm, sw and grace data from the files (the integer is the number of sublayers)

    sm, sw = buildSMDData(smF, 4)

    ##sum up all valid values
    smTotal = 0
    for line in sm:
        lineTotal = 0

```

```

for item in line:
    if not is_masked(item):
        lineTotal += item
    smTotal += lineTotal
smNOAASumDict[tmpDate] = smTotal

w = 0
z = 0

grace = buildGraceData(graceF)
yVals = list()
for y in range(0, sizeY):
    #check if we need to move grace data z position (w,z)
    if y == 4:
        z+=1
    xVals = list()
    for x in range(0, sizeX):
        #check if we need to move grace data w position (w,z)
        if x == 4:
            w+=1
        if mask[z][w]:
            #calculate
            grAvg.append(float(grace[z][w]))
            if is_masked(sm[y][x]):
                xVals.append(NODATA)
                groundwaterData[y][x] = NODATA
            else:

                smAvg.append((sm[y][x] ) / 10)
                calc = (float(grace[z][w]) - graceAvgCellList[z][w]) - (((sm[y][x] - smAvgCellList[y][x])
                    + sw[y][x]) / 10.0)

                gwAvg.append(calc)
                xVals.append(calc)

                groundwaterData[y][x]+= calc

            if not is_masked(sw[y][x]):
                swAvg.append(sw[y][x] /10)
            else:
                xVals.append(-9999)
        w = 0
    yVals.append(xVals)
#calculate and store the average
smAvgDict[tmpDate] = numpy.average(smAvg)
swAvgDict[tmpDate] = numpy.average(swAvg)
grAvgDict[tmpDate] = numpy.average(grAvg)
if tmpDate == '200501':
    print '200501 = ', smAvg
gwAvgDict[tmpDate] = numpy.average(gwAvg)
#calculate and store the average deviation
smSTDDict[tmpDate] = numpy.std(smAvg)
swSTDDict[tmpDate] = numpy.std(swAvg)
grSTDDict[tmpDate] = numpy.std(grAvg)
gwSTDDict[tmpDate] = numpy.std(gwAvg)

```

```

#reverse the data so that it will be written to the file in
# the correct order
yVals.reverse()

#write data to a file
createFile(tmpDate + '.asc', yVals)
#convert from double-value in groundwaterData to single-value

groundWaterData.reverse()

createFile("ground_water_sum_data.asc", groundWaterData)

#calculate the total average based on all monthly averages for sm and sw
totalMeansm = numpy.average(smAvgDict.values())
totalMeansw = numpy.average(swAvgDict.values())
totalMeangw = numpy.average(gwAvgDict.values())
totalMeangr = numpy.average(grAvgDict.values())

keys = smAvgDict.keys()
smDeviation = {}
smDeviation1 = {}
for k in keys:
    D = totalMeansm - smAvgDict[k]
    D1 = smAvgDict[k] - totalMeansm
    smDeviation[k] = D
    smDeviation1[k] = D1

keys = swAvgDict.keys()
swDeviation = {}
swDeviation1 = {}
for k in keys:
    D = totalMeansw - swAvgDict[k]
    D1 = swAvgDict[k] - totalMeansw
    swDeviation[k] = D
    swDeviation1[k] = D1

keys = gwAvgDict.keys()
gwDeviation = {}
gwDeviation1 = {}
for k in keys:
    D = totalMeangw - gwAvgDict[k]
    D1 = gwAvgDict[k] - totalMeangw
    gwDeviation[k] = D
    gwDeviation1[k] = D1

keys = grAvgDict.keys()
grDeviation = {}
grDeviation1 = {}
for k in keys:
    D = totalMeangr - grAvgDict[k]
    D1 = grAvgDict[k] - totalMeangr
    grDeviation[k] = D
    grDeviation1[k] = D1

#create a file with the averages of all types
f = open('LCB_results_025//avg.csv', 'w')

```

```

k = smAvgDict.keys()
k.sort()

#write header row
f.write('Date' + ',' + 'Soil Moisture Avg' + ',' + 'Snow Water Avg' + ',' + 'Grace Month-M' +
',' + 'Ground Water Avg' + ',' + 'SM STD' + ',' + 'SW STD' + ',' +
'Grace STD' + ',' + 'GW STD' + ',' + 'SM Total M-Month M' + ',' +
'SW Total m-Month M' + ',' + 'GW Total M-Month M' + ',' +
'SM Month M-Total M' + ',' + 'SW Month M-Total M' + ',' + 'GW Month M-Total M' +
',' + 'NOAA SM Sum\n')

#write the average (mean) and the average deviation
for key in k:
    f.write(key[0:4] + '-' + key[4:] + '-' + '01' + ',' + str(smAvgDict[key]) +
',' + str(swAvgDict[key]) + ',' + str(grDeviation1[key]) + ',' + str(gwAvgDict[key]) +
',' + str(smSTDDict[key]) + ',' + str(swSTDDict[key]) + ',' + str(grSTDDict[key]) +
',' + str(gwSTDDict[key]) + ',' + str(smDeviation[key]) +
',' + str(swDeviation[key]) + ',' + str(gwDeviation[key]) +
',' + str(smDeviation1[key]) + ',' + str(swDeviation1[key]) +
',' + str(gwDeviation1[key]) + ',' + str(smNOAASumDict[key]) + '\n')

f.close()

### this is the boilerplate portion
##if __name__ == '__main__':
##    main()

```

REFERENCES

- Albergel, J. "Genèse et Prédétermination des Crues au Burkina Faso; du m² au km², Étude des Paramètres Hydrologiques et de Leur Évolution." Ph.D. Thesis, Université Paris 6, Editions de l'Orston, 1987, 330 p.
- Arad, A. and U. Kafri. "Geochemistry of Groundwater in the Chad Basin." *J. Hydrol.* 25, (1975): 105-127.
- Boronina, A. and G. Ramillien. "Application of Avhrr Imagery and Grace Measurements for Calculation of Actual Evapotranspiration over the Quaternary Aquifer (Lake Chad Basin) and Validation of Groundwater Models." *J. Hydrol.* 348, (2008): 98-109.
- Bumba, J., H. Kida and Z. Bunu. "Exploitation of Underground Water in the Chad Formation - Maiduguri as a Case Study." In the *Arid Zone Hydrology and Water Resources*, edited by N.M. Gadzama, F.A. Adeniji, W.S. Richards, and G.G.R. Thambiyahpillay. Ibadan, University of Maiguguri, Nigeria, (1985): 89-98.
- Coe, M.T. and J.A. Foley. "Human and Natural Impacts on the Water Resources of the Lake Chad Basin." *J. Geophys. Res.* 106 (D4) (2001): 3349-3356.
- Crétaux, J.F. and C. Birkett. "Lake Studies from Satellite Radar Altimetry." *C. R. Geosci.* 338, (2006): 1098-1112.
- Descroix, L., G. Mahé, T. Lebel, G. Favreau, S. Galle, E. Gautier, J.C. Olivry, J. Albergel, O. Amogu, B. Cappelaere, R. Dessouassi, A. Diedhiou, E. Le Breton, I. Mamadou and D. Sighomnou. "Spatio -Temporal Variability of Hydrological Regimes around the Boundaries between Sahelian and Sudanian Areas of West Africa: A Synthesis." *J. Hydrol.* 375, no. 1-2 (2009): 90-102.
- Edmunds, W.M., E. Fellman and I.B. Goni. "Spatial and Temporal Distribution of Groundwater Recharge in Northern Nigeria." *Hydrogeological Journal*, no. 10 (2002): 205-215.
- Eilers, V.H.M., R.C. Carter and K.R. Rushton. "A Single Layer Soil Water Balance Model for Estimating Deep Drainage (Potential Recharge): An Application to Cropped Land in Semi-Arid North-East Nigeria." *Geoderm.* 140, (2007): 119-131.
- Food and Agriculture Organization (FAO). *Adaptive Water Management in the Lake Chad Basin: Addressing Current Challenges and Adapting to Future Needs*. Stockholm: Food and Agriculture Organization (FAO) Water Seminar Proceedings, 2009.
- FAO. *Irrigation Potential in Africa: A Basin Approach*. FAO Land and Food Bulletin 4. Land and Water Development Division, Chapter 6. 1997.

- Favreau, G., C. Leduc, C. Marlin, M. Dray, J.D. Taupin, M. Massault, C.L. Salle and M. Babic. "Estimate of Recharge of a Rising Water Table in Semiarid Niger from 3h and 14c Modeling." *Ground Water* 40, no. 2 (2002): 144-151.
- Fortnam, M.P. and J.A. Oguntola. *Lake Chad Basin*. Kalmar, Sweden: University of Kalmar, 2004.
- Goni, I.B., E. Fellman and W.M. Edmunds. "Rainfall Geochemistry in the Sahel Region of Northern Nigeria." *Atmos. Environ.* 35, (2001): 4331-4339.
- Grove, A.T. "African River Discharge and the Lake Levels in Twentieth Century." In *The Limnology, Climatology and Paleoclimatology of the East African Lakes*, edited by Johnson, T.C. and Odada, E. Newark: Gordon and Breach, (1996): 95-100.
- Intergovernmental Panel on Climate Change (IPCC). *Climate Change 2001: Impacts, Adaptation, and Vulnerability - Contribution of Working Group Ii to the Third Assessment Report of the IPCC. Chapter 10.2.6.3. Climatic Factors in Desertification*, 2001.
- Isiorho, S.A., J.A. Oguntola and A. Olojoba. "Conjunctive Water Use as a Solution to Sustainable Economic Development in Lake Chad Basin, Africa." 10th World Water Congress: Water, the World's Most Important Resource, (2000): 330-340.
- Isiorho, S. A. and J. Njock-Libii. "Sustainable Water Resources Management Practice." *Global Networks for Environmental Information 11*, (1996): 855-860.
- Keith, J.O. and D.C. Plowers. *Consideration of Wildlife Resources and Land Use in Chad*. Productive Sector Growth and Environment Division Office of Sustainable Development, Bureau for Africa: U.S. Agency for International Development, 1997.
- Kimmage, K. and W.M. Adams. "Wetland Agricultural Production and River Basin Development in the Hadejia-Jama'are Valley, Nigeria." *The Geographical Journal*, no. 158 (1992): 1-12.
- Kindler, J., P. Warshall, E.J. Arnould, C.F. Hutchinson and R. Varady. "The Lake Chad Conventional Basin - a Diagnostic Study of the Environmental Degradation." UNEP and UNSO, 1990.
- Koster, R.D., M.J. Suarez, A. Ducharne, M. Stieglitz and P. Kumar. "A Catchment-Based Approach to Modeling Land Surface Processes in a General Circulation Model. 1. Model Structure." *J. Geophys. Res.* 105, (2000): 24809-24822.
- Landerer, F.W. and S.C. Swenson. "Accuracy of Scaled Grace Terrestrial Water Storage Estimates." *Water Resources Research* 48, no. 4 (2012): 0-Citation W04531.

- Lake Chad Basin Commission (LCBC). "Synthèse Hydrologique Du Bassin Du Lac Tchad, Report by Lake Chad Basin Commission (LCBC)." UNESCO. ORSTROM Publication, Paris, France, 1969.
- Le Coz, M., F. Delclaux, P. Genthon and G. Favreau. "Assessment of Digital Elevation Model (Dem) Aggregation Methods for Hydrological Modeling: Lake Chad Basin, Africa." *Comp. Geosci.* 35, (2009): 1661-1670.
- Leblanc, M., G. Favreau, S. Tweed, C. Leduc, M. Razack and L. Mofor. "Remote Sensing for Groundwater Modelling in Large Semiarid Areas: Lake Chad Basin, Africa." *Hydrogeol. J.* 15, (2007): 97-100.
- Leblanc, M., M. Razack, D. Dagorne, L. Mofor and C. Jones. "Application of Meteorological Thermal Data to Map Soil Infiltrability in the Central Part of the Lake Chad Basin, Africa." *Geophys. Res. Lett.* 30, no. 19 (2003).
- Li, B., M. Rodell, B.F. Zaitchik, R.H. Reichle, R.D. Koster and M.A. Tonie. "Assimilation of Grace Terrestrial Water Storage into a Land Surface Model: Evaluation and Potential Value for Drought Monitoring in Western and Central Europe." *Journal of Hydrology (Amsterdam)* 446-447, (2012): 103-115.
- Li, K.Y., M.T. Coe, N. Ramankutty and R. De Jong. "Modeling the Hydrological Impact of Land-Use Change in West Africa." *J. Hydrol.* 337, (2007): 258-268.
- Luxereau, A., P. Genthon and J.-M.A. Karimou. "Fluctuations in the Size of Lake Chad: Consequences on the Livelihoods of the Riverain Peoples in Eastern Niger." *Reg. Environ. Change*, 12 (3), (2012): 507-521.
- Mahé, G. and J.-E. Paturel. "1896-2006 Sahelian Annual Rainfall Variability and Runoff Increase of Sahelian Rivers." *C. R. Geosci.* 341, (2009): 538-546.
- Neiland, A.E. and I. Verinumbe. *Fisheries Development and Resource-Usage Conflict: A Case Study of Deforestation Associated with the Lake Chad Fishery in Nigeria.* Centre for the Economics and Management of Aquatic Resources, 1990.
- Odada, E., L. Oyebande and A. J. Oguntola. "Lake Chad Experience and Lessons Learned Brief", N'Djamena: Lake Chad Basin Commission, 2005; R. Hassan, *Climate Change and African Agriculture*, Policy Note No. 33, Pretoria, South Africa, Centre for Environmental Economics and Policy in Africa, (2006).
- Olofin, E.A. "The Failure of Alau Reservoir to Fill: A Legacy of Unconfined, Leaking Basin of the Mega-Chad Floor." *Séminaire du Réseau Méga-Tchad (Colloques et Séminaires)*, ISBN 2-7099-1373-9, (1997): 181-189.
- Rodell, M., J. Chen, H. Kato, J. Famiglietti, J. Nigro and C. Wilson. "Estimating Groundwater Storage Changes in the Mississippi River Basin (USA) Using Grace"

- Hydrogeology J.* 15, (2007): 159–166.
- Rodell, M. and J. Famiglietti. "Detectability of Variations in Continental Water Storage from Satellite Observations of the Time Dependent Gravity Field." *Water Resour. Res.* 35, (1999): 2705–2723
- Rushton, K.R., V.H.M. Eilers and R.C. Carter. "Improved Soil Moisture Balance Methodology for Recharge Estimation." *J. Hydrol.* 318, (2006): 379-399.
- Scanlon, B.R., L. Lonquevergne and D. Long. "Ground Referencing Grace Satellite Estimates of Groundwater Storage Changes in the California Central Valley, USA." *Water Resources Research*, 48, no. W04520 (2012): 1-9.
- Schmidt, R., F. Flechtner, U. Meyer, K. H. Neumayer, C. Dahle, R. Koenig and R. Kusche. "Hydrological Signals Observed by the Grace Satellites." *Surveys in Geophysics* 29, no. 4-5 (2008): 319-334.
- Schmidt, R., P. Schwintzer, F. Flechtner, C. Reigber, A. Guentner, P. Doell, G. Ramillien, A. Cazenave, S. Petrovic, H. Jochmann and J. Wuensch. "Grace Observations of Changes in Continental Water Storage." *Global and Planetary Change* 50, no. 1-2 (2006): 112-126.
- Schneider, J.L. "Contribution of Isotopic Data to Palaeohydroclimatological Investigations - the Late Pleistocene Formations of Northern Kanem (Chad)" *Comptes rendus de l'academie des sciences serie ii* no. 312 (1991): 869-874.
- Schneider, J.L. "Carte Hydrogéologique au 1/500 000." In Rapport de Synthèse de la Feuille de Mao et Fort-Lamy, République du Tchad .BRGM LAM.67.A4, 1966.
- Schrama, E.J.O., B. Wouters and D.A. Lavalée. "Signal and Noise in Gravity Recovery and Climate Experiment (Grace) Observed Surface Mass Variations." *Journal of Geophysical Research* 112, no. B8 (2007): 0-B08407.
- Schuster, M., C. Roquin, P. Düringer, M. Brunet, M. Caugy, M. Fontugne, H.T. Mackaye, P. Vignaud and J.-F. Ghienne. "Holocene Lake Mega-Chad Palaeoshorelines from Space." *Q. Sci. Rev.* 24, (2005): 1821–1827.
- Stark, J.R., J.D. Fallon, A.L. Fong, R.M. Goldstein, P.E. Hanson, S.E. Kroening and K.E. Lee. "Water-Quality Assessment of Part of the Upper Mississippi River Basin, Minnesota and Wisconsin—Design and Implementation." U.S. Geological Survey Water-Resources Investigations Report 99-4135, (1999): 85.
- Strassberg, G., R. Bridget, B. Scanlon and D. Chambers. "Evaluation of Groundwater Storage Monitoring with the Grace Satellite: Case Study of the High Plains Aquifer, Central United States " *Water Resources Research* 45, no. W05410 (2009).

- Swenson, S., J. Famiglietti, J. Basara and J. Wahr. "Estimating Profile Soil Moisture and Groundwater Variations Using Grace and Oklahoma Mesonet Soil Moisture Data." *Water Resour. Res.* 44, no. W01413, doi: 10.1029/2007WR006057, (2008).
- Swenson, S., P. J.-F. Yeh, J. Wahr and J. Famiglietti. "A Comparison of Terrestrial Water Storage Variations from Grace with in Situ Measurements from Illinois." *Geophys. Res. Lett.* 33, no. L16401, doi: 10.1029/2006GL026962, (2006).
- Tapley, B.D., S. Bettadpur, J.C. Ries, P.F. Thompson and M.M. Watkins. "Grace Measurements of Mass Variability in the Earth System." *Science* 305, (2004): 503–505.
- Thomas, R., M. Meybeck and A. Beim. "Water Quality Assessments - a Guide to Use of Biota, Sediments and Water in Environmental Monitoring." Chapter 7 – Lakes, edited by D. Chapman (1992): 325-370.
- UN Population Division. "World Populations Prospects: The 2002 Revision Population Database." Available at: <http://esa.un.org/unpp>, (2002).
- Wahr, J., S. Swenson, V. Zlotnicki and I. Velicogna. "Time-Variable Gravity from Grace: First Results." *Geophys. Res. Lett.* 31, no. L11501, doi: 10.1029/2004GL019779, (2004).
- Wang, X., C. Linage, J. Famiglietti and S.A. Charles. "Gravity Recovery and Climate Experiment (Grace) Detection of Water Storage Changes in the Three Gorges Reservoir of China and Comparison with in Situ Measurements." *Water Resources Research* 47, no. W12502, doi; 10.1029/2011WR010534, (2011).
- Wolf, M. "Direct Measurement of the Earth's Gravitational Potential Using a Satellite Pair." *J. Geophys. Res.* 74, no. 22 (1969): 5295-5300.
- Xie, P. and P. Arkin. "Global Precipitation: A 17-Year Monthly Analysis Based on Gauge Observations, Satellite Estimates and Numerical Model Outputs." *Bull Am Meteorol. Soc.* 78, (1997): 2539–2558
- Zaitchik, B.F., M. Rodell and F. Olivera. "Evaluation of the Global Land Data Assimilation System Using Global River Discharge Data and a Source-to-Sink Routing Scheme." *Water Resources Research* 46, no. W06507, doi: 10.1029/2009WR007811, (2010).
- Zaitchik, B. F., M. Rodell and R.H. Reichle. "Assimilation of Grace Terrestrial Water Storage Data into a Land Surface Model: Results for the Mississippi River Basin." *Journal of Hydrometeorology* 9, no. 3 (2008): 535-548.

VITA

Alla Skaskevych was born on January 25, 1988 in Pervomaysk, Ukraine. In 2009, she earned a Bachelor of Science Degree in Computer Environmental and Economic Monitoring at the Sevastopol National University of Nuclear Energy and Industry, Ukraine. She began work toward her Master Degree in Environmental and Urban Geosciences at the University of Missouri-Kansas City, in the fall of 2011. During her research at the University of Missouri-Kansas City, she participated in the Lake Chad project “Interactions and feedbacks between biomass burning and water cycle dynamics across the Northern Sub-Saharan African (NSSA) region” funded by NASA and NSF as a research assistant. Her duty was conducting groundwater level analysis and geospatial analysis for groundwater, topography, and land use/land cover. Ms. Alla was awarded the Women Council scholarship in 2014. She may be reached at allaskaskevych@yahoo.com.